

Spring 5-7-2022

Modulating Cardiac Remodeling After Myocardial Infarction

Uendra Chalise
University of Nebraska Medical Center

Tell us how you used this information in this [short survey](#).

Follow this and additional works at: <https://digitalcommons.unmc.edu/etd>



Part of the [Medical Physiology Commons](#)

Recommended Citation

Chalise, Uendra, "Modulating Cardiac Remodeling After Myocardial Infarction" (2022). *Theses & Dissertations*. 614.

<https://digitalcommons.unmc.edu/etd/614>

This Dissertation is brought to you for free and open access by the Graduate Studies at DigitalCommons@UNMC. It has been accepted for inclusion in Theses & Dissertations by an authorized administrator of DigitalCommons@UNMC. For more information, please contact digitalcommons@unmc.edu.

**MODULATING CARDIAC REMODELING
AFTER MYOCARDIAL INFARCTION**

By

Upendra Chalise

A DISSERTATION

Presented to the Faculty of
the University of Nebraska Graduate College
in Partial Fulfillment of the Requirements
for the Degree of Doctor of Philosophy

Integrative Physiology & Molecular Medicine
Graduate Program

Under the Supervision of Professor Merry L. Lindsey

University of Nebraska Medical Center
Omaha, Nebraska

January 2022

Supervisory Committee

Daniel R. Anderson, MD, Ph.D. Adam J. Case, Ph.D.
Ganesh V. Halade, Ph.D. Geoffrey M. Thiele, Ph.D.
Irving H. Zucker, Ph.D.

MODULATING CARDIAC REMODELING AFTER MYOCARDIAL INFARCTION

Upendra Chalise, Ph.D.

University of Nebraska, 2022

Supervisor: Merry L. Lindsey, Ph.D.

Cardiac remodeling after myocardial infarction (MI) is indicated by infarct wall thinning, reduced ejection fraction, and dilation of the left ventricle (LV). Inflammation presides in the early days of MI as a key event in cardiac wound healing. Infiltration of inflammatory cells, predominantly neutrophils and macrophages, is stimulated by ischemic cardiomyocytes that secrete inflammatory cues. This dissertation focused on identifying factors that influence cardiac remodeling after MI. S100A9 is a neutrophil-derived factor identified that exacerbated infarct wall thinning and cardiac dilation by increasing neutrophil and macrophage infiltration. Similarly, murinoglobulin 1 (Mug1) and galectin (Lgals)3 were macrophage-derived factors identified that regulate neutrophil degranulation and correlate with infarct wall thickness. Matrix metalloproteinase (MMP)-12 was released by both neutrophils and macrophages after MI and mapping the MMP-12 signalome revealed that MMP-12 induced neutrophil apoptosis. In my current project, I identified 5 plasma markers of adverse cardiac remodeling after MI in a retrospective study at MI D3: apolipoprotein A1 (ApoA1), interleukin (IL)17E, immunoglobulin (Ig)A, haptoglobin, and tissue inhibitor of matrix metalloproteinases (TIMP)-1. ApoA1, IL-17E, IgA, and TIMP1 in the plasma mirrored cardiac dysfunction after MI in a prospective study at MI D7. In conclusion, this thesis identified prominent modulators that influenced cardiac remodeling after MI.

ACKNOWLEDGMENTS

This thesis would not have been possible without the help and support from a lot of individuals and funding sources, and I express my heartfelt gratitude to everybody who has, directly or indirectly, helped me in the completion of my dissertation.

I would like to thank Dr. Merry Lindsey for accepting me into her lab and providing incredible mentoring and guidance throughout my graduate school. I am indebted to her patience, thoughtful and kind attitude, and consistent support. Her round-the-clock availability and quick responses always kept me motivated and have inspired me to become a mentor like her in the future. It is my great privilege and honor to complete my Ph.D. journey under her supervision.

Similarly, I would like to thank the Lindsey lab members: Dr. Mediha Becirovic-Agic, Ms. Shelby Konfrst, Ms. Jocelyn Rodriguez-Paar, Dr. John Daseke II, and Dr. Sharon Morais, for their amazing support all through the project. Also, I would like to acknowledge Dr. Kristine DeLeon-Pennell for teaching me MI surgeries and animal work, Dr. Bryan Hackfort for teaching me echocardiography, and Mr. William Kalusche and Ms. Elizabeth Flynn for their help in gathering data. I am also thankful to Dr. Leah Cook for her advice for experiments and intellectual contribution to my papers.

I am highly grateful for all the advice and comments from my supervisory committee: Dr. Daniel Anderson, Dr. Adam Case, Dr. Ganesh Halade, Dr. Geoffrey Thiele, and Dr. Irving Zucker. It has helped me grow into the cardiovascular physiologist that I am today.

Dr. Matthew Zimmerman, Ms. Cindy Norton, Ms. Kim Kavan, and Ms. Charice Bryson have been incredibly helpful with all the administrative advice and support, and I owe my sincere gratitude to them.

Lastly, I would like to thank my friends and family for keeping me sane during my Ph.D. None of this would have been possible without their encouragement.

TABLE OF CONTENTS

ABSTRACT	II
ACKNOWLEDGMENT	III
TABLE OF CONTENTS	IV
LIST OF FIGURES.....	VI
LIST OF ABBREVIATIONS.....	IX
CHAPTER 1. The Cardiac Wound Healing After Myocardial Infarction.....	Error!
Bookmark not defined.	
1. Introduction	1
2. Temporal evolution of Neutrophil phenotypes.....	3
2.1 Pro-inflammatory neutrophils.....	5
2.2 Anti-inflammatory and reparative neutrophils.....	6
3. Temporal evolution of Macrophage phenotypes	9
3.1 Pro-inflammatory macrophages	10
3.2 Anti-inflammatory and reparative macrophages.....	11
4. Temporal evolution of fibroblast phenotypes	14
4.1 Pro-inflammatory fibroblasts.....	15
4.2 Anti-inflammatory and reparative fibroblasts	16
5. Conclusion.....	19
CHAPTER 2. S100A9 is a functional effector of infarct wall thinning after myocardial infarction.....	21
1. Introduction	21
2. Materials and Methods.....	23
3. Results	27
4. Discussion.....	35
5. Conclusion	40
CHAPTER 3. Macrophages secrete murinoglobulin-1 and galectin-3 to regulate neutrophil degranulation after myocardial infarction	41
1. Introduction	41
2. Methods	42
3. Results	47
4. Discussion.....	54
5. Conclusion	60
CHAPTER 4. MMP-12 POLARIZES THE NEUTROPHIL SIGNALOME TOWARDS AN APOPTOTIC SIGNATURE	61
1. Introduction	61
2. Methods	62
3. Results	68

4.	Discussion.....	78
5.	Conclusions.	83
CHAPTER 5. Harnessing the plasma proteome to predict cardiac remodeling after myocardial infarction		
1.	Introduction	84
2.	Methods	85
3.	Results	90
4.	Discussion.....	99
5.	Conclusion	103
CHAPTER 6. DISCUSSION		
1.	Neutrophil cross talk at MI day 1.....	106
2.	Neutrophil cross talk at MI day 3.....	108
3.	Neutrophils cross talk at MI days 5-7.....	109
4.	Identifying therapeutic targets after myocardial infarction.....	110
5.	Future Directions and Conclusions	111
BIBLIOGRAPHY		114

LIST OF FIGURES

Figure 1.1. Myocardial Infarction (MI) Neutrophil Signaling Network.	9
Figure 1.2. MI Macrophage Signaling Network.	14
Figure 1.3. MI Fibroblast Signaling Network.	18
Figure 1.4. MI wound healing.	20
Figure 2.1. Experimental design	24
Figure 2.2. Neutrophil proteins positively correlated with the infarct wall thinning index at MI day 1.	28
Figure 2.3. S100A8/A9 robustly increased neutrophil and macrophage infiltration without changing cardiac physiology at MI day 1.	30
Figure 2.4. S100A8/A9 increased wall thinning and impaired cardiac physiology after MI without affecting infarct sizes.	32
Figure 2.5. Infarct wall thinning observed at MI day 3 negatively correlated with neutrophils and positively correlated with macrophages.	33
Figure 2.6. S100A8/A9 did not directly stimulate MMP-9 expression in vivo or neutrophil degranulation in vitro.	34
Figure 2.7. S100A8/A9 administration increased immune cells per S100A8 or S100A9 at MI D1.	35
Figure 2.8. S100A9 is a functional effector of infarct wall thinning.	36
Figure 3.1. Experimental Design	44
Figure 3.2. D1 Macrophage secretome shows MUG1 as the highest ranked upregulated protein and USP48 as the highest ranked downregulated protein.	48
Figure 3.3. D1 MI macrophage secretome reduces neutrophil degranulation from neutrophils through MUG1 action.	49
Figure 3.4. MUG1 downregulates neutrophil degranulation and pro-inflammatory cytokine release.	50

Figure 3.5. Lgals3 is upregulated in the macrophage and increases MMP-9 release from neutrophils.....	52
Figure 3.6. MUG1 inhibits LGALS3 induced neutrophil degranulation.....	53
Figure 3.7. MUG1 peaks at MI D3 and LGALS3 peaks at MI D7 in the LV infarct, and MUG1 activity peaks at MI D1 and Lgals3 activity peaks at MI D7.	54
Figure 3.8. Macrophage coordinates neutrophil degranulation after MI.....	55
Figure 4.1. Experimental design.	63
Figure 4.2. MMP-12 increases after MI.....	69
Figure 4.3. Neutrophils are one of the sources of MMP-12 after MI.	69
Figure 4.4. IL-1 β induces neutrophil signalome towards cytokine mediated inflammation.	71
Figure 4.5. IL-4 induces neutrophil signalome towards cytokine release and intracellular signaling response.	73
Figure 4.6. MMP-12 induces neutrophil signalome towards apoptosis and intracellular signaling response.	75
Figure 4.7. MMP-12 stimulated neutrophil signalome showed IL-4 like response.	76
Figure 4.8. MMP-12 induces neutrophil apoptosis via FOXO1 and c-Jun phosphorylation.....	77
Figure 4.9. MMP-12 downregulates WNT signaling by inducing cleavage of catenins and cadherins, adherens junction proteins, and impairs cellular adhesion.	78
Figure 4.10. MMP-12 induces apoptosis in neutrophils by upregulating FOXO1 and impairs cellular adhesion through cleavage of adherens junction proteins.	79
Figure 5.1. Experimental design.	86
Figure 5.2. By retrospective analysis, we identify five plasma proteins as markers of cardiac physiology after MI.	91

Figure 5.2. By retrospective analysis, we identify five plasma proteins as markers of cardiac physiology after MI.	91
Figure 5.3. ApoA1 mirrored and predicted cardiac physiology after MI.	93
Figure 5.3. ApoA1 mirrored and predicted cardiac physiology after MI.	93
Figure 5.4. IL-17E mirrored and predicted cardiac physiology after MI.....	95
Figure 5.4. IL-17E mirrored and predicted cardiac physiology after MI.....	95
Figure 5.5. IgA mirrored and predicted cardiac physiology after MI.....	96
Figure 5.5. IgA mirrored and predicted cardiac physiology after MI.....	96
Figure 5.6. Haptoglobin is an early marker of cardiac dysfunction after MI.	97
Figure 5.6. Haptoglobin is an early marker of cardiac dysfunction after MI.	97
Figure 5.7. TIMP-1 mirrored and predicted cardiac physiology after MI.	98
Figure 5.7. TIMP-1 mirrored and predicted cardiac physiology after MI.	98
Figure 5.8. Human glycoproteome profile shows dynamic shift after MI.....	99
Figure 5.8. Human glycoproteome profile shows dynamic shift after MI.....	99
Figure 5.9. ApoA1, IgA, IL-17E and TIMP-1 predicts cardiac remodeling after MI.	100
Figure 5.9. ApoA1, IgA, IL-17E and TIMP-1 predicts cardiac remodeling after MI.	100
Figure 6.1. Wound healing after MI.....	104
Figure 6.1. Wound healing after MI.....	104
Figure 6.2. Neutrophil crosstalk after MI.	106
Figure 6.2. Neutrophil crosstalk after MI.	106

LIST OF ABBREVIATIONS

MI	Myocardial Infarction
LV	Left Ventricle
PMN	Poly Morphonuclear Neutrophil
ECM	Extra Cellular Matrix
D	Day
IL	Interleukin
MUG1	Murinoglobulin 1
LGALS3	Galectin 3
MMP	Matrix Metalloproteinase
A2M	Alpha 2 Macroglobulin
APOA1	Apolipoprotein A1
TIMP	Tissue Inhibitor of Matrix Metalloproteinase
IgA	Immunoglobulin A
FOXO1	Forkhead box O1
GSK3 β	Glycogen Synthase Kinase 3 beta
MEK1	Mitogen Activated Protein Kinase Kinase
TNF α	Tumor Necrosis Factor alpha
IFN γ	Interferon gamma
NF κ B	Nuclear Factor kappa light chain enhancer of activated B cells
CCL	Chemokine (C-C motif) Ligand
CXCL	Chemokine (C-X-C motif) Ligand
CD	Cluster of Differentiation
CTNNB1	β -Catenin
CDH3	Cadherin 3
CTNNA2	Catenin- α 2

CHAPTER 1. The Cardiac Wound Healing Response to Myocardial Infarction

1. Introduction

Myocardial infarction (MI) is defined as the presence of prolonged left ventricular ischemia due to blocked coronary artery, which causes the cardiomyocyte necrosis.(1) In the clinic, MI diagnosis includes the detection of cardiac biomarkers (e.g., troponin) above the 99th percentile of upper reference limit, along with other evidence of ischemia. Ischemia is demonstrated by the presence of symptoms, electrocardiogram changes, or imaging showing loss of viable myocardium or regional wall motion abnormality.(1) MI is also diagnosed in humans following sudden unexpected cardiac death with symptoms of ischemia or evidence of fresh thrombus at autopsy. The current optimum therapy for MI includes timely reperfusion, along with medical treatment including angiotensin converting enzyme inhibitors, beta blockers, and statins.(2-4) For the optimally treated patient who timely receives successful reperfusion, morbidity and mortality is low.

Clinically, not everyone receives timely therapy. About 25% of patients with MI will not be reperfused due to a variety of explanations, including delayed presentation or diagnosis, and lack of success in reperfusion.(5) In addition, up to 30% of those provided reperfusion therapy will experience the phenomenon of 'no-reflow', which is a state of myocardial tissue hypoperfusion due to impaired microvascular flow that occurs in the presence of a patent epicardial coronary artery.(6) Combined, this results in a significant number of patients with MI who will undergo adverse cardiac remodeling and death due to rupture of the left ventricle (LV).(7) For these patients, the risk of progression to heart failure is high, and the majority of heart failure with reduced ejection fraction have MI as the underlying etiology.(8-10)

In animal models of MI, the permanent occlusion non-reperfused MI recapitulates the phenotype of the patient with MI who progresses to heart failure and will be the focus

of this review.(11) As the mouse MI model of permanent occlusion has been extensively evaluated, we will use that as the primary model in our discussion. All animal MI models undergo a similar series of events; the major differences among them are the tolerance to ischemia and the temporal space in which each phase of wound healing occurs.(12-15)

After MI, the myocardium undergoes a series of events that initiates with inflammation and shifts to anti-inflammation before transitioning to tissue repair that culminates in scar formation to replace the necrotic myocardium. The overall response to MI is determined by two major steps, the first of which is the inflammatory response that includes the secretion of proteases to break down the extracellular matrix (ECM) and is a necessary step to clear necrotic cardiomyocytes. The second step is the generation of new ECM that comprises the scar; and this step is governed by the cardiac fibroblasts as the major source of new ECM synthesis. Leukocytes are central to both steps, contributing the proteases in the first step and stimulating the fibroblasts in the second step. Leukocytes transition from pro-inflammatory to anti-inflammatory and reparative cell phenotypes over the first week of MI. The balance between their phenotypes over the two steps of MI response determines the final quantity and quality of scar formed, which in turn contributes to chronic outcomes following MI, including the progression to heart failure.

Necrotic myocytes release complement and other mediators such as damage associated molecular patterns (DAMPs) that initiate an early robust inflammatory response.(16) Macrophages and neutrophils in the circulation and spleen respond by infiltrating to the infarct site.(17-20) Neutrophils quickly predominate, such that by MI day 1 the neutrophil is the primary cell type in the infarct.(21, 22) The macrophage peaks at MI day 3-5.(23) The lymphocyte is another leukocyte present after MI, at lower numbers than the neutrophil or the macrophage, that contributes to the MI response.(24, 25)

Cardiac fibroblasts are present through the time course, peaking in proliferative capacity at MI day 3.(26) Inflammation peaks between MI day 1 and 3, followed by anti-inflammation leading to tissue repair and scar formation over the course of MI. The early phase of response is crucial for MI wound healing, and we will discuss here the roles of the neutrophil, macrophage, and fibroblast to coordinate ECM turnover to regulate wound healing.

2. Temporal evolution of Neutrophil phenotypes

Neutrophils are among the first leukocytes to the ischemic injury after MI and serve as a crucial cell type to initiate and coordinate the early removal of necrotic debris. Neutrophil numbers peak at MI day 1 and return towards baseline values by day 7.(21) Neutrophil activation involves an increase in surface cell adhesion molecule expression that allow circulating neutrophils to enter the infarct region and mobilization of newly formed neutrophils from the bone marrow. Cardiomyocyte necrosis releases complement, DAMPs (e.g., high mobility group box1 (HMGB-1), S100A8/A9, mitochondrial DNA, adenosine triphosphate) and other signaling molecules that activate cell adhesion molecule expression on circulating neutrophils to trigger extravasation into the infarct region and stimulate maturation and recruitment of further neutrophils from the bone marrow. Reduced secretion of CXCL12 in the bone marrow allows mobilization of myeloid cells to the circulation through CXCL12/CXCR4 (fusin, CD184) axis.(27) CXCL12/CXCR4 axis is very important in early neutrophil and monocyte mobilization from the bone marrow to the circulation and hence for overall MI wound healing. CXCR4 blockade by use of antagonist improves tissue repair after MI.(28, 29)

Once extravasated, neutrophils shed L-selectin (CD62L) to allow diapedesis to the infarct and activation by binding toll like receptor (TLR)-4.(30) Activated neutrophils are characterized as CD62L^{low} and CXCR4^{high}.(31, 32) Inhibition of neutrophil recruitment by using CD18 antibody reduces infarct size and improves cardiac

remodeling in a mouse reperfused MI model.(33) Neutrophils, once activated, traverse to the infarct region where they degranulate and release a number of proteases (e.g., matrix metalloproteinase (MMP)-8 and MMP-9 and neutrophil elastase) to breakdown ECM into fragments to remove necrotic cardiomyocytes.(34) Neutrophils also release a number of pro-inflammatory cytokines and chemokines that serve to amplify the inflammatory signal and herald in the macrophage.

While the net effect of the neutrophil is destructive overall, neutrophil presence is required and essential for MI resolution.(35) A number of groups have shown that blocking neutrophil entry using anti-inflammatory strategies increases the incidence of rupture in mouse models of permanent occlusion MI. Neutrophil depletion started before MI worsens cardiac physiology after MI by altering the role of the macrophage.(35) While macrophage numbers are elevated in the neutrophil depleted mice due to increased infiltration, at the same time there is a reduction in their conversion to a reparative phenotype and reduced phagocytic capacity. Neutrophil gelatinase-associated lipocalin (NGAL) was identified in the MI neutrophil secretome as being the driver of the effect on macrophages, and NGAL alone could rescue the neutrophil depleted phenotype and convert macrophages to become phagocytic. Neutrophil depletion, therefore, was detrimental to cardiac repair.

Prolonged pro-inflammation is also detrimental and has negative effects on cardiac physiology and survival. Inhibition of MMP-12 prevents neutrophil apoptosis from occurring and results in excessive infarct wall thinning and exacerbated LV remodeling due to the prolonged presence of neutrophils.(36, 37) The neutrophil, therefore, has a complex cellular role in MI remodeling. One reason for this complexity is that neutrophils across the MI time continuum undergo a full shift in cell polarization from early pro-inflammation to anti-inflammation to repair.(21, 38) The change in MI microenvironment across the first week of MI dictates neutrophil phenotype, as neutrophils polarize in

response to the environment into which they enter. Single cell analysis revealed distinct neutrophil profiles across the response to MI. At MI day 1, neutrophils show higher expression of CD62L, CXCL3, CCL6, and CD177 that shifts to expression of ICAM1, tumor necrosis factor (TNF) α , and interleukin (IL)-23 α at day 3 indicating activated or aged neutrophils. (32, 39) At day 5, neutrophils express higher nuclear receptor 4A2 (NR4A2) indicated resolution of inflammation with increased apoptosis. The MI neutrophil signaling map is shown in **Figure 1.1**.

2.1 Pro-inflammatory neutrophils

Activated neutrophils in the infarct show a pro-inflammatory phenotype. Upon entry to the ischemic site, neutrophils degranulate to release tissue degrading proteases, reactive oxygen species, chemokines, and cytokines.(19) The overall phenotype of the neutrophil at MI day 1 is pro-inflammatory, with invasion and degranulation being primary features. Proteomic analysis showed high upregulation of S100A9, fibrinogen, histones, and activin A indicating positive regulation of secretion.(38) The predominant MMPs are MMP-8 and MMP-9, although recently MMP-12 was shown to be expressed by the neutrophil.(19, 35, 36) Neutrophils also secrete myeloperoxidase, NGAL, and neutrophil elastase in response to MI. MMP-9 secreted by neutrophils in turn stimulates production of CXCR4 to further increase cell mobilization through a positive feedback loop.(40, 41) In the presence of the pro-inflammatory stimulus, fibronectin induces neutrophil degranulation to release MMP-9, which then breaks down fibronectin to its 120 kDa fragment.(38)

Neutrophils at MI days 1 and 3 are characterized by expression of pro-inflammatory cytokines and chemokines, including IL-1 β , IL-8, IL-12 α , CC chemokines (CCL)3 and CCL5, CXCL1/2, lipopolysaccharide-induced CXC chemokine (LIX), TNF α .(19) Pro-inflammatory neutrophils also show low expression of anti-inflammatory proteins, including macrophage mannose receptor 1 (MRC1/CD206) and IL-10.(21) The

release of pro-inflammatory mediators creates a gradient for chemotaxis to stimulate the entry of more neutrophils from circulation to the site of MI as part of the amplification process. This gradient also stimulates the entry of macrophages.(42) Pro-inflammatory neutrophil numbers correlate with the extent of infarct wall thinning.(21) Pro-inflammatory neutrophils can sustain inflammation by forming neutrophil extracellular traps (NETs).(43, 44)

At the same time, the presence of pro-inflammatory neutrophils is also essential in cardiac wound healing, as inflammation is required before resolution and repair can be initiated. For timely resolution of inflammation, it is important that pro-inflammatory neutrophils undergo apoptosis to remove them after cardiac wound healing has been initiated. Neutrophil apoptosis occurs through activation of caspase 3, and MMP-12 can stimulate neutrophil apoptosis directly.(36) MMP-9 reduces macrophage phagocytosis of apoptotic neutrophils, and MMP-9 also reduces neutrophil apoptosis indicated by reduced caspase 9.(45) MMP-9 therefore prevents neutrophils from becoming apoptotic and prevents macrophages from phagocytosing apoptotic neutrophils. Induction of neutrophil apoptosis also initiates the polarization to anti-inflammatory neutrophil phenotype, indicating there is a built-in shut off mechanism to temporally limit inflammation.

2.2 Anti-inflammatory and reparative neutrophils.

Within the infarct zone, by MI day 3 the progression to anti-inflammation and repair commences. The infarct environment shows increased expression of anti-inflammatory molecules and growth factors such as IL-10, transforming growth factor- β (TGF- β) and vascular endothelial growth factor (VEGF), and this is the environment into which new neutrophils infiltrate. The overall phenotype of the neutrophil at MI day 3 is apoptotic, with cathepsin activity and ECM reorganization being primary features. The anti-inflammatory neutrophil is characterized by high expression of Ly6G and CD206,

which continue to increase until MI day 7.(21) CD206 in neutrophils is locally produced, as neutrophils in circulation at MI days 1, 3, or 5 were all CD206 negative.(21) Proteomic analysis showed high expression of cathepsin D, Epo-R, α -synuclein, fibronectin and fibrinogen indicating positive regulation of vasoconstriction.(38) By MI day 5, there is reduced neutrophil recruitment, and the neutrophils present have reduced pro- and elevated anti-inflammatory gene expression. By MI day 7, the overall phenotype of the neutrophil is reparative, with neutrophils contributing to ECM synthesis and reorganization as the top enriched pathway.(38)

Cathepsins degrade ECM and stimulate apoptosis and autophagy, providing shut-off values to prevent extended neutrophil activity. Cathepsins degrade BCL-2 to stimulate apoptosis.(46) Cathepsin D mediates cytochrome c and primes caspase 8 activation to stimulate apoptosis.(47) Fibronectin is 22-fold induced in neutrophils at MI day 3 compared to pre-MI resident neutrophils.(38) Fibronectin amplifies TNF α stimulated neutrophil apoptosis and augments macrophage uptake of apoptotic neutrophils, thus serving a dual role in promoting neutrophil removal from the MI.(48, 49).

The overall phenotype of the neutrophil at MI day 7 is reparative, with ECM reorganization being the primary feature. The direct role of neutrophils in tissue repair has been understudied, and neutrophils at MI day 5 and 7 have increased ECM protein expression, including fibrinogen, fibronectin, thrombospondin-2, galectin-3, MMP-2, tissue inhibitor of metalloproteinase (TIMP)-2, and vitronectin.(38) Neutrophils at MI day 7 also express cathepsin B and S100A4.

Fibrinogen stimulates fibroblast proliferation, indicating an upregulation of neutrophil to fibroblast cross-talk.(50) The increase in TIMP-2 indicates that neutrophils at later times of MI prevent further ECM breakdown by both reducing their expression of MMP-8 and -9 while upregulating TIMP. At the same time, the increased expression of

MMP-2 in the day 7 neutrophil indicates that it may also serve a neo-homeostatic role to help maintain the infarct scar, as MMP-2 is associated with cardiomyocyte homeostasis.(51) In vivo, exogenous IL-4 infusion started 24 h after MI reduced neutrophil expression of CCL3, IL-12a, TGF- β 1, and TNF α at MI day 3.(52) Neutrophils stimulated in vitro with IL-4 show a strong anti-inflammatory polarization with increased expression of anti-inflammatory markers (i.e., arginase (ARG)1, CD206, TGF- β 1, and chitinase-3-like protein 3 (YM1)).(53)

As neutrophil directly regulate inflammatory response and tissue microenvironment in MI, targeting neutrophils or neutrophil components could be therapeutically viable. In cancer, training neutrophils towards granulopoiesis has shown to have a positive effect.(54) Inhibition of neutrophil dimer protein S100A8/A9 improves infarct size after MI.(55-57) Resolution promoting factors (resolvin D, annexin A1, and MMP-12) impact neutrophil infiltration and pro-inflammation.(37, 58, 59) Selective transdifferentiation of neutrophils from an inflammatory to reparative phenotype may provide improved response to MI. A significant challenge lies in identifying the appropriate time point to start the therapy, as pro-inflammatory neutrophils and subsequent signaling are essential for MI resolution. Sex as a biological variable may also need to be considered. While neutrophil numbers were lower in female mice at MI day 1, the neutrophils from the female mice showed higher per cell release of MMP-9 to maintain tissue clearance rates.(60, 61) The net effect of sex differences on remodeling remains to be fully elucidated.

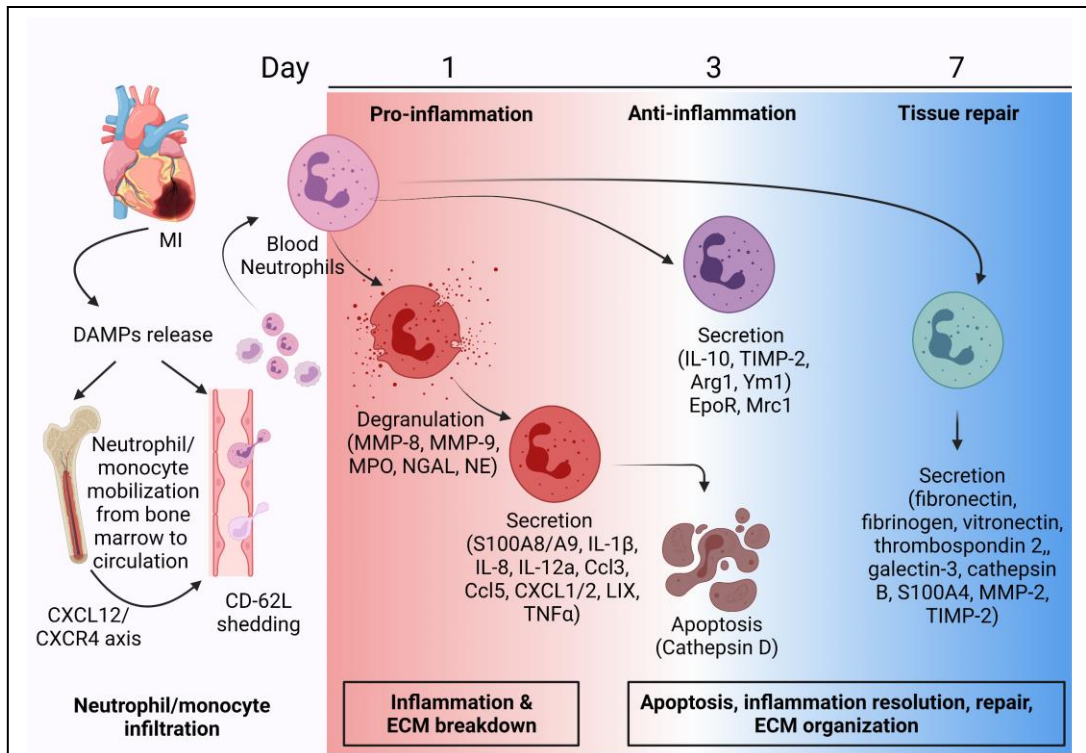


Figure 1.1. Myocardial Infarction (MI) Neutrophil Signaling Network.

After MI, necrotic cardiomyocytes release damage associated molecular patterns (DAMPs) that stimulate neutrophil infiltration from the circulation and mobilization of new neutrophils from the bone marrow, a process regulated by CXCL12/CXCR4 signaling. Blood neutrophils infiltrate to the infarct, shedding CD-62L along the way. MI neutrophils are polarized to a pro-inflammatory phenotype at MI day 1. Pro-inflammatory neutrophils undergo degranulation to release various proteases such as matrix metalloproteinase (MMP)-8, MMP-9, myeloperoxidase (MPO), neutrophil gelatinase associated lipocalin (NGAL) and neutrophil elastase. Pro-inflammatory neutrophils also secrete pro-inflammatory proteins (e.g., S100A8/A9, interleukin (IL)-1 β , IL-8, IL-12a, CCL3, CCL5, CXCL1/2, LIX, and tumor necrosis factor (TNF) α). With the change in tissue microenvironment to anti-inflammatory status, pro-inflammatory neutrophils undergo apoptosis and newly infiltrating neutrophils polarize to an anti-inflammatory phenotype. Anti-inflammatory neutrophils are characterized by increased expression of IL-10, Arginase (Arg)1, Ym1, tissue inhibitor of matrix metalloproteinase (TIMP)-2, and mannose receptor C-type 1 (Mrc1). By MI day 7, neutrophils show a reparative phenotype with predominant secretion of extracellular matrix (ECM) proteins such as fibronectin, fibrinogen, vitronectin, thrombospondin 2, galectin-3, cathepsin B, S100A4, MMP-2 and TIMP-2. Created with BioRender.com.

3. Temporal evolution of Macrophage phenotypes

Blood monocytes infiltrate to the LV infarct in response to chemotactic signals and initially differentiate into pro-inflammatory macrophages. Macrophages also

phenotypically evolve over the first week of MI (**Figure 1.2**).⁽²³⁾ Pro-inflammatory macrophages amplify the inflammatory signaling cascade, while anti-inflammatory and reparative macrophages phagocytose apoptotic neutrophils to shut off inflammation, and secrete growth factors and ECM components to initiate scar formation, and stimulate neovascularization in the infarct zone.

3.1 Pro-inflammatory macrophages

The overall phenotype of the macrophage at MI day 1 is pro-inflammatory, with cytokine upregulation and ECM degradation being primary features. Similar to neutrophils, pro-inflammatory macrophages express cytokines and chemokines, including IL-1b, IL-6, and TNF α .⁽⁵³⁾ CD14 is also upregulated at MI day 1. Th1- related cytokines activate M1 macrophages and induce pro-inflammatory activity. In addition to cytokine release, another major role of pro-inflammatory macrophages is to secrete MMP-8 and -9 to coordinate necrotic tissue removal in conjunction with the neutrophils. Enrichment analysis of the day 1 MI macrophage transcriptome showed upregulation of degranulation or release of tissue degrading proteases, and downregulation of ECM organization.

In vivo, macrophages at MI day 1 are activated by binding of TLR ligands to TLR in a MYD88 dependent manner to induce transcription of interferon (IFN) γ and TNF α . Macrophages stimulated by pro-inflammatory cytokines secrete pro-inflammatory cytokines to maintain the inflammatory condition that extends neutrophil survival.⁽⁴²⁾ At MI day 1, pro-inflammatory macrophages (F4/80^{low}Ly6C^{high}) predominantly exhibit NF- κ B and MAPK signal activation to increase IL-1 β , IL-12a, CXCL4, ILR-2, MMP-8, and IL-24 expression.⁽²³⁾ Hypoxic response is indicated in M1 macrophages at day 1 with differential expression of HIF-1 α . Glycolysis, a metabolic hallmark of the pro-inflammatory macrophage, is upregulated at MI day 1.^(62, 63)

Pro-inflammatory macrophages associate with adverse cardiac remodeling after MI. In humans with acute MI, peak in pro-inflammatory monocytes (CD14⁺CD16⁻) in the blood negatively associated with recovery of ejection fraction 6 months after MI.(64) Peak circulating monocyte counts were higher in patients with acute MI who had pump failure or LV aneurysm, with monocyte counts correlating positively with LV end diastolic volumes and negatively with ejection fraction.(65) Similar results have been observed in mouse models of MI with increased macrophages correlated to higher incidences of LV rupture.(66) ApoE^{null} mice after MI have exacerbated infiltration and prolonged presence of pro-inflammatory macrophages resulting in reduced ejection fraction measured at MI day 21.(67) When the ApoE^{null} mice were treated with siRNA targeting CCR2, they were protected from heart failure and had improved MI wound healing.(67) Excessive inflammatory response caused by pro-inflammatory macrophages, therefore can be deleterious and appropriate targeting of this macrophage subtype may improve MI outcomes.

3.2 Anti-inflammatory and reparative macrophages

At about MI day 3, macrophages begin to polarize with the overall phenotype of the macrophage being anti-inflammatory, with proliferation, phagocytosis, and metabolic reprogramming being primary features.(23) These cells are characterized by high expression of IFN γ , IL-12a, and CXCL4, indicating a combination of pro- and anti-inflammation. Anti-inflammatory macrophages can be stimulated *in vitro* by IL-4, IL-10, or IL-13.(53) While IL-4 is not endogenously expressed at high levels after MI, cells in the heart express IL-4 receptors and can respond to IL-4 stimulation.(52) Anti-inflammatory genes expressed by macrophages include ARG1, IL-10, CD206, TGF β , and YM1.(68) By MI day 7, the macrophage converts to a reparative phenotype, producing collagen, periostin (Postn), secreted protein acidic and rich in cysteine (SPARC), and lysyl oxidase.(26).

Engulfing of apoptotic neutrophils by macrophages involves GAS6 binding and MerTK activation through upregulation of AKT signaling.(69, 70) Acute inhibition of CD47 during reperfused MI promotes macrophage phagocytosis and improves cardiac repair.(71) Neutrophil phagocytosis by macrophages reduces IL-23 release and triggers an anti-inflammatory response.(72) The anti-inflammatory macrophage stimulates fibroblast proliferation and ECM synthesis to initiate scar formation. TGF- β secreted by macrophages initiates the proliferative phase and induce repair and regeneration of ECM in the infarct region.(73). Anti-inflammatory macrophages also communicate with endothelial cells through release of growth factors (e.g., platelet derived growth factor) to stimulate the formation of new blood vessels necessary to vascularize the infarct scar.(74)

As macrophages play various crucial physiological roles which are essential for infarct wound healing, complete depletion or early inhibition of macrophages holds less therapeutic potential. Depletion of macrophages by clodronate liposomes or genetic ablation both impairs wound repair.(68) In humans, pro-inflammatory M1 macrophages (CD14⁺CD16⁻) were lower in patients with thrombus after MI compared to patients without thrombus.(75, 76) In patients with ST segment elevation MI, blood CD14⁺CD16⁻ monocyte counts negatively correlate with MI resolution.(77) Increasing macrophages proliferation by administration of macrophage colony-stimulating factor (M-CSF, CSF-1) reduces MI cardiac remodeling,(78) while administering an inducer of granulocyte-macrophage colony-stimulating factor (GM-CSF) has the opposite effect.(79).

Optimization or refinement of macrophage subtype kinetics may be beneficial in the MI response. A blunted or accelerated pro-inflammatory phase or an enhanced or early anti-inflammatory phase may provide an improved balance of phenotypes that allow the essential inflammation while promoting repair. CCR2 inhibition targets pro-inflammatory monocytes (Ly-6C^{high}) and is beneficial for MI repair.(77) Similarly, RNA

inhibition of the IRF5 transcription factor reduces pro-inflammatory macrophage numbers without altering anti-inflammatory or reparative macrophage numbers.(80) IL-10, an anti-inflammatory agent, administered 24 h after MI, improved ejection fraction and reduced cardiac dilation by reducing macrophage numbers, and shifting the phenotype to anti-inflammation and repair.(81) IL-10 induces phagocytosis by acting through an IL-10-STAT3-galectin 3 axis to upregulate production of osteopontin.(82) Macrophage induced phagocytosis is essential for tissue repair by clearing apoptotic cells and coordinating ECM reorganization during scar formation.(83) Effective strategies targeting the macrophage, therefore, will need to consider the necessity of inflammation.

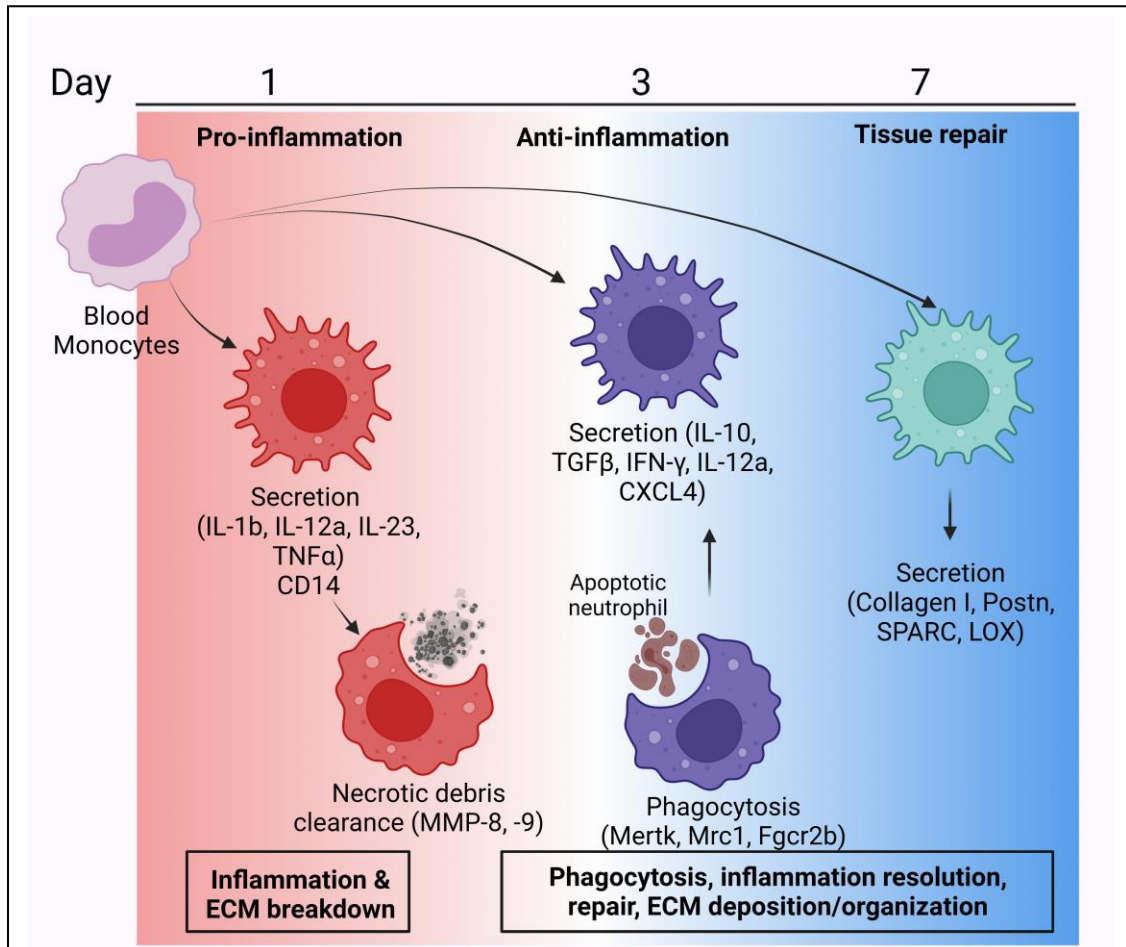


Figure 1.2. MI Macrophage Signaling Network.

Blood monocytes infiltrate to the infarct area and are initially polarized to pro-inflammatory macrophages by processes similar to neutrophils. Pro-inflammatory macrophages highly express cytokines (e.g., IL-1 β , IL-12a, IL-23, and TNF α), as well as high expression of CD14. At MI day 1, macrophages aid the neutrophils in necrotic debris clearance by secreting tissue degrading proteases such as MMP-8 and MMP-9. By MI day 3, macrophages transition to an anti-inflammatory phenotype and phagocytose apoptotic neutrophils through cell surface expression of MERTK, MRC1 and Fc γ R2b. Anti-inflammatory macrophages secrete IL-10 and TGF- β , along with IFN- γ , IL-12a, and CXCL4, indicating a mixed profile. By MI day 7, macrophages continue to transition towards a reparative phenotype with secretion of ECM proteins such as collagen I, periostin (Postn), secreted protein acidic and rich in cysteine (SPARC) and lysyl oxidase (LOX). Created with BioRender.com.

4. Temporal evolution of fibroblast phenotypes

The cardiac fibroblast is a resident cell type that actively participates in homeostasis of the myocardium by providing continuous low-grade turnover of ECM, contributing to vascular maintenance, and aiding in transduction of electrical signals.(26,

74, 84-89) Following MI, the fibroblast transitions from supporting homeostatic functions to actively participating in all phases of infarct wound healing.(26, 74) While ECM synthesis and deposition is the major and most known role of the fibroblast during infarct healing, the fibroblast polarizes and shows a spectrum of phenotypes in response to changes in the microenvironment over the MI time continuum (**Figure 1.3**).(26) During the early inflammatory phase, ECM degradation is favoured over ECM deposition as removal of debris is necessary before scar formation.(90, 91) Consequently, fibroblasts polarize to support ECM degradation and necrotic debris removal. (26, 90) During the anti-inflammatory and reparative phase, changes in the microenvironment stimulate fibroblast proliferation and ECM synthesis resulting in scar formation.(26, 90)

4.1 Pro-inflammatory fibroblasts

The overall phenotype of the fibroblast at MI day 1 is pro-inflammatory, with cytokine upregulation and anti-migration being primary features. Cardiac fibroblasts both contribute and respond to pro-inflammatory signaling during MI.(84) DAMPs released by necrotic myocytes and leukocytes stimulate fibroblasts through pattern recognition receptors (TLRs, NLRs, IL-1R1, RAGE) to produce and release a range of chemokines (CXCL1, CXCL2, CXCL5, CXCL8, CXCL10, CX3C11, CCL2, CCL3, and CCL5) and cytokines (IL-1 β , IL-6, IL-8, IL-12p40, IL-12p70, IL-13, TNFRSF9, and TNF α).(92-94) The MI day 1 fibroblast also produces colony stimulating factor (CSF)-1, which is needed for macrophage differentiation.(95) The production of pro-inflammatory cytokines by fibroblasts stimulates the influx of leukocytes into the infarct zone.(96-101) Cultured fibroblasts also produce pro-inflammatory chemokines and cytokines in response to IFN γ and TNF α , indicating a positive feedback loop is initiated in the presence of a pro-inflammatory environment.(84, 102, 103) By transcriptomics, the most upregulated pathway in MI day 1 fibroblasts is chemokine- and cytokine-mediated inflammation indicating that cardiac fibroblast actively regulate the inflammatory response.(26) Pro-

inflammatory fibroblasts also display a pro-survival, anti-proliferative and anti-migratory phenotype. The expression of anti-apoptotic BCL2 is increased in MI day 1 fibroblasts indicating a pro-survival phenotype, which would also prevent neutrophils from undergoing apoptosis.(26) This in conjunction with reduced migration rate and absence of proliferation favours ECM degradation.(26, 90) Thus pro-inflammatory fibroblasts promote leukocyte infiltration, ECM degradation and necrotic debris removal.

4.2 Anti-inflammatory and reparative fibroblasts

The inflammation starts to subside around MI day 3.(84) The overall phenotype of the fibroblast at MI day 3 is proliferative, with promotion of angiogenesis and ECM production being primary features. The shift from an inflammatory to an anti-inflammatory environment induces transdifferentiation of the fibroblasts into myofibroblasts, which start to proliferate and migrate into the infarcted area, resulting in increased wound contraction and repair capacity.(26, 104, 105) The main function of the fibroblast is to synthesize and secrete ECM, a function fundamental for formation of the collagen rich scar that replaces the necrotic myocytes.(74, 84, 90) Even though replacing myocytes with scar tissue results in loss of contractility and is suboptimal compared to the pre-MI state, formation of an infarct scar is crucial for structural integrity to prevent the formation of LV aneurysm and cardiac rupture and is an optimal response to MI.(104)

TGF- β 1, secreted by most myocardial cell types, including cardiomyocytes and macrophages, is the central mediator of myofibroblast activation.(34, 73, 105) IL-1, cardiotrophin-1, and fibroblast growth factor are additional factors that can stimulate fibroblast migration into the infarct, but their effect on infarct scar formation is still uncertain.(105-108) The myofibroblast is commonly defined as a post-injury fibroblast, a definition loosely based on the binary expression of alpha smooth muscle actin.(105) This terminology however, is limiting since it does not include all the different

phenotypes that the fibroblasts display during the MI time continuum.(84) MI day 3 fibroblasts have a proliferative and pro-angiogenic phenotype.(26) Cholesterol biosynthesis, necessary for membrane synthesis and proliferation, is the major upregulated pathway in the MI day 3 fibroblast. Increased proliferation in combination with downregulation of pro-apoptotic genes (*Caspase3*) explains the increased fibroblast numbers detected around MI day 3.

Angiogenesis, cell migration involved in sprouting angiogenesis, and blood vessel endothelial cell migration are additional processes upregulated in the MI day 3 fibroblasts. In vitro, the secretome from day 3 fibroblasts stimulate endothelial cell tube formation, supporting the pro-angiogenic phenotype.(26) Collagen content in the infarcted area does not increase measurably until 3-7 days after MI and peaks after 3-6 weeks.(104, 109) The fibroblasts that we typically think of, a prominent producer of ECM, are seen at MI day 7.(90) The overall phenotype of the fibroblast at MI day 7 is scar forming, with ECM production and anti-angiogenesis being primary features. The secretome of day 7 fibroblasts is rich in collagen I alpha 1 and 2 chains, secreted protein acidic and rich in cysteine, and lysyl oxidase. At the same time, day 7 fibroblasts also secrete TIMP-1, TIMP-3 and THBS1, which inhibits ECM degradation and angiogenesis.(26) Thus, the anti-inflammatory and reparative fibroblasts support scar formation through ECM deposition and revascularization.

Fibroblasts are very changeable in character and therefore amenable to therapy.(110) Promoting pro-angiogenic fibroblasts early on may be a way to accelerate revascularization and infarct healing. To do this, a better understanding of the factors that promote different fibroblast phenotypes is warranted. TGF- β 1, in addition to stimulating ECM synthesis and deposition, is a very potent suppressor of inflammation and may therefore be used to promote infarct healing.(73) On the other hand, excessive

ECM deposition may induce arrhythmias and diastolic dysfunction, showing the importance of having the right amount at the right time.(111, 112)

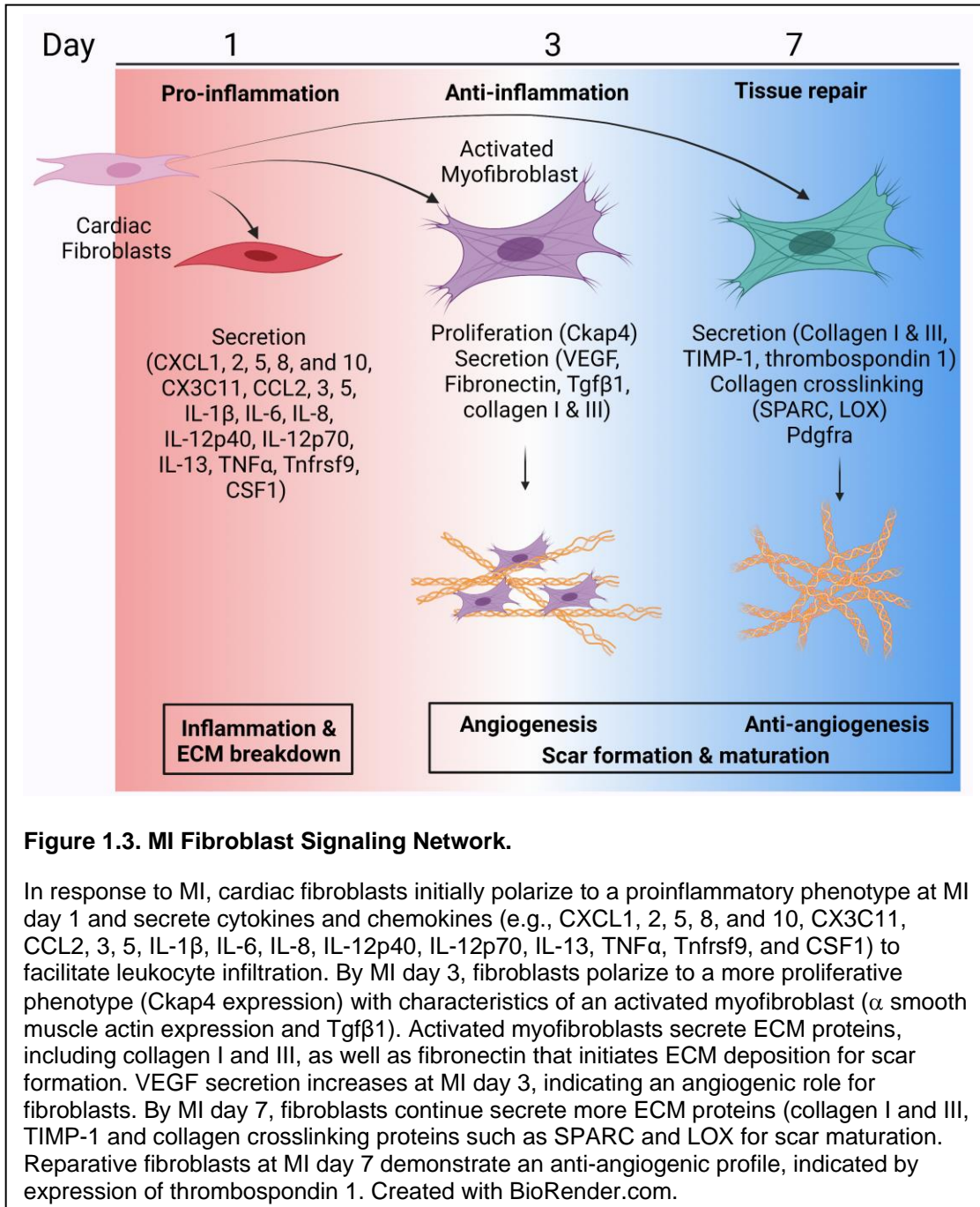


Figure 1.3. MI Fibroblast Signaling Network.

In response to MI, cardiac fibroblasts initially polarize to a proinflammatory phenotype at MI day 1 and secrete cytokines and chemokines (e.g., CXCL1, 2, 5, 8, and 10, CX3C11, CCL2, 3, 5, IL-1 β , IL-6, IL-8, IL-12p40, IL-12p70, IL-13, TNF α , Tnfrsf9, and CSF1) to facilitate leukocyte infiltration. By MI day 3, fibroblasts polarize to a more proliferative phenotype (Ckap4 expression) with characteristics of an activated myofibroblast (α smooth muscle actin expression and Tgf β 1). Activated myofibroblasts secrete ECM proteins, including collagen I and III, as well as fibronectin that initiates ECM deposition for scar formation. VEGF secretion increases at MI day 3, indicating an angiogenic role for fibroblasts. By MI day 7, fibroblasts continue secrete more ECM proteins (collagen I and III, TIMP-1 and collagen crosslinking proteins such as SPARC and LOX for scar maturation. Reparative fibroblasts at MI day 7 demonstrate an anti-angiogenic profile, indicated by expression of thrombospondin 1. Created with BioRender.com.

5. Conclusion

The cardiac response to MI involves a series of wound healing events categorized as temporal shifts from pro-inflammation to anti-inflammation to repair and scar formation (**Figure 1.4**). The neutrophil, macrophage, and fibroblast all evolve in phenotype along this time continuum. Understanding the balance in interactions among these three cells types will provide insight into both the mechanisms involved as well as provide targets for therapeutic modulation. With increased awareness of the importance of rigor and reproducibility, a number of resources have been provided by the research community to aid in MI research.(5, 113)

Fine tuning the system, rather than total ablation or overexpression of components, will likely yield a better outcome. Strategies that temper inflammation or accelerate the transition to turn off inflammation may provide a means to modify the response. Using resolution promoting factors is one such arena of promising research.(37, 59, 114) While clinical treatment of acute MI has improved dramatically over the last 40 years, preventing the progression to heart failure remains a significant clinical issue.

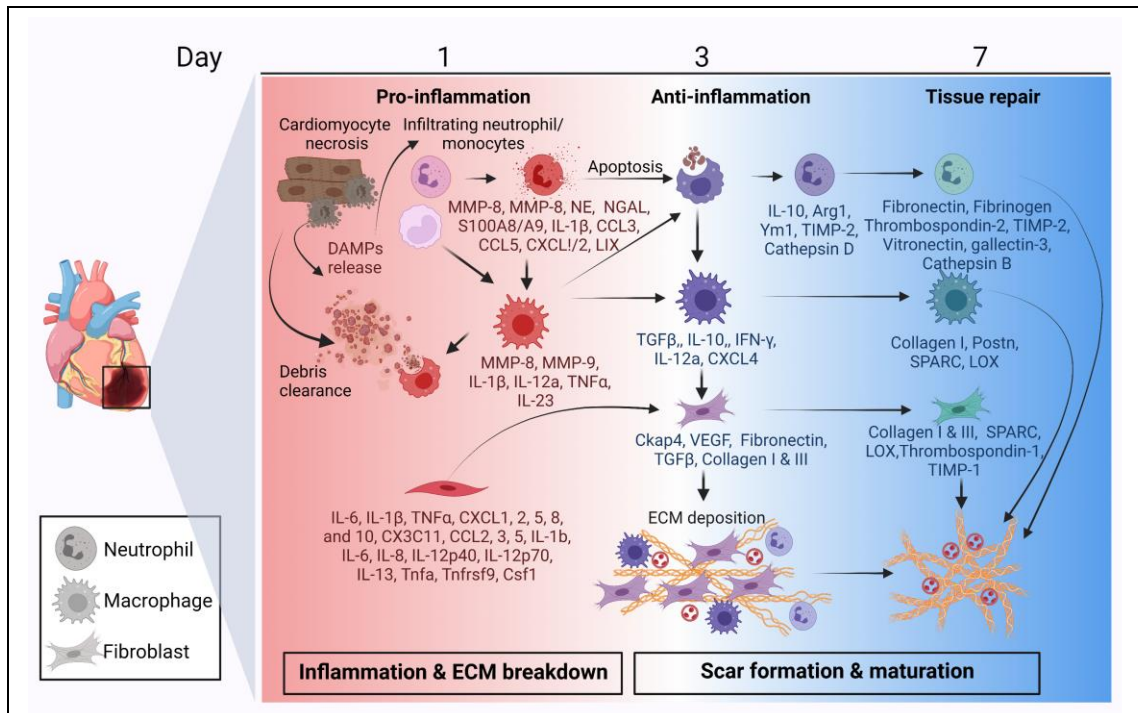


Figure 1.4. MI wound healing.

Cardiac wound healing after MI is a balance between the breakdown of existing ECM and construction of new ECM to form an infarct scar. Changes in cellular phenotypes transition from early pro-inflammatory to anti-inflammatory and reparative polarization phenotypes. Pro-inflammatory cells clear necrotic tissue, while anti-inflammatory cells turn off the inflammatory response and reparative cells promote scar formation and maturation through secretion of ECM and ECM-modifying proteins. Created with Biorender.com.

CHAPTER 2. S100A9 is a functional effector of infarct wall thinning after myocardial infarction

1. Introduction

The response to myocardial infarction (MI) involves a robust immune response with inflammatory cell infiltration initiated within the first hours after coronary artery occlusion. Pro-inflammatory neutrophils and monocytes are early responders to danger associated molecular patterns (DAMPs) released from necrotic cardiomyocytes.(115-117) Leukocytes infiltrate the infarct regions and commence the inflammatory cascade by secreting cytokines, chemokines, and proteases essential for extracellular matrix (ECM) breakdown and remodeling. Excessive infiltration of pro-inflammatory cells after MI can have a negative impact on cardiac remodeling and repair mechanisms.(91, 118) While tempering the pro-inflammatory cascade will curb excessive cardiomyocyte and ECM turnover, pro-inflammation is an essential preceding guide for later anti-inflammatory and reparative signaling. For this reason, anti-inflammatory strategies that totally block pro-inflammation have often resulted in negative impacts on cardiac remodeling.(119)

Cardiomyocyte necrosis and subsequent loss after MI defines the magnitude of infarct wall thinning that occurs.(38, 120) In the mouse MI model, maximum myocyte loss occurs within 24 h of ischemia initiation, with wall thinning peaking at day(D)1. Infarct wall thinning can be measured *in vivo* by echocardiography. Wall thinning weakens cardiac structure and can lead to formation of left ventricle (LV) aneurysms which can further progress to LV rupture. LV rupture, while less prevalent clinically due to the advent of reperfusion, is still a major cause of MI mortality in preclinical MI animal models and clinically with failed reperfusion or ineffective cardiac repair.(66, 121) About 25% of MI cases in humans are non-reperfused due to inaccessibility or delayed presentation of MI or other medical contraindications. An additional ~30% of MI cases

undergoing percutaneous intervention fail and are categorized as no-reflow.(122, 123) No-reflow accounts for about 500,000 patients yearly in the United States alone.(122, 123) In both of these cases, the patient is at high risk for adverse cardiac remodeling that progresses to heart failure. In mice, the non-reperfused MI model best replicates this clinical scenario.

Neutrophil numbers positively associate with LV rupture.(124) Neutrophils secrete a variety of proteases including serine proteases, matrix metalloproteinases (MMPs), and neutrophil elastase to orchestrate the removal of necrotic debris. The neutrophil expresses several MMPs, particularly MMP-8 and MMP-9, which are stored in pre-formed granules.(125) MMP-8 and MMP-9 proteolytically cleave a number of substrates including ECM, chemokines, and cytokines. Increased MMP-8 or MMP-9 in the infarct zone associates with LV rupture and heart failure progression after MI.(121, 126-128)

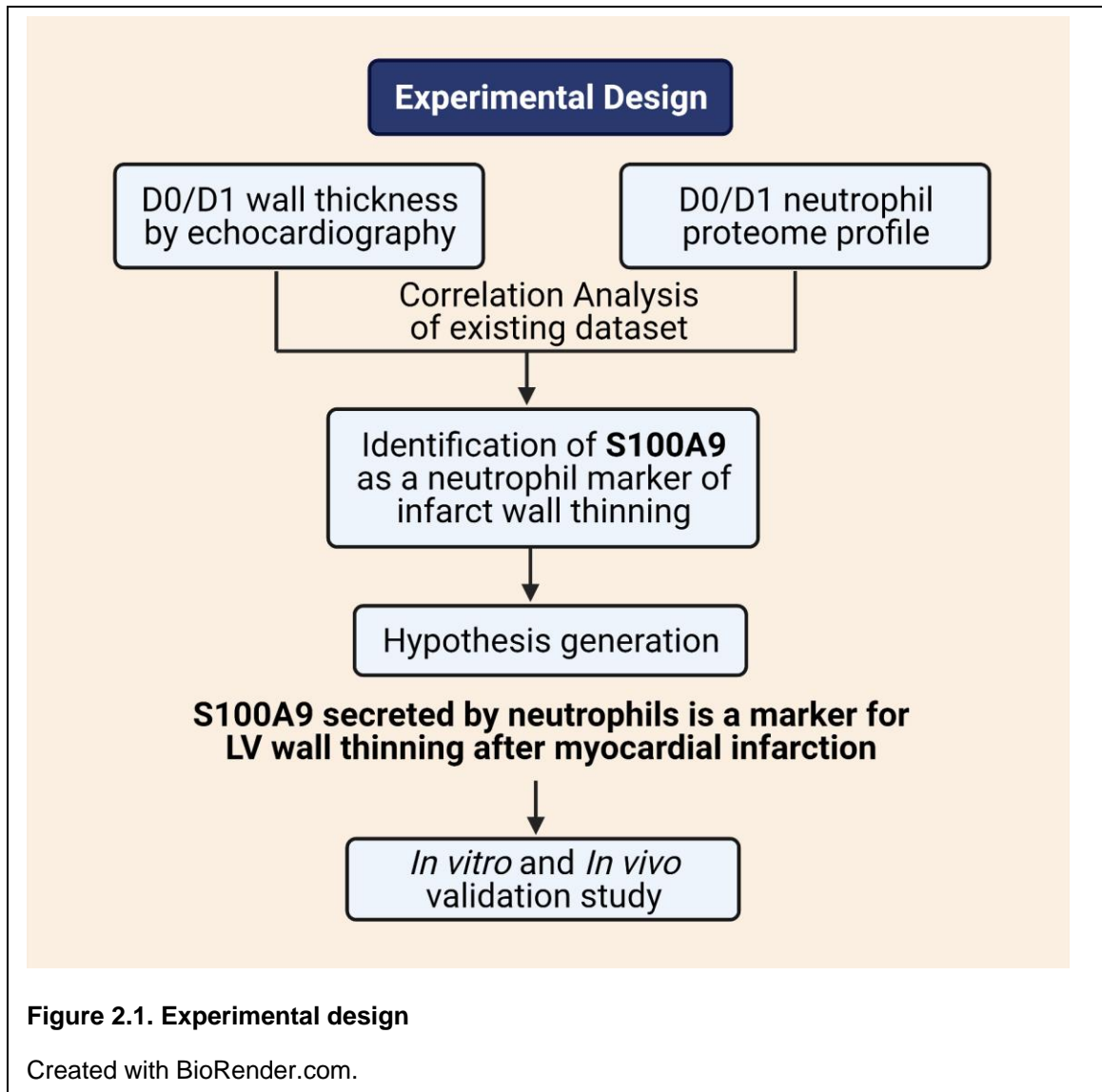
The S100A8/A9 complex, also known as calprotectin, is a DAMP secreted by neutrophils and monocytes and regulates inflammatory responses through its role in innate immunity.(129) The two subunits belong to the S100 family of proteins, which regulates various cellular functions including calcium balance, cellular migration, proliferation, and inflammation.(130) S100A8 and S100A9 combined account for approximately 45% of total cytosolic protein content in neutrophils. S100A9 is a calcium binding protein that primarily exists as a heterodimer with S100A8.

The goal of this study was to identify proteins derived from the neutrophil that best correlate with infarct wall thinning and could serve as causal mediators. Our results identified 4 proteins, of which S100A9 was the highest extracellular component. We then tested the hypothesis that as a direct regulator, S100A9 administration after MI would increase infarct wall thinning.

2. Materials and Methods

Identification of protein candidates

The experimental design workflow is detailed in **Figure 2.1**. We retrospectively interrogated a previously published MI neutrophil proteome and echocardiography dataset to identify proteins that best linked to infarct wall thinning.(38) The dataset included 123 neutrophil proteins, which were correlated with infarct wall thickness measurement by echocardiography (anterior wall thickness in systole, AWTs).(38) Infarct wall thinning index was calculated as the inverse of wall thickness ($1/\text{AWTs}$). The dataset included results for 3-6 month old C57BL/6J male(M) mice at control no MI D0 (n=10) or MI D1 (n=10). Neutrophils were isolated from the infarct region at MI D1 and compared with no MI D0 LV neutrophils. By Pearson correlation analysis, the correlation coefficient (r) and p value were used to determine ranking. Positive correlations between wall thinning index and protein concentration (negative correlation between infarct wall thickness and protein concentration) were used for target selection and hypothesis generation for the prospective study.



Coronary artery ligation and echocardiography

For the prospective evaluation, all animal procedures were approved by the Institutional Animal Care and Use Committee at the University of Nebraska Medical Center and were conducted in accordance with the Guide for the Care and Use of Laboratory Animals published by the National Institutes of Health.(131) We enrolled a new set of mice for validation assessment. C57BL/6J male mice (3-6 months old) were used for MI surgery using the same protocol as described previously.(21, 81, 118, 132-134) Isoflurane (~2%) was used for anesthesia and buprenorphine-SR (0.5 mg/kg,

subcutaneously) was given before surgery for analgesia. MI was confirmed at surgery by visual blanching of the left ventricle and changes in the electrocardiogram (ST segment elevation) and validated by terminal echocardiography and infarct sizing by 1% 2,3,5-triphenyltetrazolium chloride (Sigma) staining. Mice were randomized to treatment groups and investigators were blinded for data acquisition and analysis.

At the time of MI, recombinant S100A8/A9 (RnD Systems #8916-S8-050; 4.4 ng/g/h or 3.2 g/day, endotoxin-free) was given subcutaneously by osmotic minipump (Alzet #2001D for D1 and #1003D for D3). Osmotic minipumps were activated for 3 h for D1 pumps and overnight for D3 pumps per manufacturer recommendation. S100A9 was given as a complex with S100A8 because *in vivo* the proteins exist as a stable heterodimer. The dose used was similar to previous reports.(55-57, 135) Saline was infused as the vehicle control. Echocardiography was performed prior to MI and at MI D1 and D3 using the Vevo 3100 (FUJIFILM Visualsonics) in accordance to the guidelines for measuring cardiac physiology in mice.(136) Following echocardiography, the mice were sacrificed and the tissue was collected, snap frozen, and stored at -80 °C. Infarct sizes were calculated as the percentage infarcted area of total LV area using Adobe Photoshop. The LV infarct region was separated from the remote non-infarcted region and stored individually. Sample sizes were D1 saline (n=6M), D1 S100A8/A9 (n=7M), D3 saline (n=6M), and D3 S100A8/A9 (n=5M).

Degranulation assay

Bone marrow derived neutrophils were isolated from C57BL/6J male mice (3-6 months old; n=3) using the autoMACS Pro Separator (Miltenyi Biotec) with anti-Ly6G microbeads (Miltenyi Biotec; #130-120-337) as previously described.(118) Neutrophils (1.5×10^6 cells) were resuspended in 1 mL RPMI 1640 (Gibco, #21875034) with 1% penicillin/streptomycin (Thermo, #15140-122). The cells were stimulated with S100A8/A9 (RnD Systems, #8916-S8-050; 500 ng/mL) for 15 min at 37C. Unstimulated

neutrophils served as negative controls. At the end of stimulation, samples were centrifuged at 800xg for 8 min. The secretome (supernatant) and cell pellet were separated, individually snap frozen, and stored at -80 °C until use. MMP-9 release into the secretome was measured by immunoblotting, as an indicator of degranulation status.

Immunoblotting

Immunoblotting was performed according to the published guidelines.(137) For immunoblotting of infarcted LV, total protein (10 µg) was loaded on 4–12% Criterion XT Bis-Tris precast gels (Bio-Rad) and transferred to nitrocellulose membranes using the Trans-Blot Turbo Transfer Pack (Bio-Rad). Membranes were stained with Pierce Reversible Protein Stain Kit (Thermo Scientific). Membranes were blocked with Blotting Grade Blocker (5%, Bio-Rad) in phosphate buffer solution (PBS) containing 0.1% Tween 20 and incubated overnight at 4°C with the primary antibody (Cedarlane, anti-mouse neutrophils #CL8993AP, 1:1000; Cedarlane, anti-mouse Mac-3 #CL8943AP-3, 1:1000; Invitrogen, anti- mouse S100A8 #PA5-79948, 1:1000; Invitrogen, anti-mouse S100A9 #PA1-46489, 1:1000), followed by incubation at room temperature for 1 h with the secondary antibody (Vector laboratories, anti-rat IgG, #PI-9400, dilution 1:5000, anti-rabbit IgG, #PI-1000, dilution 1:5000). Chemiluminescent images were captured using the iBright FL1000 imaging system (Thermo Fisher) and quantified using iBright analysis software 4.0.0. The blots were normalized to the total protein and the data are presented as normalized arbitrary units. Antibodies were validated using positive controls, including bone marrow derived neutrophils for the neutrophil Ly6b blot, LV macrophages for the Mac-3 blot, and recombinant mouse MMP-9 for MMP-9 blot. Spleen was used as a standard positive control for all blots.

For immunoblotting of the neutrophil secretome, the above protocol was followed with the following modifications. Equal volume (10 µL) was loaded for each sample, because the cell number per volume was equal. The primary antibody used was against

MMP-9 (Millipore Sigma, #AB19016, dilution 1:1000), and the secondary antibody was anti-rabbit IgG (Vector Laboratories, #PI-1000, dilution 1:5000). The data are presented as arbitrary units.

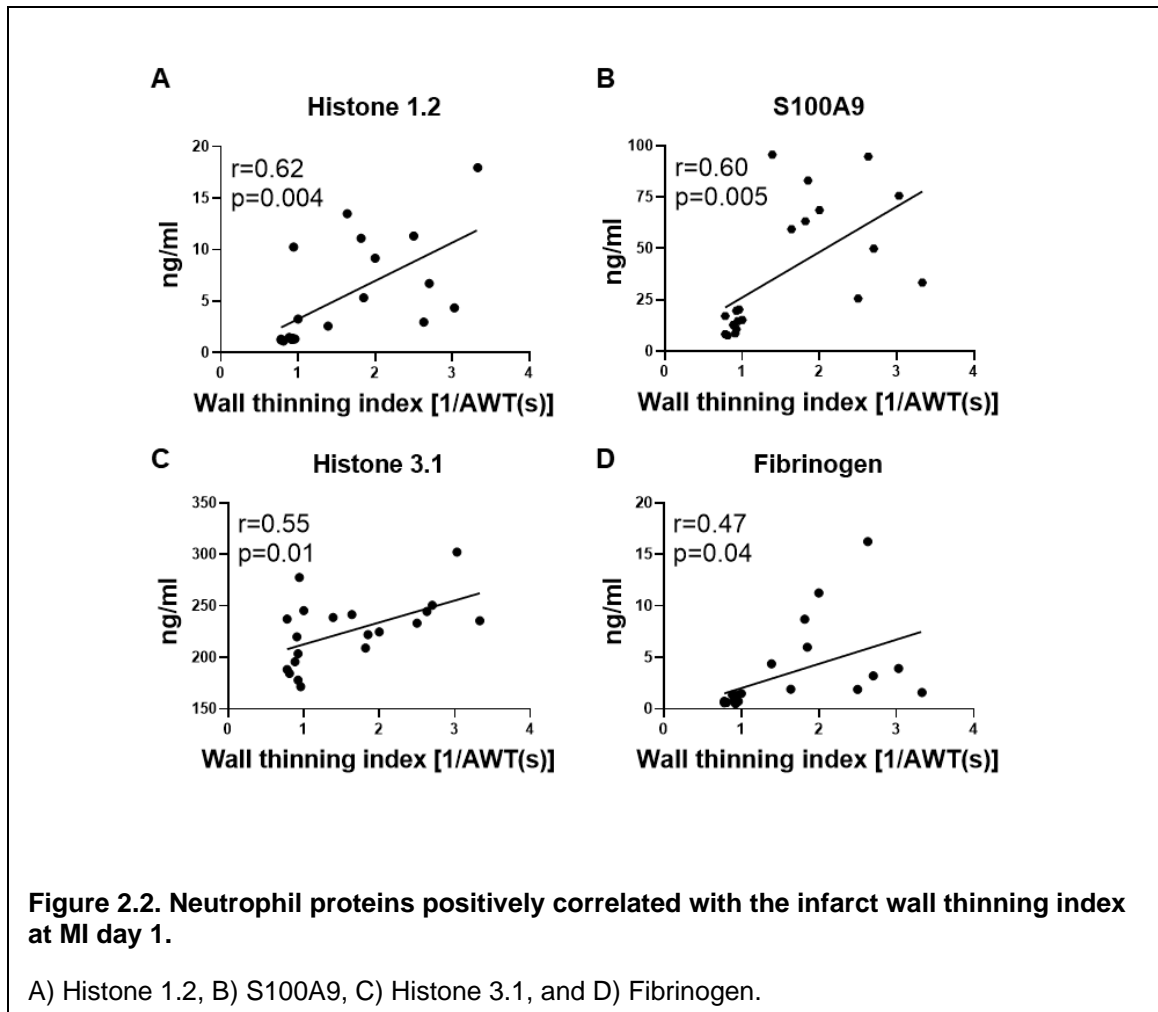
Statistics

Statistical analyses were performed with GraphPad Prism 9, according to the guidelines outlined in Statistical Considerations in Reporting Cardiovascular Research.(138) Data were reported as mean±SEM. Normality was evaluated using the Shapiro-Wilk test, and all data passed normality. For correlation analysis, association between two variables was determined by calculating the Pearson correlation coefficient. Survival curves were analyzed by Mantel-cox (log-rank) test. The Students t-test was used to compare two groups; unpaired t-test was used for the *in vivo* data and paired t-test was used for the *in vitro* data. A p value <0.05 was considered statistically significant.

3. Results

Neutrophil proteins positively correlated with the wall thinning index

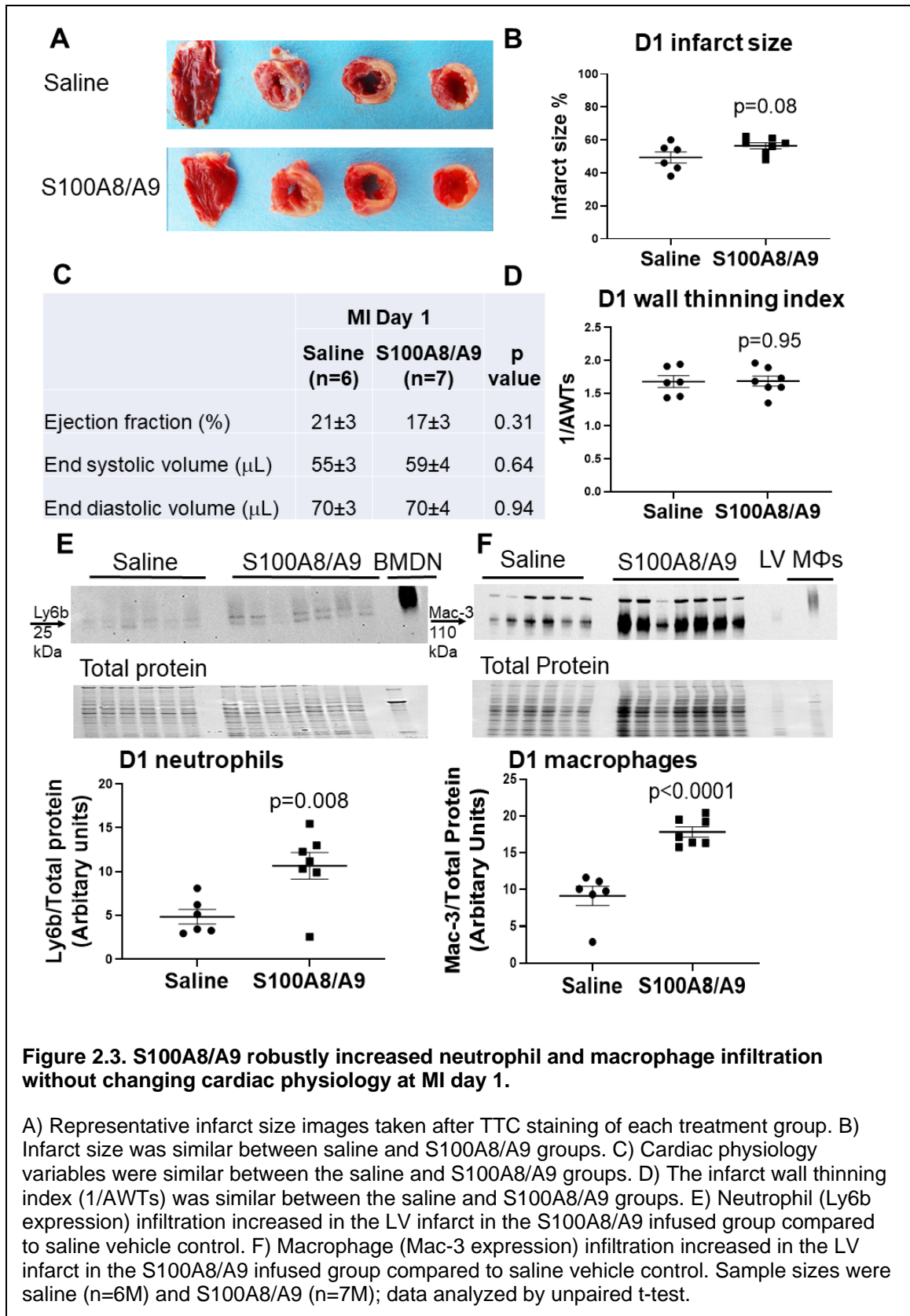
Out of 123 proteins examined, four proteins positively correlated with the wall thinning index (**Figure 2.2**). Ranked by r, these were histone 1.2, S100A9, histone 3.1, and fibrinogen. The histone proteins identified are intracellular components and likely reflect the change in metabolic status of the neutrophil.(139-141) Because S100A9 was the highest ranked secreted factor, we evaluated whether it was causally involved in infarct wall thinning and could serve as a functional effector biomarker.



S100A8/A9 administration increased neutrophil infiltration at MI D1

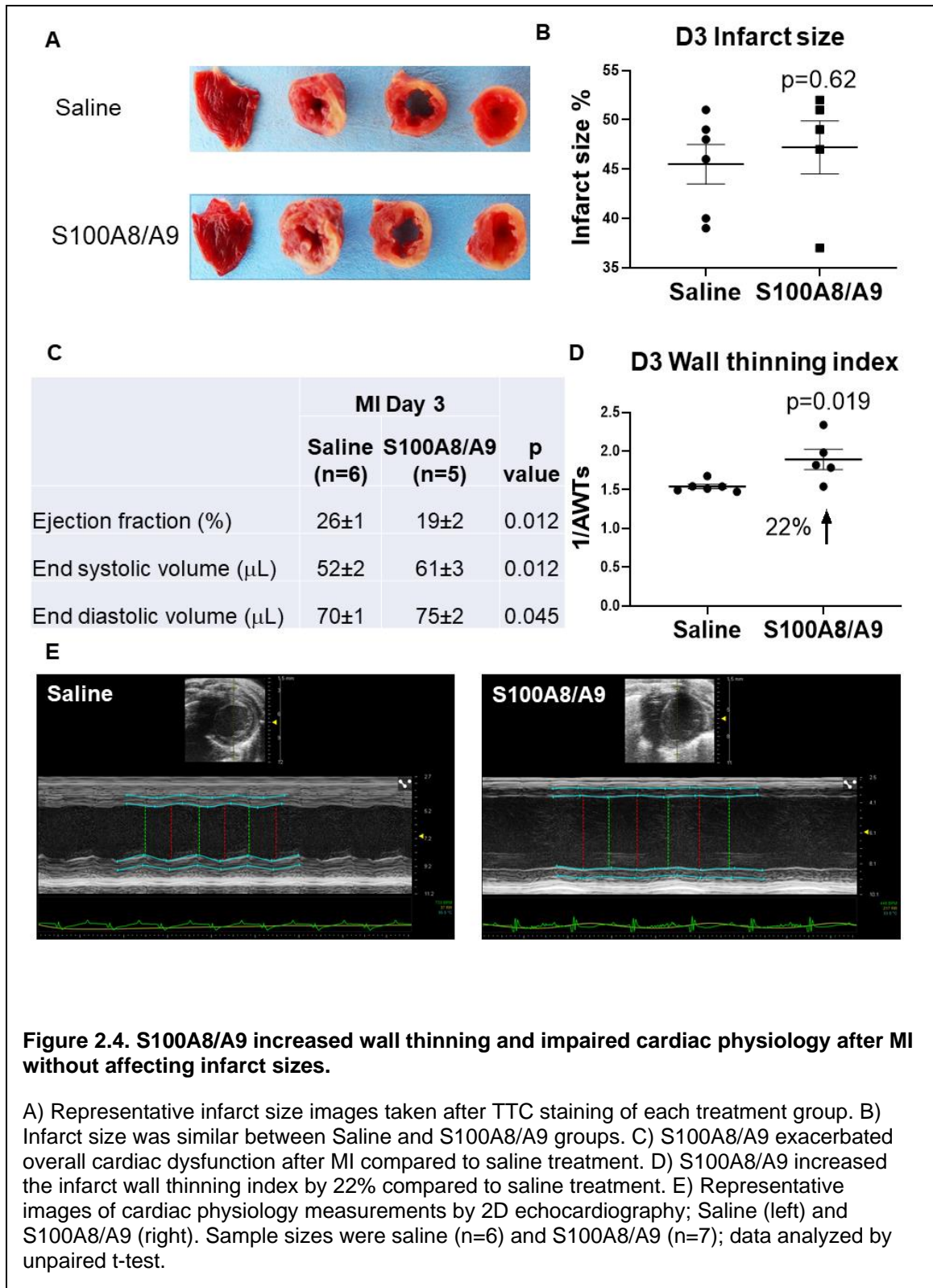
To test whether exogenous administration of S100A8/A9 stimulated infarct wall thinning, we infused S100A8/A9 beginning at the time of MI. At MI D1, neutrophil and macrophage infiltration were measured by immunoblotting and infarct wall thickness by echocardiography. Survival at MI D1 was identical between MI groups, with 100% of mice enrolled with successful MI surviving to D1. Infarct size was also similar in both groups at MI D1 (**Figure 2.3A and B**); the saline group had an infarct size of $49 \pm 3\%$ and the S100A8/A9 group $56 \pm 3\%$ ($p=0.082$). Cardiac physiology, including wall thinning, was also similar between saline and S100A8/A9 treated groups at MI D1 (**Figure 2.3C and D**). To test whether exogenous administration of S100A8/A9 increased neutrophil and

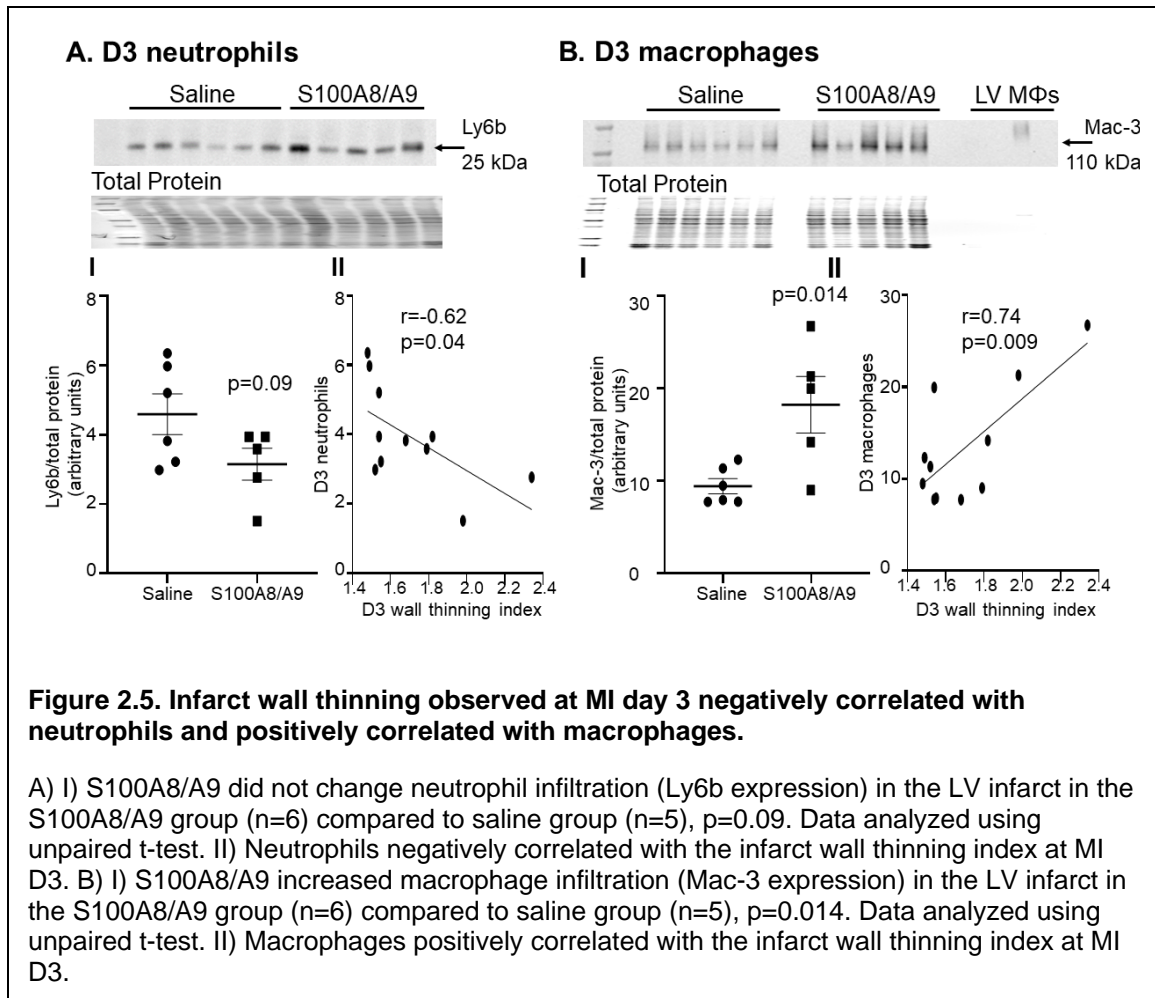
macrophages influx to the infarct, we measured ly6b and mac-3 in the LV infarct by immunoblotting. Neutrophil and macrophage infiltration were robustly increased by S100A8/A9 treatment compared to saline control (**Figure 2.3E and F**). As expected, there was little to no neutrophil infiltration in the LV remote region and S100A8/A9 had no effect (0.54 ± 0.14 normalized arbitrary units for saline and 0.62 ± 0.13 normalized arbitrary units for S100A8/A9, $p=0.66$). This indicated that that the primary effect of S100A8/A9 at MI D1 was to amplify pro-inflammatory neutrophil and macrophage entry to the infarct.



S100A9 administration increased infarct wall thinning at MI D3

To determine if the increased neutrophils at MI D1 would lead to increased infarct wall thinning later, we evaluated MI D3. Survival was not different between the saline group (6/6 survived, 100%) and the S100A8/A9 group (5/6 survived, 83%, $p=0.31$), and infarct sizes were similar (**Figure 2.4A and B**). Compared to saline control, S100A8/A9 administration worsened cardiac physiology, as indicated by decreased ejection fraction and increased end systolic and end diastolic volumes (**Figure 2.4C**). S100A8/A9 treatment resulted in a 22% increase in the wall thinning index (**Figure 2.4D**). By D3, neutrophil infiltration was not different between saline and S100A8/A9 groups (**Figure 2.5A (I)**). There continued to be a sustained two-fold increase in macrophages in the S100A8/A9 group compared to saline (**Figure 2.5B(I)**). Neutrophil count at MI D3 negatively correlated with infarct wall thinning index ($r=-0.62$, $p=0.04$; **Figure 2.5A(II)**), whereas macrophage count at MI D3 positively correlated with infarct wall thinning index ($r=0.74$, $p=0.009$; **Figure 2.5B (II)**). These results indicate that sustained S100A8/A9 treatment increased macrophages at MI D3 to exacerbate infarct wall thinning.

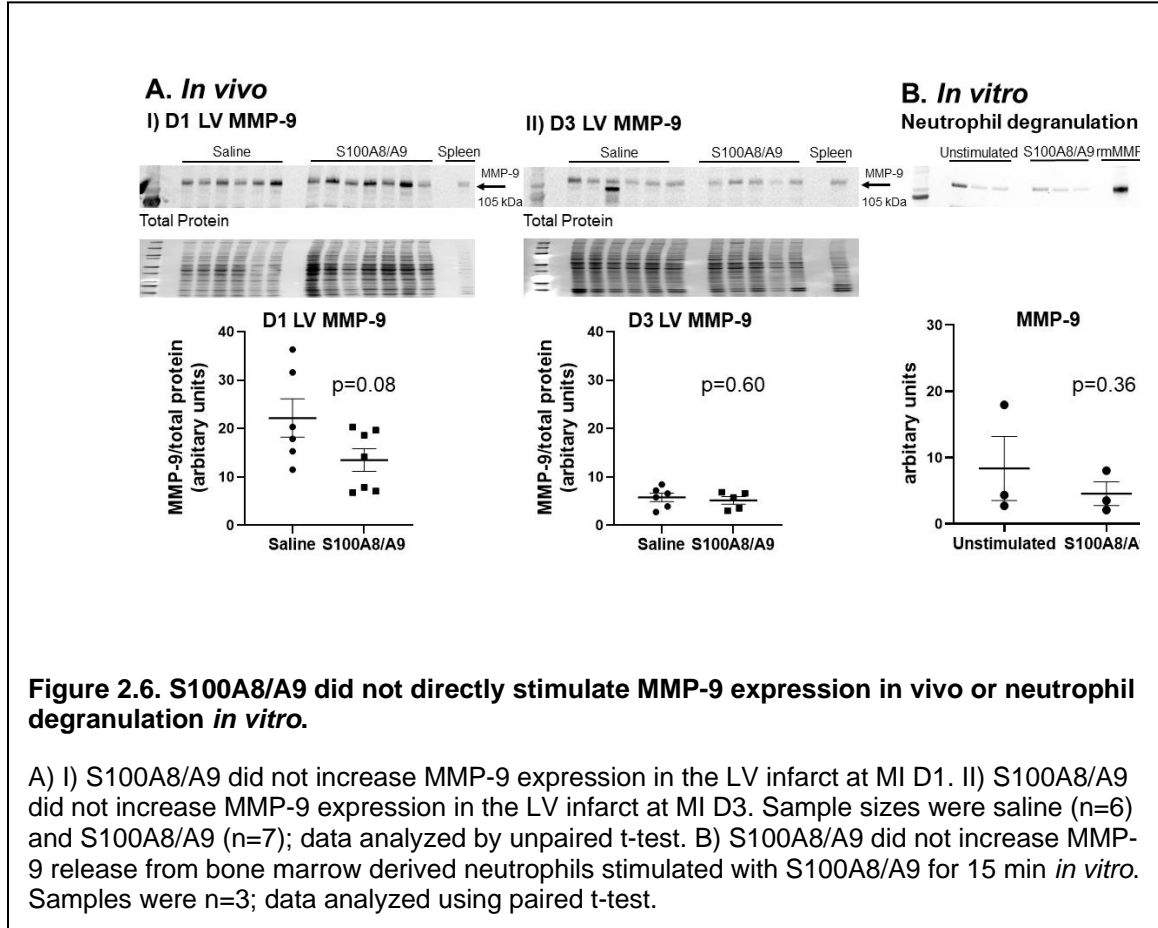




S100A8/A9 did not increase MMP-9 *in vivo* and did not directly stimulate neutrophil degranulation *in vitro*

To evaluate whether the correlation of S100A9 to infarct wall thinning was linked to MMP-9, as MMP-9 is associated with MI death and LV rupture, we evaluated MMP-9 protein expression in the LV infarct. There were no differences between groups at MI D1 or D3 (**Figure 2.6A(I) and (II)**). To determine if S100A8/A9 had a direct effect on neutrophil degranulation, we stimulated bone marrow derived neutrophils *in vitro* with S100A8/A9 and measured MMP-9 release into the secretome as an index of degranulation. As shown in **Figure 2.6B**, S100A9 did not directly induce release of MMP-9. This indicates that the exacerbated LV physiology – increased wall thinning and

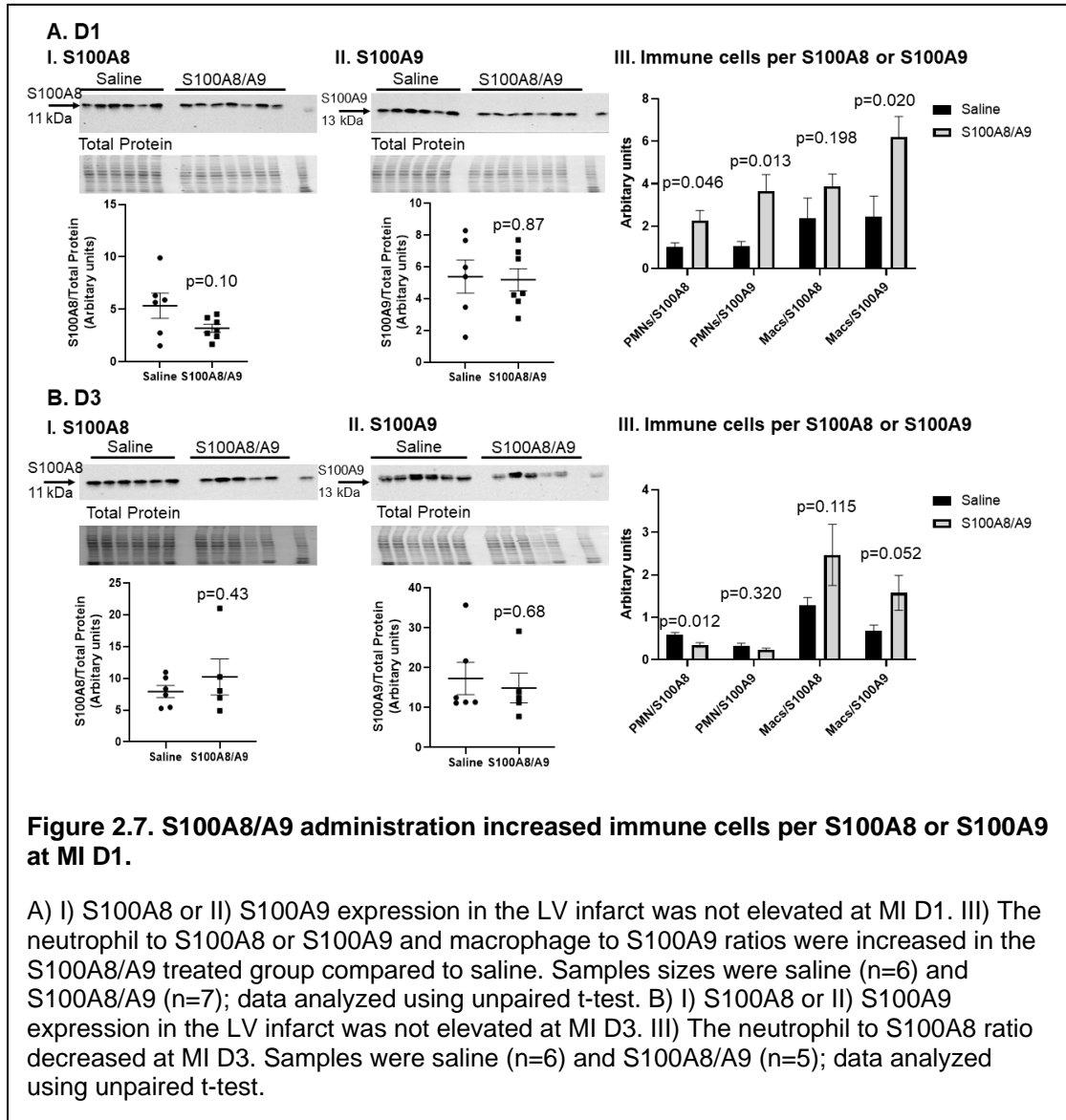
dilation – seen due to administration of S100A8/A9 was primarily due to stimulating the influx of pro-inflammatory leukocytes at MI D1 and D3, and through stimulating tissue degrading action of macrophages more than neutrophils.



S100A8/A9 activity increased with treatment

S100A8 or S100A9 was not elevated at MI D1 or D3 in the infarct region of the S100A8/A9 treated mice (**Figure 2.7A (I), (II) and B (I), (II)**). This is consistent with past reports that S100A8/A9 has an auto-inhibitory feedback mechanism that turns off its production.(142, 143) To measure activity, we calculated the ratio of neutrophils and macrophages (immune cells) per unit of S100A8 or S100A9 expression in the LV infarct (**Figure 2.7A (III) and B (III)**). The neutrophil to S100A8 or S100A9 ratio and the macrophage to S100A9 ratio were all higher at MI D1, while the neutrophil to S100A8

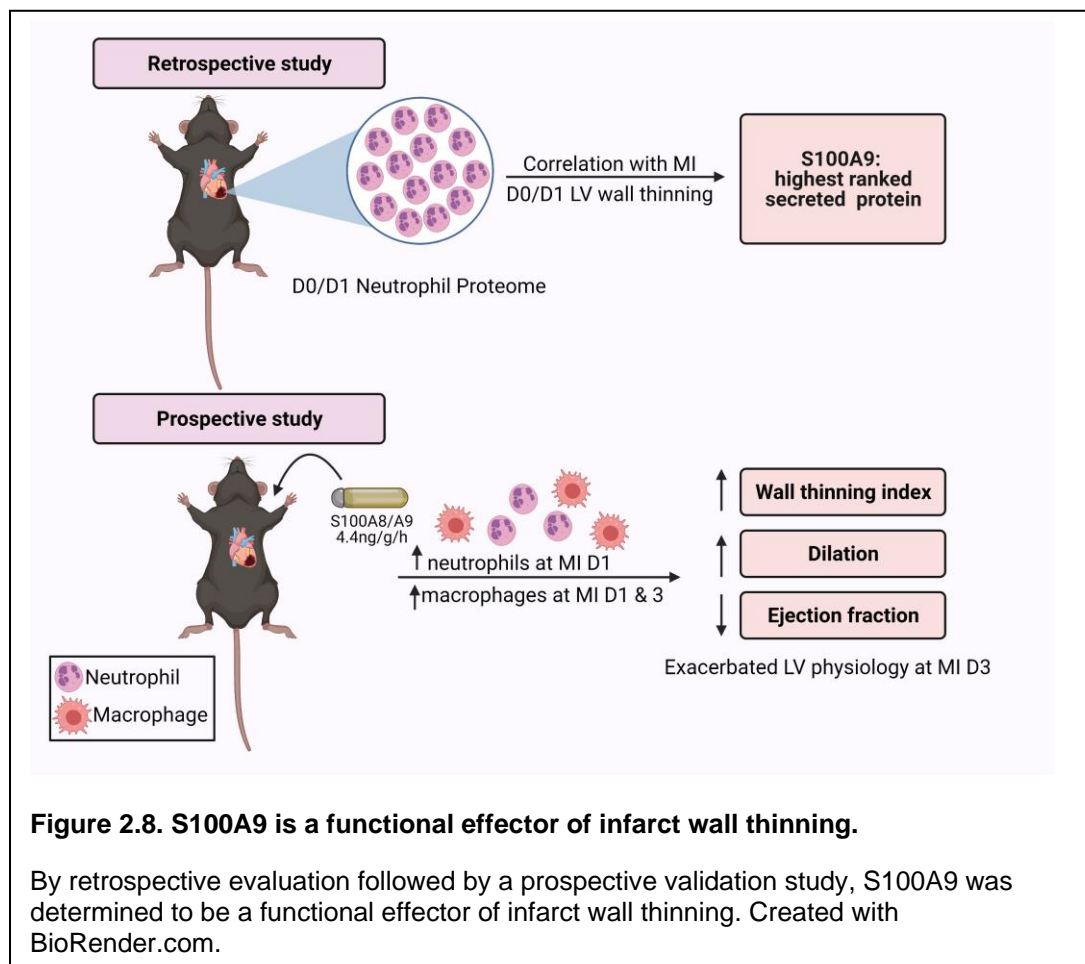
ratio was lower at MI D3. This indicates that S100A8/A9 activity was higher in treated group compared to control, and administration of S100A8/A9 elevates inflammatory cell infiltration early as its primary mechanism of action for exacerbating LV physiology later in MI.



4. Discussion

The goal of this study was to identify proteins derived from the neutrophil that best correlate with infarct wall thinning and serve as causal mediators. We selected to evaluate the relationship between wall thinning and the neutrophil proteome at MI D1

because both peak at this time point. There were four proteins identified that positively tracked with wall thinning: S100A9, Histone 1.2, Histone 3.1 and Fibrinogen. Of these, S100A9 was the highest ranked secreted factor. By *in vivo* exogenous S100A8/A9 administration, S100A8/A9 increased leukocyte influx at MI day 1 and 3 and infarct wall thinning at MI day 3. Our results indicate that S100A9 is a functional effector of infarct wall thinning (**Figure 2.8**).



Activated neutrophils secrete DAMPs to maintain inflammatory status by renewing leukocyte infiltration. S100A8/A9 is a pro-inflammatory alarmin abundantly expressed in neutrophils.(119, 144) S100A8/A9 acts through toll-like receptor 4 (TLR4) and receptor of advanced end glycation end-products (RAGE) to activate innate immune responses.(125, 142, 145) S100A8/A9 primes the nucleotide-binding oligomerization

domain (NOD)-like receptor family pyrin domain-containing protein 3 (NLRP3) inflammasome to produce interleukin (IL)-1 β , which leads to myeloid cell recruitment to the infarct.(142, 146) Genetic disruption of S100A8/A9 or its downstream signaling mediators improves cardiac physiology after MI.(142) A similar study by Marinkovic and colleagues showed that short term pharmacological inhibition of S100A8/A9 also improves cardiac function at MI D3, which is similar to our findings.(147)

A primary role of the neutrophil in the infarct is to secrete proteases to remove necrotic myocytes and damaged ECM, which prepares the infarct for scar deposition. While neutrophils are essential for cardiac wound healing, excessive neutrophils amplify inflammation and promote excessive tissue proteolysis. Neutrophils secrete proteases by degranulation, including MMP-9, which regulates early clearance of the necrotic debris. Our lab has shown that neutrophils polarize over the course of MI, with the neutrophil proteome showing a functional shift from pro-inflammatory to reparative phenotype over the first week in mice.(21, 38) This study validates that increased influx of pro-inflammatory neutrophils, macrophages, and associated proteins after MI D1 leads to sustained inflammation, which can debilitate the wound healing process. Targeting neutrophil polarization in cancer has shown positive results by decreasing tumor size and may be a potential avenue for MI therapy as well.(54) S100A9 could be a neutrophil specific therapeutic switch point.(148)

In the present study, S100A8/A9 increased neutrophil and macrophage infiltration in the infarct at MI D1, leading to sustained increase of macrophages and increased wall thinning at MI D3. The LV samples were snap frozen and collected for biochemical analysis; as such, we were not able to perform immunohistochemistry to show localization of leukocytes within the infarct region. The effect on infiltration is limited to the infarct region, as the remote region showed little or no influx of neutrophils either with saline or S100A8/A9 treatment, which is consistent with past reports.(149)

Our results highlight that the effect of S100A8/A9 is not a direct effect on neutrophil degranulation. Degranulation was defined as MMP-9 release, which is one surrogate marker. Other markers of degranulation include MMP-8, myeloperoxidase, and serine elastase.(125) Rather, the effect was indirect in stimulating a greater influx of pro-inflammatory leukocytes. In addition, S100A9 is a calcium binding protein and as such could also have a direct effect on the cardiomyocyte sarcomere.(150) This would be consistent with the decrease in ejection fraction observed at MI D3 in the treated group. Our *in vivo* and *in vitro* results combined indicate that S100A8/A9 does not itself specifically target wall thinning through neutrophil degranulation.

S100A8/A9 peaks within 6 h of MI and is autoregulated for its activity by the formation of oligotetramers, which competitively bind TLR-4 to block signaling and negatively feedback to reduce further production.(142, 143) S100A8/A9 acts as a major inducer for granulopoiesis and mobilization of granulocytes within the infarct.(142, 151) We observed that S100A8/A9 induced early changes in immune cell infiltration. S100A8/A9 potentiated inflammation by increasing pro-inflammatory leukocyte influx into the heart and exacerbated LV dysfunction after MI. S100A8/A9 stimulation of TLR4 activates nuclear factor kappa-B (NF- κ B) to induce translation of various pro-inflammatory cytokines (e.g., tumor necrosis factor alpha (TNF α), IL-1 β , IL-6, and IL-8).(57, 125, 129, 152) Serum S100A9 is a potential prognostic marker of major cardiovascular events in patients with acute MI and CXCR2+ neutrophils in the heart are the main producers of S100A9 early during reperfusion.(153, 154) There is strong evidence, therefore, that S100A9 is an effector marker.

The infarct wall thinning index directly correlated with increased neutrophils and macrophages at MI D1 and with only macrophages at MI D3. While neutrophil influx was elevated at MI D1, macrophage numbers remained elevated at D3. Similar to neutrophils, pro-inflammatory macrophages peak at MI D1.(21, 133) S100A9 induces a

pro-inflammatory macrophage phenotype in osteoarthritis.(155) Macrophages also express S100A9, which is lost during conversion from pro- to anti-inflammatory phenotype.(152) Exogenous administration of S100A9 stimulates the transition from inflammatory Ly6C^{hi} monocytes to reparatory Ly6C^{lo} macrophages through upregulation of the transcription factor Nur77.(147, 156)

Increased pro-inflammatory macrophage influx has been associated with LV rupture.(66) MI D3 macrophage numbers directly correlated with the infarct wall thinning index, which could be either a reflection or consequence of S100A8/A9 treatment, or both. MI D3 neutrophils show a negative correlation with infarct wall thinning, indicating that wall thinning seen with S100A8/A9 administration is due initially to action on the neutrophil and macrophage and later to the potentiation of macrophage activity. S100A9 could be influencing neutrophil to macrophage cross-talk, as it is known that neutrophils coordinate the influx of macrophages.(157, 158) Disrupted leukocytes kinetics after MI induced by S100A8/A9 could explain the physiological effects observed.(114, 159) One limitation of this study was the use of only male mice. Future studies exploring the role of S100A8/A9 on MI remodeling in female mice is warranted.

For this study, we focused on the highest ranked secreted protein, which was S100A9. For the S100A8/A9 (calprotectin) heterodimer complex, only S100A9 was measured in the protein array. The other proteins identified, histone 1.2, histone 3.1, and fibrinogen, were also strong indicators of wall thinning and should be evaluated in future studies. Histones are markers of NETosis and likely reflect intracellular re-organization of the neutrophil at MI D1.(145) Increased histones suggest formation of extracellular traps and sustenance of inflammation, which is also in line with our findings.(160) In a clinical study, Liu et al showed that neutrophils obtained from infarct related arteries released NETs and that dsDNA levels were significantly higher in coronary plasma samples and independently associated with in-hospital major adverse cardiac

events.(161) Inhibition of peptidyl arginine deiminase (PAD)-4, an enzyme responsible for citrullination of arginine in histones, by PAD4 specific chemical inhibitor GSK484 protected against left ventricular dysfunction after MI.(162) Further, excessive NETs is associated with Reactive oxygen species(ROS)–dependent aggravation of myocardial injury in MI in Apolipoprotein E deficient mice.(163) Nagareddy et al linked the potential of NETosis to S100A8/A9 release from neutrophils in a recent article, demonstrating a requirement of NETosis in S100A8/A9-induced granulopoiesis.(145)

Fibrinogen is a novel neutrophil marker of degranulation previously identified by our team which remains upregulated in neutrophil proteome throughout D7.(38) Increased production of fibrinogen at D1 of MI by neutrophils indicates a significant role of neutrophils in MI wound healing with key inputs in ECM reorganization. Early secretion of ECM proteins like fibrinogen from neutrophils could aid in formation of a provisional matrix scaffold for infiltrating neutrophils and monocytes in the infarct, hence sustaining inflammation.(164) Fibrinogen is also known to activate fibroblasts and increased fibrinogen early in MI can potentially be linked to fibrosis.(165) Fibrinogen has previously been suggested by many as a marker for stroke and MI.(166-169) However, this is the first time that fibrinogen has been linked with LV wall thinning and neutrophils, and is worth pursuing in future evaluations.

5. Conclusion

In summary, S100A9 is an early functional effector of LV infarct wall thinning in the mouse MI model of permanent occlusion. The mechanism of action of S100A9 is directed more at stimulating influx of neutrophils and macrophages rather than direct activation of neutrophil degranulation. Neutrophil proteins are not only potential early biomarkers, but also functional effectors for worsened LV physiology after MI and could be therapeutically targeted to promote infarct healing.

CHAPTER 3. Macrophages secrete murinoglobulin-1 and galectin-3 to regulate neutrophil degranulation after myocardial infarction

1. Introduction

In response to myocardial infarction (MI), the cardiac wound healing response involves an early phase of robust inflammation, which is an essential prerequisite event for later transition to resolution and repair that culminates in infarct scar formation.(52, 91, 119, 170) Leukocyte infiltration is a key hallmark of the early inflammatory phase, with neutrophils and macrophages serving as the predominate cell contributions.(32, 95, 171, 172) During the inflammatory phase, the neutrophils and macrophages instigate tissue repair by stimulating pro-inflammatory cytokines and proteases that remove necrotic cardiomyocytes.(14) Proteases such as matrix metalloproteinase (MMP)-9 induce tissue degradation and extracellular matrix fragmentation.(128)

Neutrophils that are activated to pro-inflammatory polarization release preformed granules by a process termed degranulation.(128, 173) Neutrophil granules contain MMP-8, MMP-9, myeloperoxidase (MPO), neutrophil granule associated lipocalin (NGAL), and neutrophil elastase (NE), all of which support infarct debris removal.(173) While neutrophil degranulation is essential to create an optimum environment for later scar formation, excessive degranulation can lead to excessive infarct wall thinning and dilation of the left ventricle (LV).(174, 175) Neutrophil numbers, MMP-9, and MPO have all been positively associated with increased risk of heart failure progression after MI and mortality.(124, 176-179)

Various attempts have been made to globally target neutrophils or neutrophil activity after MI, and each of these studies showed detrimental effects on cardiac remodeling, indicating the importance of neutrophils in MI wound repair.(180-182) Neutrophil depleted mice given MI showed impaired clearance of apoptotic

cardiomyocytes and reduced phagocytic macrophage subtype, though anti-inflammatory macrophage phenotype increased early in the heart.(180) Neutrophil degranulation is a crucial step for the initiation of macrophage transdifferentiation to reparative phenotype. Neutrophil gelatinase-associated lipocalin (NGAL), is secreted from the neutrophil as a required switch for reparative macrophage polarization and negative feedback induction of phagocytosis to remove neutrophils.(180) Neutrophil to macrophage cross talk, therefore, is relevant for MI remodeling.

Macrophages are the crucial cell types in the wound healing.(66, 75, 183) Monocytes infiltrate the infarct along with neutrophils, differentiates into macrophages in the infarct regions and initially serve as a pro-inflammatory cell.(32, 184) At MI day (D)1, macrophages are the second most abundant cell type in the infarct, transiting to the most abundant cell by MI D3-5.(95) By MI D3, macrophages are transitioning to anti-inflammatory polarization, with efferocytosis of apoptotic neutrophils being a key feature.(52, 95) Neutrophil to macrophage cellular communication has been well studied by several groups,(185, 186) and the converse – macrophage to neutrophil cellular communication – is understudied. Because anti-inflammatory and reparative macrophages regulate other cell types (e.g., endothelial cells and cardiac fibroblasts), the pro-inflammatory macrophage may regulates neutrophil physiology as well.(187)

The goal of this study, accordingly, was to explore the hypothesis that macrophages communicate to neutrophils at MI D1 to regulate degranulation during the pro-inflammatory phase. We catalogued the macrophage secretome and coupled results with a previously acquired transcriptomics dataset to identify major MI D1 secreted proteins secreted that regulated neutrophil degranulation.

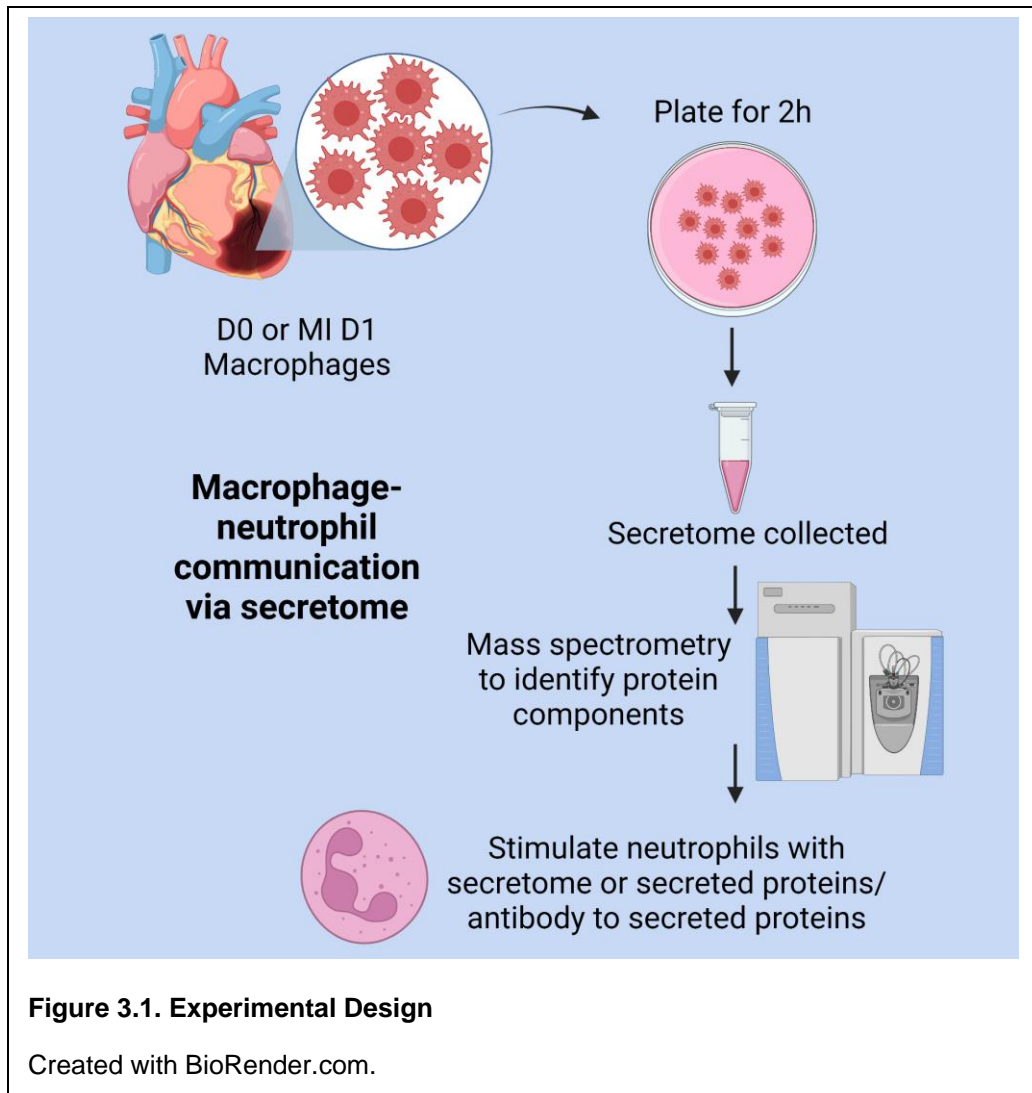
2. Methods

Animal Use

All animal procedures were performed according to the Guide for the Care and Use of Laboratory Animals, and all protocols were pre-approved by the Institutional Animal Care and Use Committee at the University of Mississippi Medical Center or the University of Nebraska Medical Center.(188) C57BL/6J wild-type mice of both sexes (3–6 months old) were either purchased from Jackson Laboratory or in house bred and housed in the animal facility. All mice were maintained together in the same room, under a 12:12 h light-dark cycle and given ad libitum access to standard mouse chow and water.

Mapping the MI D1 macrophage secretome

The experimental design is detailed in **Figure 3.1**. We evaluated the MI D1 macrophage secretome from male mice (C57BL/6J, ages 3-6 months) subjected to coronary artery ligation surgery as described previously.(95, 113) Macrophages from no MI D0 were used as the control, and sample sizes were n=4 pooled sets per group. Transcriptomics was performed in the cell pellets from the same paired cell sets, and this dataset has previously been evaluated and published.(95) Macrophage secretomes were evaluated by mass spectrometry using the Q Exactive (ThermoFisher, Waltham, MA) as previously described.(26) The mass spectrometry proteomics data have been deposited to the ProteomeXchange Consortium via the PRIDE partner repository with the dataset identifier PXD011780.(189) Volcano plotting was used to rank individual proteins.



Bone marrow derived neutrophil isolation and stimulation

Bone marrow derived neutrophils were isolated from male and female mice using the autoMACS Pro Separator (Miltenyi Biotec) with anti-Ly6G microbeads (Miltenyi Biotec; #130-120-337) as previously described.(118) To isolate bone marrow derived cells, bone marrow was flushed from femur and tibia using a 26-gauge needle and 10 mL syringe filled with RPMI 1640 media supplemented with 1% penicillin/streptomycin (Thermo, #15140-122) and 2 mM EDTA. Single cell suspension was obtained by passing over 30 µm pre-separation filters (Miltenyi Biotec, #130-041-407). Red blood cell lysis buffer (Miltenyi Biotec, #130-094-183) was added to the suspension to lyse

erythrocytes. The single cell suspension was centrifuged at 400 x g for 10 min, and the cell pellet was resuspended in PEB buffer (PBS containing 2 mM EDTA and 0.5% BSA). Neutrophils were labeled using magnetic anti-Ly-6G MicroBeads, ultrapure by incubation for 10 min at 4°C (Miltenyi Biotec, #130-120-337) and sorted using a AutoMACS Pro Separator. Cells were counted using a hemocytometer and plated at 1 x 10⁶ cells/mL. Neutrophils were stimulated for 15 min at 37°C in RPMI 1640 media (Gibco) with 1% antibiotics (Thermo).(36, 171)

For the first set of experiments, the groups were: a) unstimulated, b) phorbol myristate acetate (PMA, 2 nM), c) PMA + MI D1 macrophage secretome (10%), d) PMA + MI D1 macrophage secretome + murinoglobulin-1 blocking antibody (200 ng/mL). For the second set of experiments, the groups were: a) unstimulated, b) IL-1 β (200 ng/ml) as an MI relevant positive control stimulus, c) MUG1 (500 ng/ml), d) IL-1 β + MUG1. For the third set of experiments, the groups were: a) unstimulated, b) IL-1 β (200 ng/ml) c) Lgals3 (500 ng/ml), and d) IL-1 β + Lgals3. MUG1 and Lgals3 stimulation was done using separate sets of mice. For the fourth set, the groups were: 1) unstimulated, 2) Lgals3, and 3) Lgals3 + MUG1. Following stimulation, the cells were centrifuged at 800 g for 8 min to separate secretome (supernatant) and cell pellets, which were separately snap frozen at -80C and stored until use.

Cytokine Array

Proteome Profiler Mouse XL Cytokine Array Kit (ARY028; RnD Systems) containing 111 mouse proteins was used to analyze the secretome from stimulation set 1 according to manufacturer instructions.(190) Images were captured using the iBright FL1000 imaging system (Thermo Fisher) and chemiluminescence intensity was quantified using HImage++ (Western vision) software. Duplicate technical replicates were averaged for each sample and reported as relative intensity.

Immunoblotting

Immunoblotting was performed according to the published guidelines.(137) For immunoblotting of the neutrophil secretome, samples were volume loaded (10 μ L) onto 4–12% Criterion XT Bis-Tris precast gel (Bio-Rad) and transferred to nitrocellulose membranes using the Trans-Blot Turbo Transfer Pack (Bio-Rad). MMP-9 antibody (EMD Millipore, #Ab19016 dilution:1:1000) was used as the primary antibody, and goat anti-rabbit IgG (Vector Laboratories, #PI1000 dilution:1:1000) was used as secondary antibody. The data were plotted as relative chemiluminescence intensity.

For immunoblotting of LV infarct for the MI time-course of MUG1 and Lgals3, total protein (10 μ g) was run on 4–12% Criterion XT Bis-Tris precast gels (Bio-Rad) and transferred to nitrocellulose membranes using the Trans-Blot Turbo Transfer Pack (Bio-Rad). Membranes were stained with Peirce Reversible Protein Stain Kit (Thermo Fisher) and images were taken for total membrane protein estimation. Rabbit anti-MUG1 (MyBiosource, #MBS1496515, dilution:1:1000) and rat anti-mouse Lgals3 (Invitrogen, #MAI-940, dilution:1:1000) were used as primary antibodies. The corresponding secondary antibodies used were goat anti-rabbit IgG (Vector Laboratories, #PI1000 dilution:1:1000) and horse anti-mouse (Vector Laboratories, #PI2000; dilution:1:1000). Liver was used a positive control for MUG1, and lung was used as a positive control for Lgals3. Chemiluminescent images were captured using the iBright FL1000 imaging system (Thermo Fisher) and quantified using iBright analysis software 4.0.0. The blots were normalized to the total membrane protein, and the data plotted as normalized relative intensity.

Statistics and bioinformatics analysis

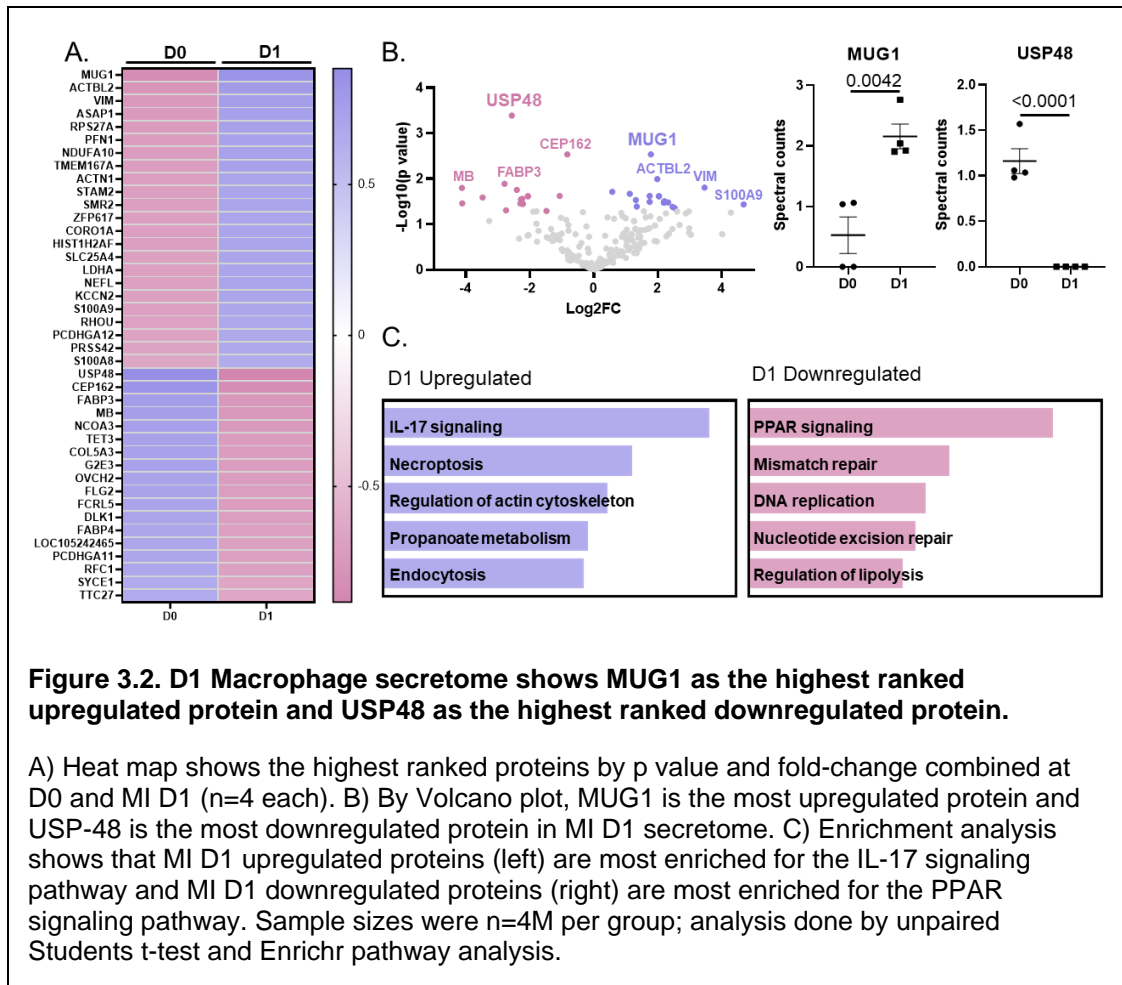
Statistical analyses were performed using GraphPad Prism 9 according to the guidelines outlined in Statistical Considerations in Reporting Cardiovascular Research.(138) Data are reported as mean \pm SEM for group comparisons. One-way ANOVA was used to compare more than 2 groups with a Newman-Keuls post-hoc test

for multiple comparisons. A paired Students t-test was used to compare two groups from the paired stimulus experiments. Data was autoscaled and run in Metaboanalyst 5.0 (<https://www.metaboanalyst.ca/>) for data visualization by volcano plot.(191) Enrichment analysis was done using Enrichr, a bioinformatics tool developed by Ma'ayan Laboratory.(192) GO and KEGG pathways were used for enriched processes and pathways. A p value <0.05 was considered statistically significant. We coupled our proteomics data with bioinformatics analysis for a comprehensive multi-omics evaluation of data.(193, 194)

3. Results

MUG1 was the major upregulated protein in the MI D1 macrophage secretome.

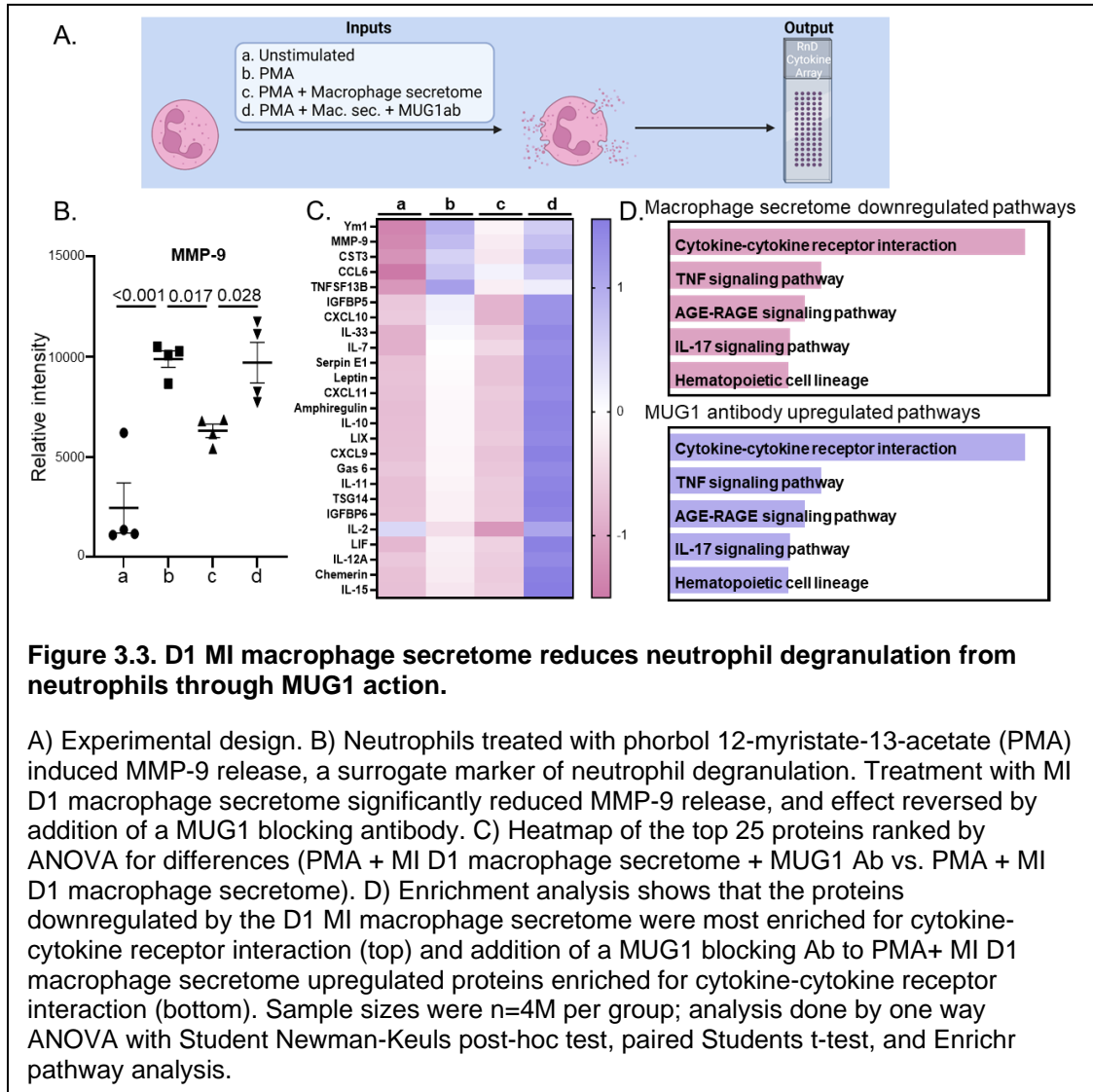
By mass spectrometry, 246 proteins were detected in either no MI D0 or MI D1 macrophage secretomes. Out of 246 proteins, 39 proteins were statistically different (all $p < 0.05$); 22 of which were upregulated and 17 were downregulated (**Figure 3.2A**). By volcano plot, MUG1 was the highest ranked upregulated protein, followed by β -actin like protein 2 (ACTBL2), vimentin (VIM), arf-GAP with SH3 domain, and ANK repeat and PH domain-containing protein 2 (ASAP1). Ubiquitin carboxyl-terminal hydrolase 48 (USP48) was the highest ranked downregulated protein, followed by centrosomal protein of 162 kDa (CEP162), fatty acid-binding protein heart (FABP3), myoglobin (MB), and nuclear receptor coactivator 3 (NCOA3; **Figure 3.2B**). For the upregulated proteins, IL-17 signaling was the most enriched pathway, while for the downregulated proteins, PPAR signaling was the most enriched pathway (**Figure 3.2C**).



MI D1 macrophage secretome signaled through MUG1 to blunt neutrophil degranulation.

The experimental design is detailed in **Figure 3.3A**. Bone marrow derived neutrophils treated with PMA, a positive control for neutrophil degranulation, showed robust release of MMP-9 into the secretome (**Figure 3.3B**). Degranulation of MMP-9 was attenuated by the addition of D1 MI macrophage secretome, an effect reversed by addition of a MUG1 blocking antibody. Out of 111 cytokines examined, 62 proteins were different by ANOVA, and the top 25 differentially expressed proteins are shown in **Figure 3.3C**. For the proteins induced by PMA that were attenuated by the MI D1 macrophage secretome, cytokine-cytokine receptor interaction was the major enriched pathway (**Figure 3.3D top**). The ability of the MI D1 macrophage secretome to reduce

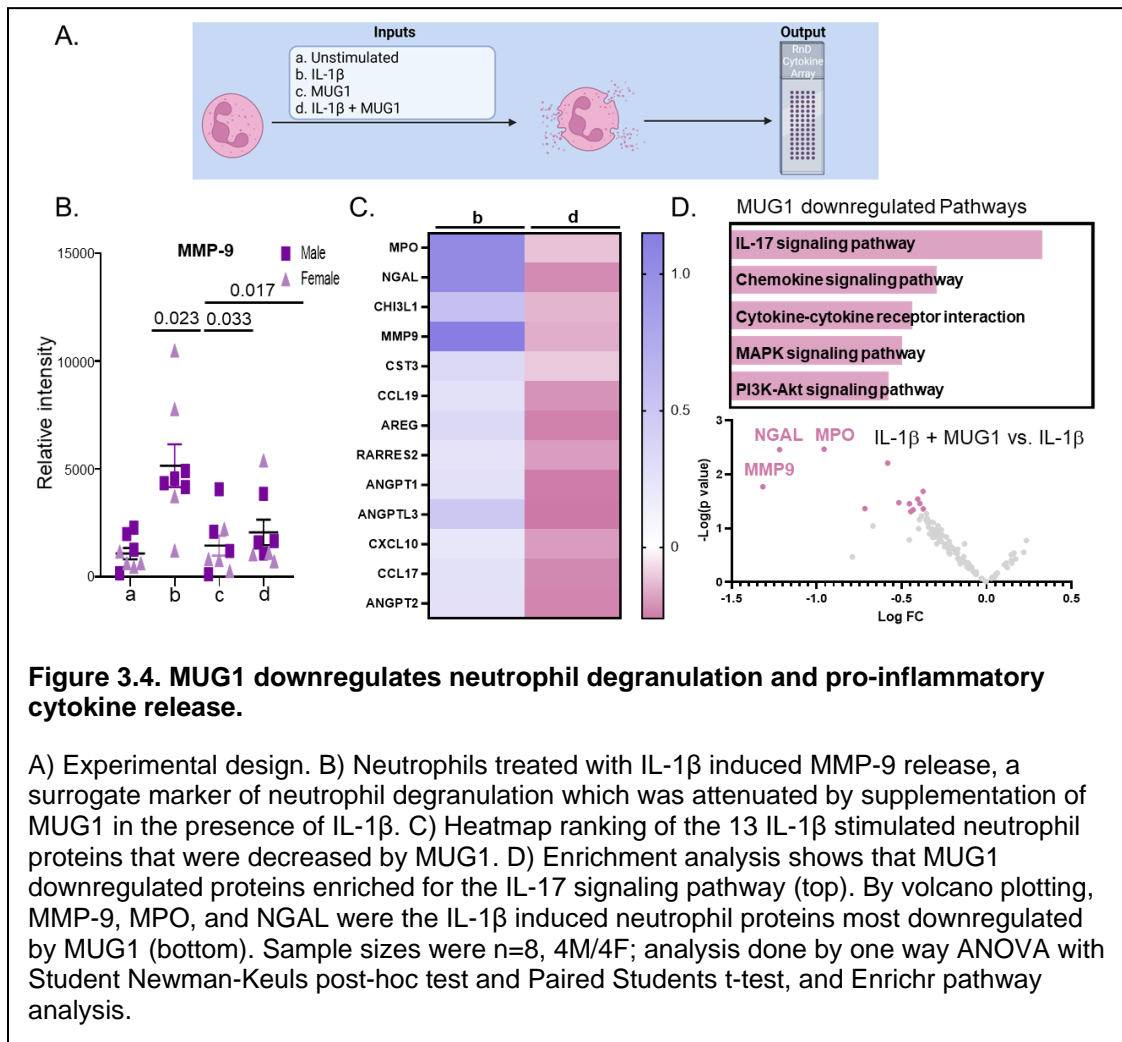
proteins induced by PMA stimulation was reversed by addition of a blocking MUG1 antibody, and cytokine-cytokine receptor interaction was the major pathway enriched pathway affected (**Figure 3.3D bottom**). The MI D1 macrophage secretome, therefore, acted in part through MUG1 to blunt neutrophil degranulation.



MUG1 directly inhibited IL-1 β stimulated neutrophil degranulation.

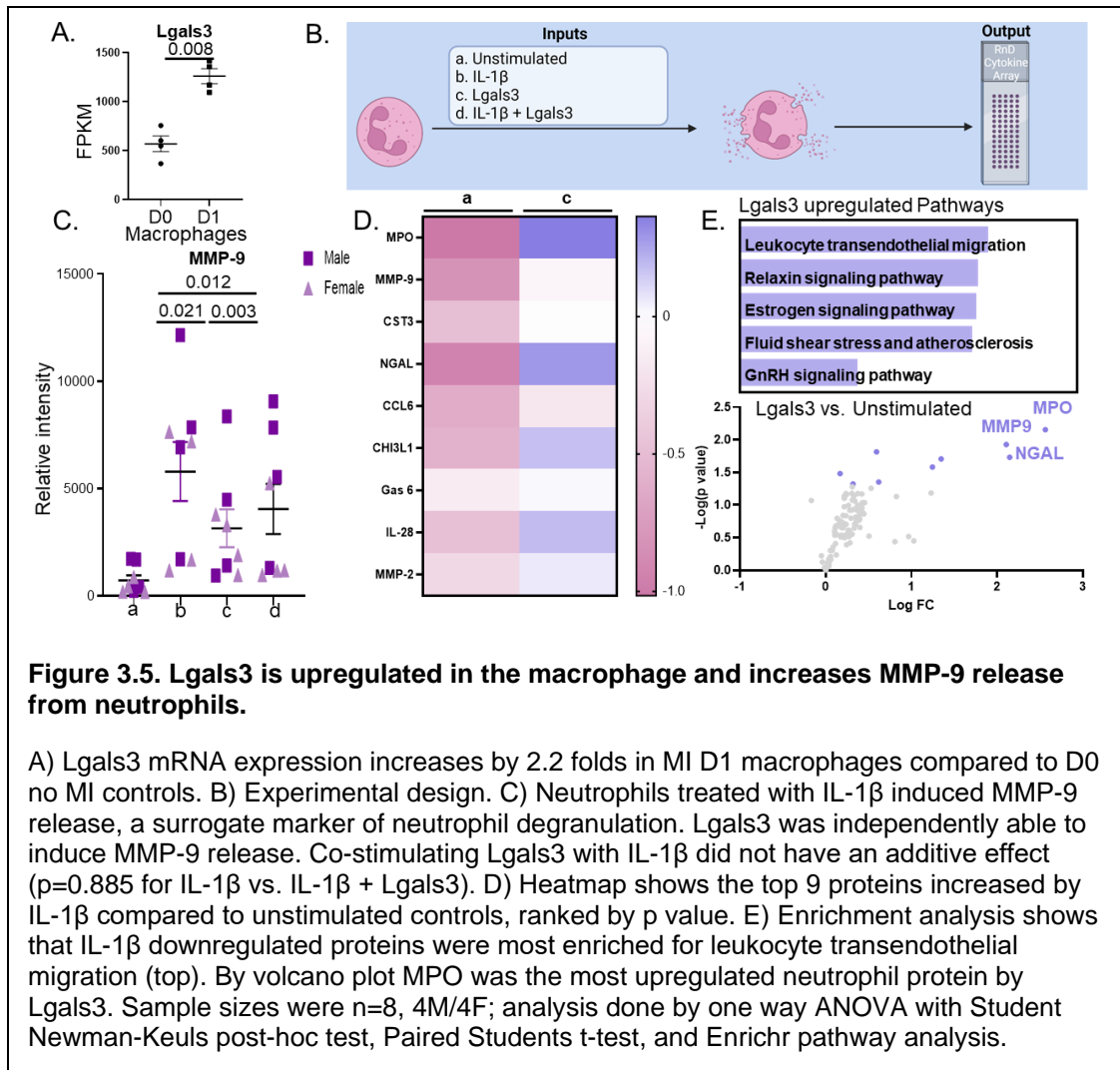
The experimental design is detailed in **Figure 3.4A**. IL-1 β upregulated 92 proteins out of 111 (all $p < 0.05$ for IL-1 β vs. unstimulated). The top 4 were NGAL (3.9-fold, $p < 0.0001$), MMP-9 (5.7-fold, $p < 0.0001$), CCL6 (2.2-fold, $p = 0.0006$) and CHI3L1

(2.0-fold, $p=0.001$). MUG1 attenuated IL-1 β stimulated neutrophil degranulation measured by the release of MMP-9 by 60% (**Figure 3.4B**). Of the 92 proteins induced by IL-1 β , MUG1 reduced expression for 13 of the proteins (**Figure 3.4C**). Of these, MMP-9, MPO, and NGAL had the greatest reduction (**Figure 3.4D top**). MUG1 by itself did not induce changes in the neutrophil secretome (all 111 proteins were p =not significant), indicating that MUG1 blunted degranulation only in the presence of a pro-inflammatory stimulus. Enrichment analysis of the 13 proteins downregulated by MUG1 treatment showed that IL-17 signaling and chemokine and cytokine mediated signaling were the two most enriched pathways (**Figure 3. 4D bottom**).



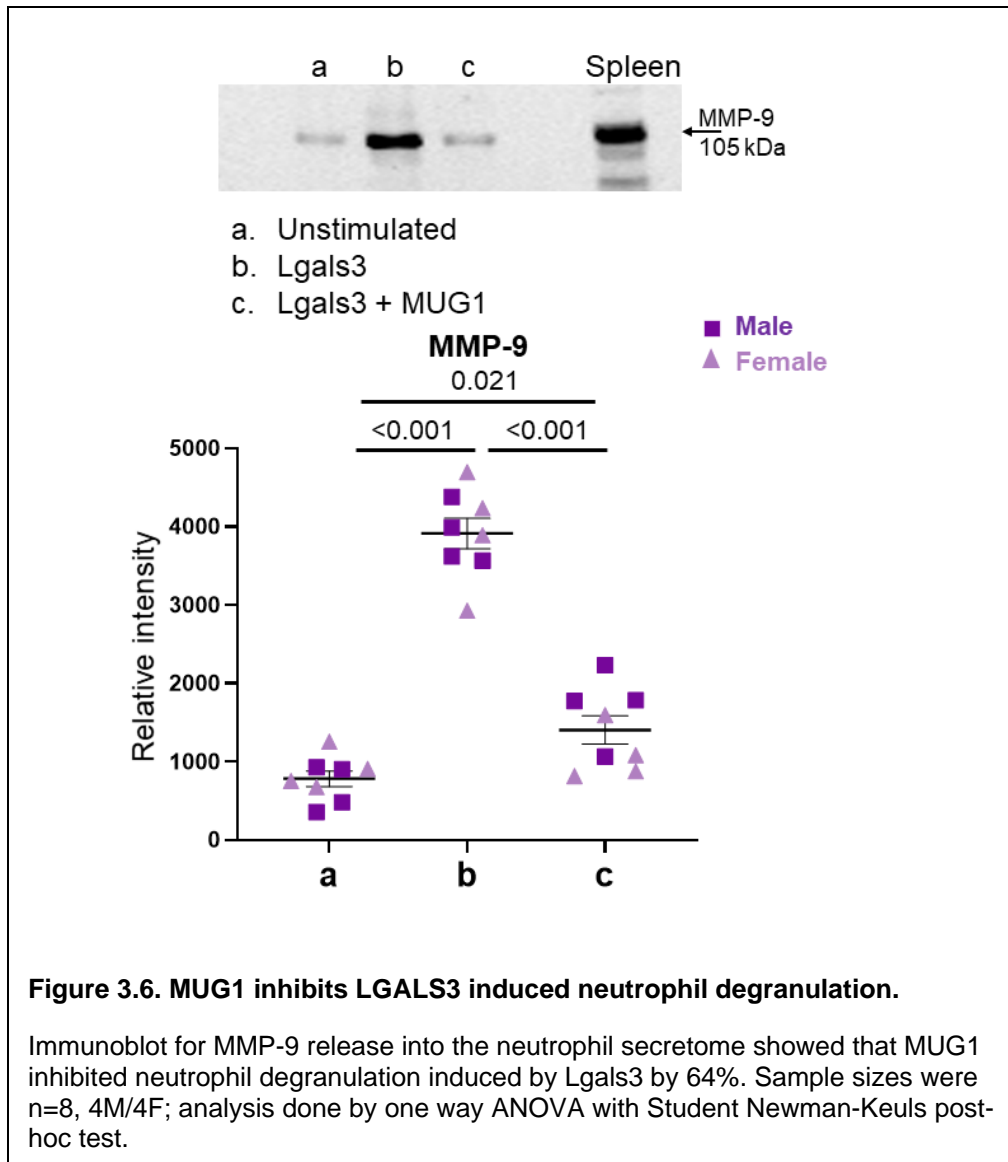
Lgals3 was expressed by MI D1 macrophages and promotes neutrophil degranulation.

Lgals3 is a pro-inflammatory protein highly expressed by MI D1 macrophages (**Figure 3.5A**).⁽⁹⁵⁾ Lgals3 interacts with soluble fibrinogen, a neutrophil protein increased in MI D1 that correlates with infarct wall thinning, we hypothesized Lgals3 could be another macrophage secreted protein that affected neutrophil physiology.^(195, 196) The experimental design is detailed in **Figure 3.5B**. IL-1 β alone robustly increased neutrophil degranulation. Lgals3 alone also showed strong pro-degranulatory activity (**Figure 3.5C**). Lgals3 stimulation did not amplify the IL-1 β effect, indicating that Lgals3 and IL-1 β may use the same signaling pathways. Compared to unstimulated, Lgals3 directly increased expression of 9 proteins (**Figure 3.5D**); top of which were MPO, MMP-9, CST3, NGAL and CCL6. All 9 proteins were also upregulated by IL-1 β , indicating similar pathways were induced by the two stimuli. Enrichment analysis of the proteins upregulated by Lgals3 revealed leukocyte transendothelial migration as the most upregulated pathway (**Figure 3.5E top**), indicating the Lgals3 may also serve a role in stimulating neutrophil influx to the infarct. Volcano plot visualization showed that the highest ranked proteins was MPO, followed by MMP-9 and NGAL, all of which are the components of neutrophil degranulation (**Figure 3.5E bottom**) This experiment demonstrated that Lgals3 directly stimulates neutrophil degranulation.



MUG1 prevented Lgals3 induced degranulation.

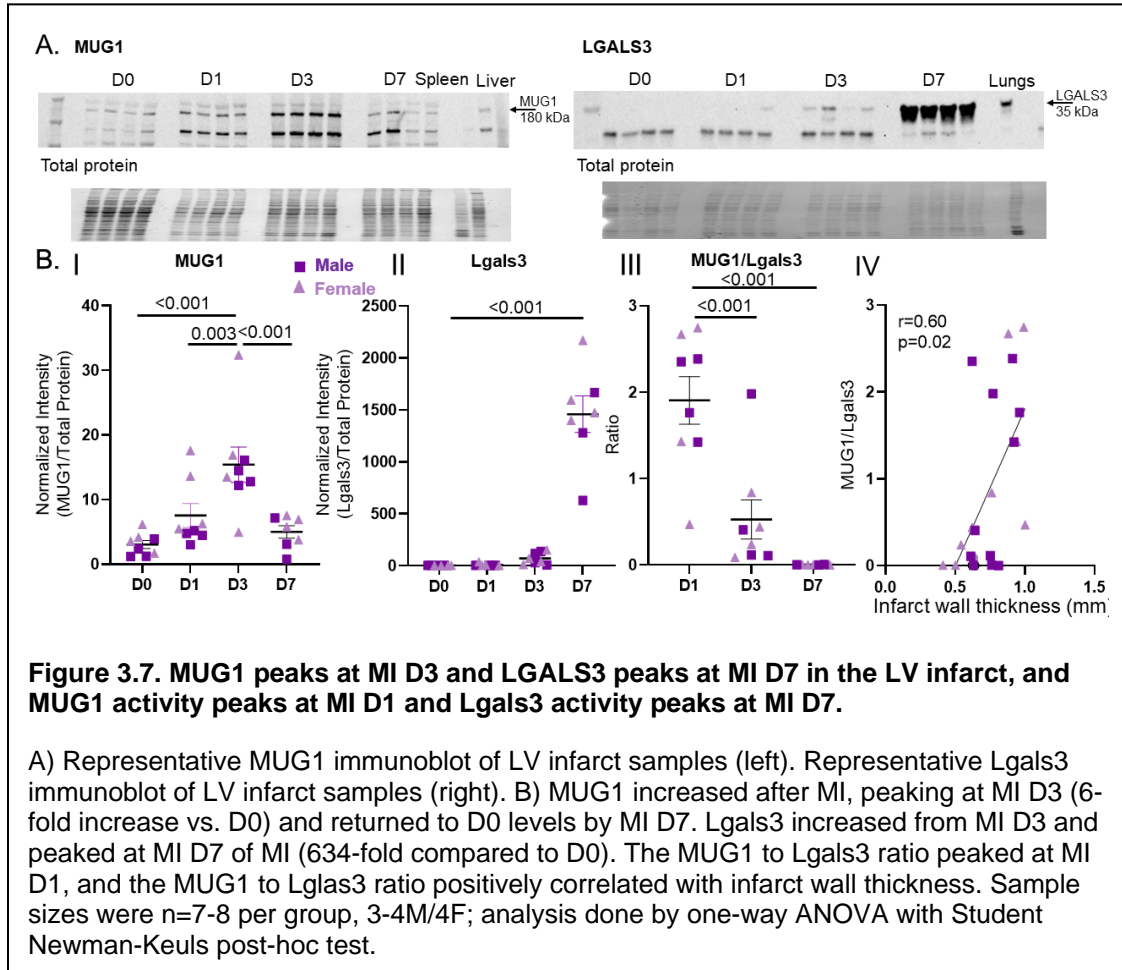
Lgals3 binds $\alpha 2$ -macroglobulin, a homologue of MUG1; therefore, MUG1 may bind Lgals3 to inhibit its action on neutrophil degranulation.(197) Indeed, neutrophils stimulated with a combination of MUG1 and Lgals3 showed a 64% reduction in Lgals3-induced release of MMP-9 (**Figure 3.6**). MUG1 and Lgals3 therefore, could be endogenous mechanisms employed by macrophages to regulate neutrophil degranulation.



The MUG1 to Lgals3 ratio peaked at MI D1 and positively correlated with infarct wall thickness.

To evaluate MUG1 and Lgals3 expression in the LV infarct, we measured the expression time course by immunoblotting (**Figure 3.7A**). MUG1 protein expression peaked at MI D3 (6-fold increased vs. D0) and returned to D0 values by MI D7 (**Figure 3.7B (I) & (II)**). Lgals3 protein expression peaked at MI D7 (634-fold increase vs. D0). The MUG1 to Lgals3 ratio peaked at MI D1 (**Figure 3.7B (III)**), and infarct wall thickness at all MI times correlated positively with the MUG1 to Lgals3 ratio ($r=0.60$, $p=0.02$)

(Figure 3.7B (IV)). This indicates that macrophage MUG1 expression is an endogenous protective mechanism to limit neutrophil degranulation and excessive infarct wall thinning early in MI.



4. Discussion

The goal of this study was to determine how the MI D1 macrophage secretome regulates neutrophil degranulation. The striking findings from this study were: 1) Mug1 was the highest ranked protein secreted by the MI D1 macrophage; 2) The MI D1 macrophage secretome attenuated neutrophil degranulation induced by PMA, an effect reversed by addition of a Mug1 blocking antibody; 3) Mug1 attenuated IL-1 β induced degranulation, while Lgals3 also induced degranulation, and the effects of both IL-1 β and Lgals3 were blocked by Mug1; and 4) the MUG1 to Lgals3 ratio in vivo linked with

infarct wall thickness. Combined, our results revealed that the D1 MI macrophage regulates neutrophil degranulation by secreting Lgals3 as a pro- and Mug1 as an anti-degranulatory protein (**Figure 3.8**) . At MI D1, the balance favors Mug1 activity to contain and prevent excessive neutrophil degranulation early in MI when inflammation is high.

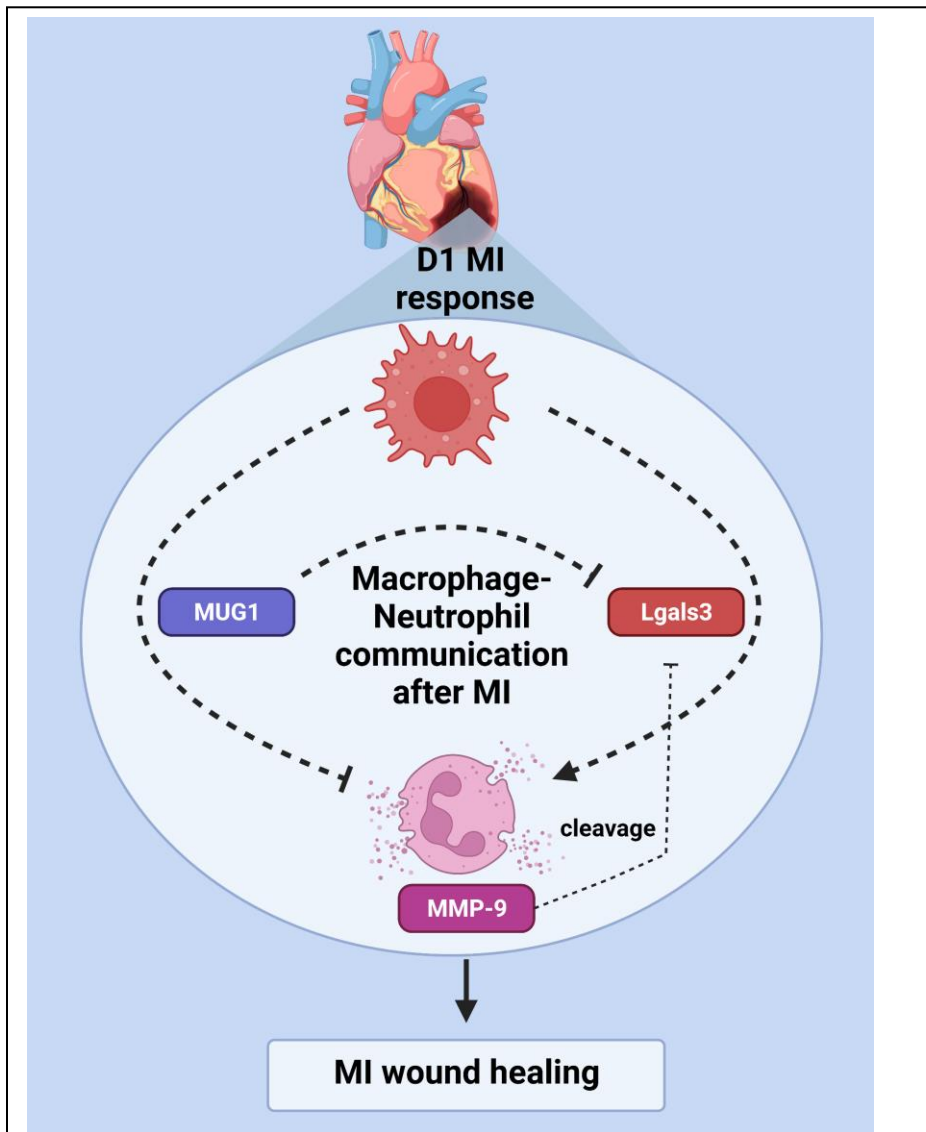


Figure 3.8. Macrophage coordinates neutrophil degranulation after MI.

Macrophages inhibit neutrophil degranulation by secretion of MUG1 and induce neutrophil degranulation by secretion of Lgals3 to coordinate early MI wound healing. Release of MMP-9 provides an additional feedback to degrade Lgals3. Created with BioRender.com.

Excessive neutrophil activation and degranulation can exacerbate inflammation after MI and worsen cardiac dysfunction, though neutrophil activation and degranulation early in MI is essential for initiation of the infarct wound healing.(19, 198) Increased neutrophil activity can induce wall thinning after MI and lead to LV aneurysms and death due to LV rupture.(196, 199) LV wall thinning after MI peaks at D1, which occurs due to the loss of cardiomyocyte due to ischemia, along with neutrophil infiltration. Neutrophils remove the necrotic debris and lays ground for ECM deposition by releasing ECM degrading enzymes from its granules.(173) As inhibition of early ECM fragmentation is necessary, our study sheds light on an endogenous mechanism of regulation of excessive neutrophil activity through macrophage-neutrophil communication. MUG1 release by macrophages limiting neutrophil degranulation could potentially be an initiation in resolution of inflammation and tissue repair.

MUG1 was the highest ranked upregulated protein secreted by D1 macrophages and USP48 was the highest ranked downregulated protein. Our data shows that D1 macrophage secretome hints for IL-17 signaling upregulation. Necroptosis and endocytosis enrichment hints for crucial role of macrophages in early wound healing phase and regulation of removal of necrotic debris.(200) Regulation of actin-cytoskeleton by macrophages indicates its role in neutrophil degranulation.(201) PPAR signaling pathway coming as a most enriched downregulated pathway further establishes central role of macrophages in MI wound healing as activation of PPAR signaling has been implicated for Ischemia reperfusion repair and reduction of infarct sizes.(202-204) PPAR γ activation in neutrophils is known to turn off NF- κ B activation and stimulate LXR/RXR signaling to initiate resolution.(205)

As we focused on macrophage-neutrophil communication through its major upregulated protein in the secretome for this study, we observed that macrophage secretome neutrophil degranulation was one of the components modulated by D1 MI

macrophages. Macrophage secretome treatment downregulated most of the cytokine release and cytokine-cytokine receptor interaction was the major enriched downregulated pathway in neutrophils followed by TNF signaling and Age-RAGE signaling pathway. This shows that D1 macrophages secretes factors to limit major inflammatory pathways in neutrophils. Macrophage secretome could be the negative feedback required to dwindle neutrophil numbers after D1.(171) With addition of MUG1 blocking antibody to the macrophage secretome and PMA we see upregulation of cytokine release. Also, it is hard to miss that cytokine-cytokine receptor interaction, TNF signaling and AGE-RAGE signaling pathway come back as enriched upregulated pathways with MUG1 blocking antibody treatment. This shows us that MUG1 is a key regulator of neutrophil activity.

MUG1 is a 180 kDa protein that has been characterized as a widespread protease inhibitor belonging to α 2-macroglobulin family.(206) Our study is the first to our knowledge to suggest MUG1 release from the macrophages. The amount of literature available on MUG1 is meager. It is known that murine MUG1 is a homologue of human α 2-macroglobulin, another protease inhibitor and a major component of human plasma(207). Comparisons of MUG1 and mouse α 2-macroglobulin show that they inhibit thrombin, plasmin, and pancreatic elastase. In addition to those mouse α 2-macroglobulin further inhibited clotting factor Xa, plasma kallikrein, submaxillary gland trypsin-like proteinase, and neutrophil elastase.(208) Before this study, MUG1 was thought to act primarily in the plasma as a protease inhibitor. Interestingly, MUG1 deficient mice also show elevated plasma levels of TNF α and IFN γ indicating its role in inflammation.(209, 210) Here, we show that MUG1 secreted by macrophages blunts neutrophil degranulation with reduced secretion of MPO, MMP-9 and MPO as its major action. Cytokines downregulated by MUG1 matched similar pathway enrichment as shown by macrophage secretome with chemokine signaling and cytokine-cytokine receptor

interaction as most enriched pathways. Our study shows enrichment for downregulation of MAPK and PI3K-AKT signaling pathway, however further work on signaling paradigm affected by MUG1 is warranted.

Lgals3 was the second protein we focused on this study as it was one of the pro-inflammatory protein secreted by macrophages at MI D1. Lgals3 stimulated release of degranulation component such as MPO, MMP-9 and NGAL by itself. Enrichment analysis was showed maximum enrichment for leukocyte transendothelial migration. It has previously been shown that Lgals3 includes β 1 integrin mediated cellular adhesion and migration by increasing binding to fibronectin, laminin and collagen 1.(211) Lgals3 is a lectin of approximately 35 kDa that has been identified as a biomarker of inflammation and fibrosis.(212-215) 2013 guidelines from American College of Cardiology Foundation/American Heart Association has recognized Lgals3 as a predictive biomarker for hospitalization and death in heart failure patients.(216, 217) Activated macrophages secretes Lgals3 and are the major source.(213) Lgals3 is highly expressed when monocytes differentiate to macrophages.(218) We have previously shown that neutrophils also secretes Lgals3, and MI neutrophils show their peak Lgals3 expression at MI D7.(38) Most of the literature available has focused the role of Lgals3 in fibrosis, fibroblast activation and proliferation.(219, 220) Our study uniquely identifies role of Lgals3 in neutrophil degranulation.

Time course of MUG1 and Lgals3 in the LV infarct shows that both proteins increase after MI and peaks at different time points in MI; MUG1 early in MI and Lgals3, later, at D7 in MI. Highest expression of MUG1 at D3 shows that MUG1 activity (MUG1/Lgals3) was highest at D1, this suggests that MUG1 culminates as pro-inflammation peaks in the LV. This is also in line with our findings that MUG1 activity requires pro-inflammatory stimuli, while Lgals3 action does not require pro-inflammation as Lgals3 peaks when inflammation is subsiding in the infarct region. As both MUG1 and Lgals3

were macrophage secreted proteins, we looked if both proteins work through similar signaling pathway and is an inbuilt mechanism to regulate neutrophil degranulation. Decrease in MMP-9 release seen with combined stimulation of bone marrow derived neutrophils with MUG1 and Lgals3 suggest Lgals3 as a downstream of MUG1. Lgals3 can bind to various protease inhibitors including α 2-macroglobulin.(197) Therefore, there is a potential for MUG1 inhibition of Lgals3 induced degranulation through Lgals3 binding to MUG1.(197)

Lgals3 is degraded by MMP-2 and MMP-9.(221) This suggests that Lgals3 action on neutrophil degranulation is similar to fibronectin as we have shown before, which is also a substrate of MMP-9. MMP-9 degradation of Lgals3 further stimulates MMP-9 release.(222) Lgals3 is a downstream regulator of MMP-9 and Lgals3 degraded by MMP-9 induces further activation of MMP-9 in chondrocytes *in vitro*, while full length Lgals3 induces MMP-9 null like effect.(223) Therefore, it is really intriguing that Lgals3 could have different functions based on its enzymatic fragmentation. Early action of Lgals3 on neutrophil degranulation could be due to degraded Lgals3 whereas later MI action of Lgals3 on cellular proliferation and migration could be due to decreased Lgals3 degradation as MMP-9 peaks early in MI.(222) Lgals3 null mice shows reduced macrophage infiltration and early polarization to M2 like phenotype worsening cardiac physiology after MI. Lgals3 null mice shows increased neutrophils after infiltration and reduced apoptosis.(224, 225) This indicates that Lgals3 has a complex role in MI would healing and careful tapping of the MUG1-Lgals3 signaling axis for optimization of neutrophil degranulation after MI could be of potential value to improve LV physiology.

As direct targeting neutrophils numbers and activity has negative impact in MI resolution, optimal regulation of neutrophil degranulation by aiming at the neutrophil kinetics could be next frontier for neutrophil specific therapies. Neutrophil specific proteins such as S100A8/A9 has been shown as a potential target, our paper shows a

new way to modulate neutrophils i.e. through macrophages.(196) While rupture is not as common now in humans with the advent of reperfusion, excessive wall thinning can lead to LV aneurysms.(5, 8) Hence, treatments that could limit excessive wall thinning could prove useful in preventing poor outcomes and exogenous MUG1 treatment following MI could mitigate excessive wall thinning after MI.

5. Conclusion

In conclusion, we show that MI D1 macrophages secretes various factors to regulate neutrophil degranulation. MUG1 secreted by macrophages inhibits neutrophil degranulation, whereas Lgals3 secreted by macrophages can induce neutrophil degranulation. The key lies on the temporal expression of these two proteins in the LV infarct. MUG1 which peaks at D3 of MI can inhibit neutrophil degranulation signals caused by Lgals3. Therefore, effective optimization of MUG1 to limit excessive neutrophil degranulation and, hence, the tissue damage could rescue early rescue of the adverse LV remodeling after MI.

CHAPTER 4. MMP-12 Polarizes The Neutrophil Signalome Towards An Apoptotic Signature

1. Introduction

Macrophage polarization is a well-studied process, and macrophages transdifferentiate phenotypes based on the type of stimulus present in the environment.(226) For example, interleukin (IL)-1 β , interferon (IFN) γ , lipopolysaccharide (LPS), or phorbol 12-myristate 13-acetate (PMA)-stimulated macrophages convert to a pro-inflammatory phenotype, also termed classical activation or M1 polarization.(227, 228) Similarly, IL-4 or IL-10-stimulated macrophages convert to an anti-inflammatory phenotype, also termed alternative activation or M2 polarization.(81, 229)

In contrast to macrophages, neutrophils have predominantly been considered a pro-inflammatory cell type, degranulating proteases and other proteins from preformed granules in response to inflammatory or infectious stimuli.(230, 231) We have recently shown that neutrophils actually display a large range of phenotypes over the course of the myocardial infarction (MI) wound healing phase.(171) Neutrophil phenotypes range from pro-inflammatory early in MI to anti-inflammatory and reparative later. (173, 222) The same stimuli that polarize macrophages (e.g., IL-1 β and IL-4) also polarize neutrophils.(232)

Matrix metalloproteinase (MMP)-12 is produced by neutrophils, and neutrophils stimulated with MMP-12 upregulate caspase-3 *in vitro*.(36) Further, MMP-12 inhibition affects neutrophil phenotype in the left ventricle to impair cardiac wound repair after MI by prolonging neutrophil presence and pro-inflammatory status.(36) Understanding how neutrophils signal in response to MMP-12 stimulation would provide insight into MMP-12 regulation of inflammation.

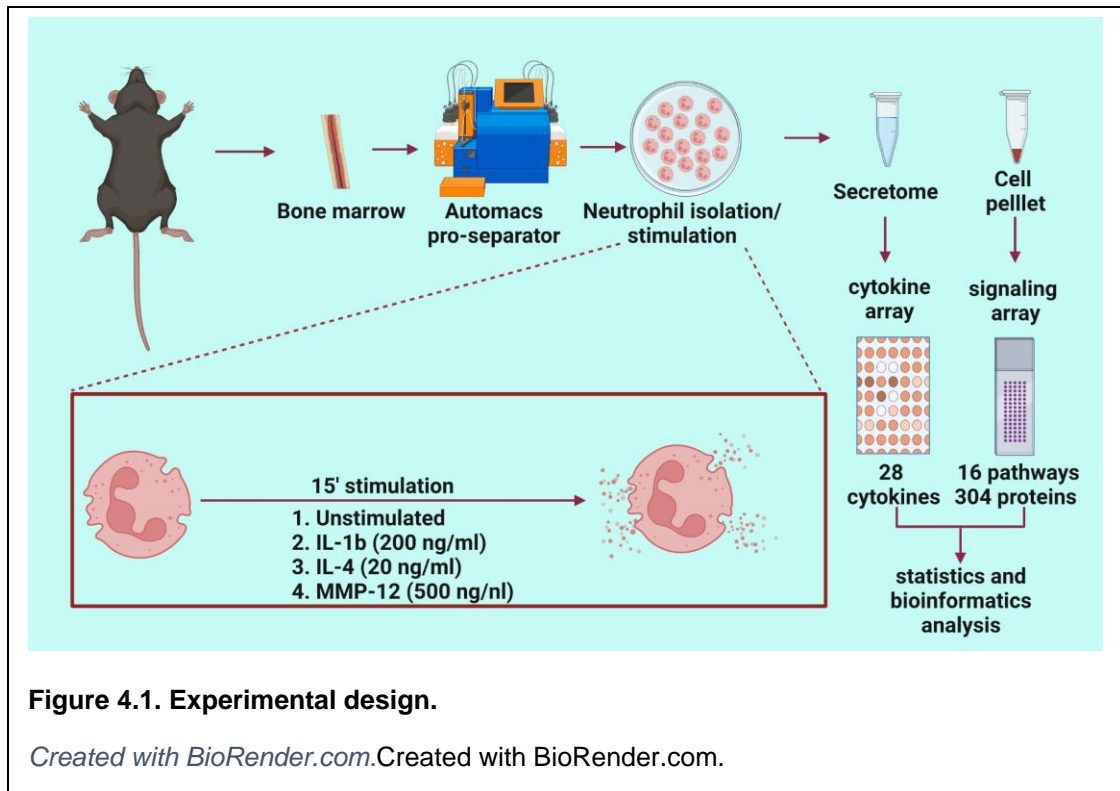
During the shift from pro-inflammation to anti-inflammation, neutrophils undergo apoptosis to remove the inflammatory signal. Neutrophil apoptosis is one important mechanism for inflammation resolution.(173, 233) In MI wound healing, neutrophils start to undergo apoptosis starting day 3 of MI in mice and they are phagocytosed by macrophages.(52) Compared to necrosis, apoptosis subdues inflammation as it avoids release of danger associated molecular patterns (DAMPs), and further inactivates DAMPs such as high mobility group box protein 1 (HMGB1).(234) Apoptotic cells are inactive but can decoy cytokines and scavenge receptors, aiding in inflammation resolution.(235) Neutrophil apoptosis delays in acute myocardial infarction with prolonged inflammation.(236)

We hypothesized that MMP-12 is a novel modifier of PMN signaling. To address this hypothesis, we mapped the neutrophil protein signalome in response to MMP-12 and compared the response to stimulation by IL-1 β as a prototypical pro-inflammatory stimulus and IL-4 as a prototypical anti-inflammatory stimulus.

2. Methods

Animal use.

The overall experimental design is detailed in **Figure 4.1**. All animal procedures were performed according to the Guide for the Care and Use of Laboratory Animals, and all protocols were pre-approved by the Institutional Animal Care and Use Committee at the University of Nebraska Medical Center.(188) C57BL/6J wild-type mice of both sexes (3–6 months old) were obtained either by purchasing from Jackson Laboratory or from an in house breeding colony and were housed in the animal facility. All mice were housed together in the same room, under a 12:12 h light-dark cycle and given ad libitum access to standard mouse chow and water.



Dot-blot analysis.

Human plasma samples were obtained from the University of Mississippi Medical Center and used for subsequent dot-blot for MMP-12 plasma concentration. Plasma was collected at 48h after admission in patients with MI (n= 41) or from healthy controls (n=18) with Institutional Review Board at the University of Mississippi Medical Center (IRB# 2013-0164) approval. All participants gave written consent before participation in the study. The investigation conformed to the principles outlined in the Declaration of Helsinki.

Plasma was diluted 10 folds and 2 μ L of was added to 6 μ L of loading buffer (without dye) and 22 μ L of distilled water for a total of 30 μ L. The samples denatured by heating to 95 $^{\circ}$ C for 5 mins. Final volume was made to 510 μ L by adding 480 μ L of PBS and loaded to the nitrocellulose membrane. Membrane was incubated overnight with primary human anti-MMP-12 (Epitomics, #EP1906, dilution 1:500), followed by

secondary goat anti-rabbit (Vector, #PI1000, dilution 1:5000) for 1 hour.

Chemiluminiscent images were taken and analyzed. Data is normalized to total protein and concentration is reported as $\mu\text{g}/200\text{nL}$.

***In situ* hybridization.**

LV mid-sections were fixed in 10% zinc-buffered formalin, paraffin-embedded, and sectioned at 5 μm . Slides were deparaffinized and rehydrated. 4 RNAscope probes were used: *Mmp12* (ACD, #406551), *L6g6e*- Neutrophil (ACD, #506391-C2), *Lamp2*- Macrophage (ACD, #422851-C3), and *Pdgfra*-Fibroblast (ACD, #480661-C4), as well as the kits from Advanced Cell Diagnostics and Akoya Biosciences. RNAscope Protease Plus was added within the barrier on the tissue, placed into the HybEZ II Hybridization oven (ACD) at 40°C for 30 minutes followed by addition of mixture of RNAscope probes and subsequent incubation in the HybEZ oven for 2 hours at 40°C. RNA amplification was done one at a time by incubation at 40°C for 30 minutes. HRP-conjugated channel was added followed by fluorophore addition to the channel and addition of HRP blocker. This step was repeated 4 time for 4 channels. Opal 520 was used for C1, Opal 620 was used for C2, Opal 690 was used for C3 and Polaris 780 was used for C4. The slides were then incubated in diluted DAPI (Akoya, #FP1490) for 5 minutes and mounted using Prolong Antifade Mountant (Invitrogen, #P36980). The slides were acquired using an Akoya Mantra Quantitative Pathology Workstation (Perkin Elmer) and analyzed using Akoya inFrom Tissue Analysis Software.

Bone marrow derived neutrophil isolation and stimulation.

Neutrophils were isolated from the femur and tibia of mice as previously described.(222) Using a 26-gauge needle and 10 mL syringe filled with RPMI 1640 media supplemented with 1% penicillin/streptomycin and 2 mM EDTA, bone marrow cells were flushed from the bones. The cell suspension was filtered through 30 μm filter to obtain single cell suspension. Single cell suspension was incubated with anti-Ly6G

magnetic ultrapure microbeads (Miltenyi Biotec, #130-120-337), and neutrophils were sorted through magnetic columns in the AutoMACS Pro Separator. Neutrophils (1×10^6) were stimulated with IL-1 β (200 ng/ml, RnD systems, #401-ML), IL-4 (20 ng/ml, RnD systems, #404-ML), or MMP-12 (500 ng/ml, Enzo Life Sciences #BML-SE138-0010) and incubated for 15 min at 37°C in 1 ml of RPMI 1640 media. The negative control was unstimulated cells. Samples sizes were n=3 M and 3 F biological replicates for each stimulus group, performed as a paired stimulation. Following stimulation, cells were centrifuged at 800xg for 8 min and cell pellets were used for the transcription factor signaling array, while the secretome was used for the cytokine array.

Signaling protein array.

The Cell Signaling Phospho Antibody Array (Full Moon Biosystems, #PCS300 <https://www.fullmoonbio.com/product/cell-signaling-phospho-antibody-array/>) contains 16 known pathways and 304 proteins. Each glass array slide contains replicate spots for each protein. All procedures were performed according to manufacturer recommendations. Cell pellets (1×10^6 cells) were washed in 1 mL of ice-cold phosphate buffered saline (PBS) for 2 min at 500 x g, repeated twice for a total of 3 washes. The cells were lysed with lysis beads in 50 μ L of Extraction Buffer, vortexed for 30 seconds, placed on ice for 10 min and the process was repeated for 6 times. The samples were then centrifuged at 10,000 x g for 5 min at 4°C. The supernatant was transferred to a new tube, centrifuged at 18,000 x g for 15 min at 4°C, and transferred to a new tube. The spin columns with dry gel were reconstituted with 650 μ L of labeling buffer, vortexed for 5 sec, and incubated for 30 min at RT. After hydration, the spin columns were put into a wash tube and spun down at 750 x g for 2 min to remove excess fluid. The wash tubes were discarded, and the spin columns were placed into collection tubes. The clear supernatant was transferred to a spin column and centrifuged at 750 x g for 2 min. The purified protein in the collection tube was quantified and

assessed for quality using a Nanodrop 2000 and measuring absorbance at A280. To a new tube, 25 μ L of the sample, 50 μ L of labeling buffer, and 3 μ L of Biotin/DMF solution were added. This mixture was incubated for 1 h at RT with vortexing every 10 min. Stop reagent (35 μ L) was added to the tube, and the samples were incubated for 30 min at RT with vortexing every 10 min. The samples were stored at -80°C and used within a month on the arrays.

The antibody arrays were equilibrated to RT for 1 h, removed from the package, and allowed to dry at RT for another 30 min. The arrays were put into blocking solution on an orbital shaker rotating at 55 rpm for 30 min at RT. The arrays were placed in 50 mL conical tubes and rinsed with water, shaking for 10 sec repeated 10 times. The prepared samples were added to 6 mL of coupling solution and incubated with the arrays on an orbital shaker at 35 rpm for 1 h at RT. The arrays were washed in 30 ml of 1x wash solution at 55 rpm for 10 min 3 times. The arrays were rinsed again in water as described above. To 60 mL detection buffer, 60 μ l of Cy-3 streptavidin (GE Healthcare, #PA43001) was added and the array was incubated with 30 mL for 20 min at 35 rpm at RT covered with aluminum foil. The arrays were washed and rinsed as described above and dried in a centrifuge at 1300 x g for 5 min. The glass slides were packaged and sent to Fullmoon biosystem for analysis. Microarray scanner was used to image and images were used to quantify signal intensity. Average of two replicate spots are taken and data is normalized to median value of average signal intensity for all antibodies in the array.

Multi-analyte cytokine profiling of the secretome.

The secretome from the neutrophil stimulation were used for V-PLEX Mouse Cytokine 29-Plex Kit (Mesoscale Discovery, #K15267D), which contained three plate (Proinflammatory panel with 10 proteins, Cytokine panels with 9 proteins and TH17 panel with 9 proteins) for total of 28 cytokines. The V-PLEX arrays are validated by Mesoscale Discovery as per the guidelines for fit-for-purpose method development and

validation for successful biomarker measurement.(237) Plate comes with a kit for all the required reagents and buffers used. 0.05% tween containing phosphate-buffered saline (TPBS) was made in the lab as a wash buffer as recommended. The 96 well plates were filled with two columns of standards at serial dilutions and 80 different secretome samples for each run. Before loading the samples, the plates were washed 3 times with 150 μ L per well of 0.05% TPBS. Standards (50 μ L each) were loaded into the plate, followed by the neutrophil secretome (25 μ L) diluted in 25 μ L of diluent 41 (1:1). The plates were sealed and placed on a shaker to incubate at RT for 2 h. The plates were washed again 3 times with 150 μ L per well of 0.05% TPBS. Detection antibody solution (25 μ L) was added to each well. The plates were sealed and incubated at RT with shaking for 2 h. The plates were washed as described above, and 150 μ L of 2x read buffer T was added to each well. The plates were read in the Mesoscale Quikplex SQ 120, and the data was processed through the discovery workbench software analysis program (Mesoscale Discovery).

MMP-12 substrate analysis.

Human recombinant proteins – β -Catenin (Abnova, #H00001499-P01), Cadherin-3 (Abnova, #H00001001-P01), Cadherin-1 (RnD Systems, #8875-EC) and Catenin- α 2 (Abnova, #H00001496-P01) – were incubated with the active catalytic domain of human MMP-12 (Enzo life sciences, #BML-SE138-0010) at a 5:1 ratio (1 μ g recombinant protein: 0.2 μ g enzyme) at 37°C in 10 μ L of 1x zymogram buffer (Life technologies, #LC2671) for up to 24h. Experiments were run in triplicate. The reaction was stopped at each timepoint by addition of 0.5 μ L of 0.5M EDTA to each 10 μ L reaction, which was then stored at 4°C until the next day and run on SDS-PAGE gels. Timing was adjusted for each protein to see maximum range of enzymatic degradation. Silver staining was performed using Pierce™ Silver Stain Kit (Thermo Scientific, 24612) as per manufacturer recommendation. The gels were imaged using iBrightFL1000.

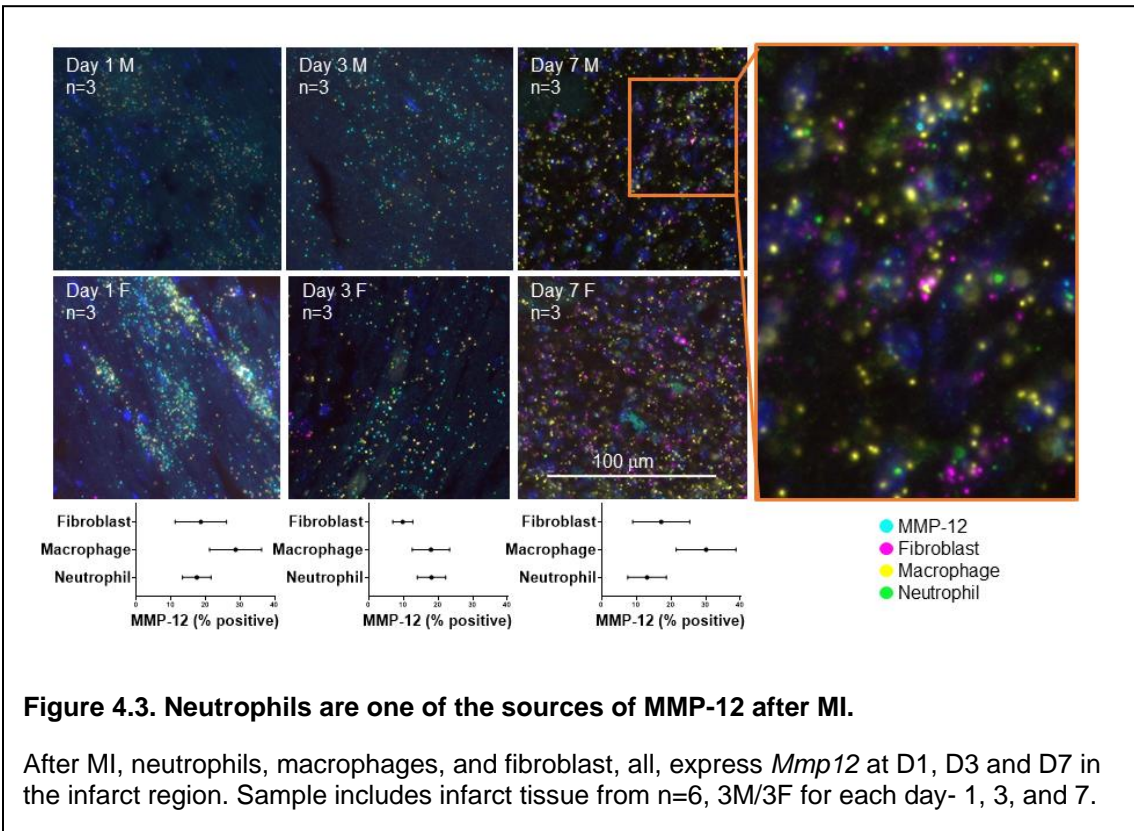
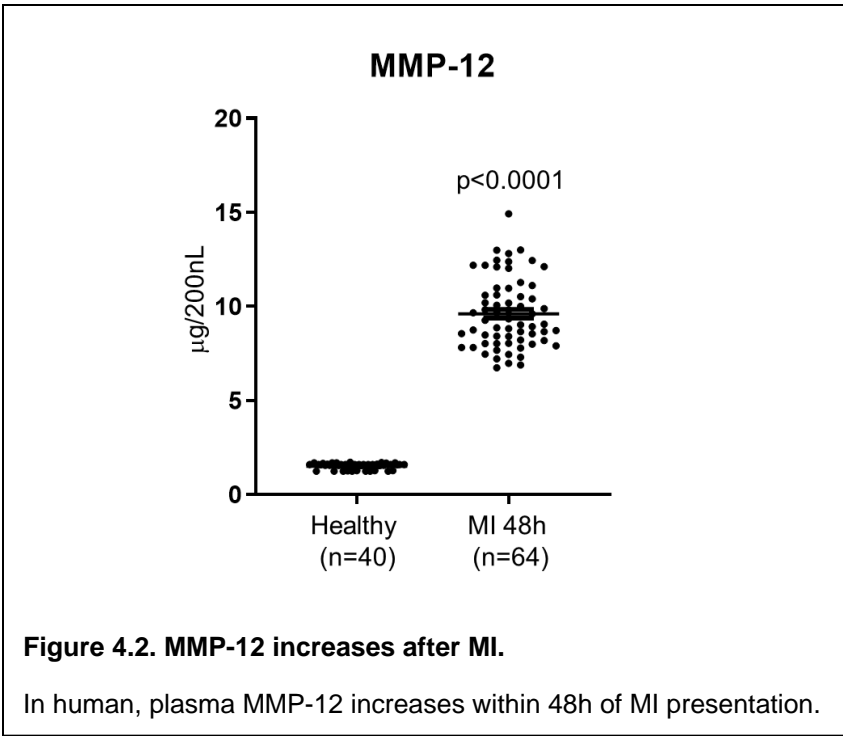
Statistics and Bioinformatics.

Statistical analyses were performed using GraphPad Prism 9 according to the guidelines outlined in Statistical Considerations in Reporting Cardiovascular Research.(138) Data are reported as mean±SEM for group comparisons. To compare each stimulus group to the unstimulated negative control, a paired Students t-test was used. A volcano plot was generated to rank based on p value and log-fold change. A Venn diagram was created to visualize inter-group overlap using DeepVenn (<http://www.deepvenn.com/>).(238) Enrichment analysis was performed using Enrichr (<https://maayanlab.cloud/Enrichr/>), a bioinformatics tool developed by the Ma'ayan Laboratory.(192) Statistically significant proteins were used for enrichment analysis. GO Biological process 2021 and were used for enriched biological processes. Transcription factor protein-protein interactions was used to identify pathways enriched transcription factors. A p value <0.05 was considered statistically significant.

3. Results

MMP-12 increases early in MI in humans and neutrophils are a source of MMP-12.

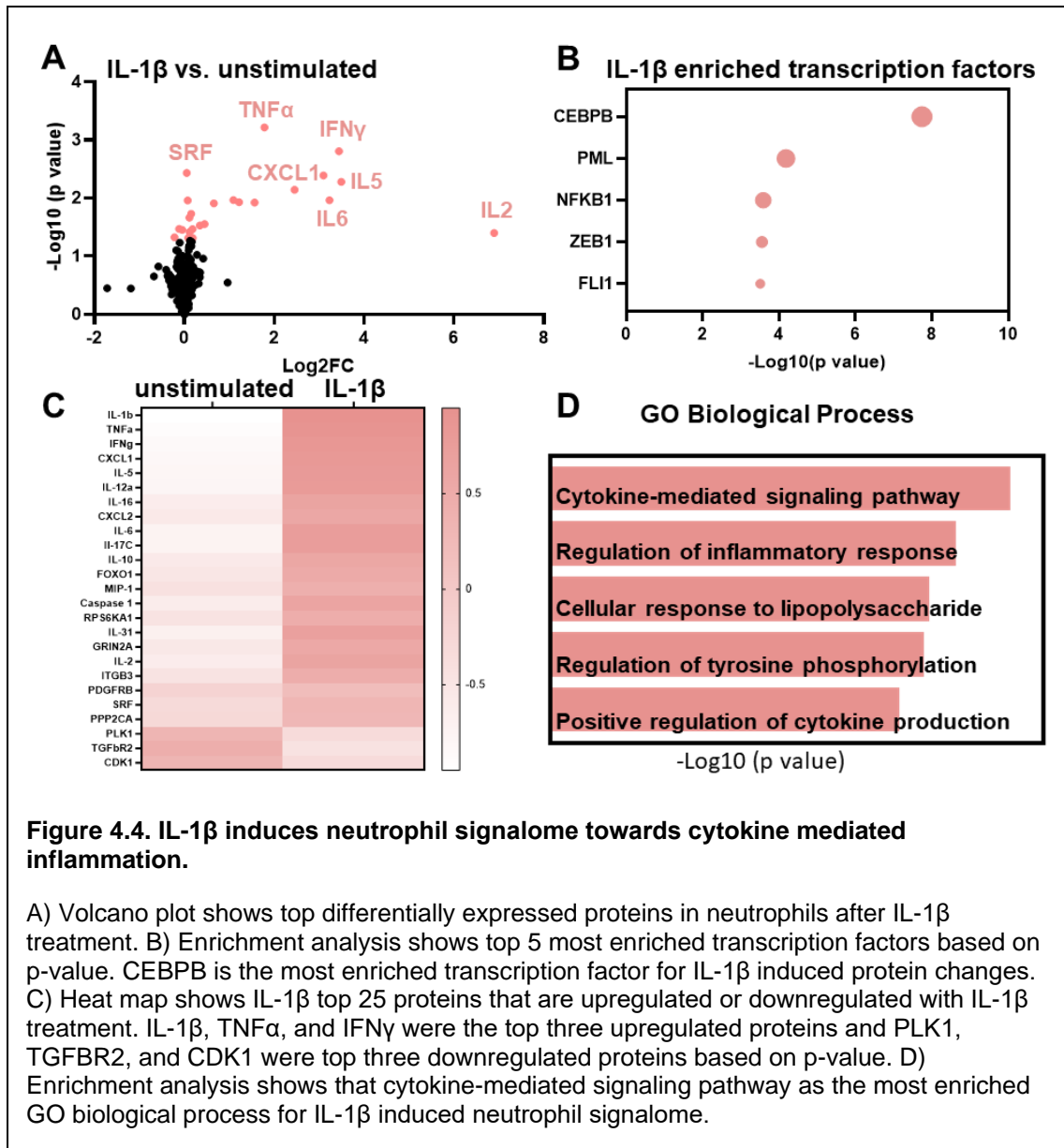
After MI, MMP-12 increased 6.3-fold in plasma compared to healthy controls (**Figure 4.2**). In situ hybridization of mouse LV sections show that neutrophils express *Mmp12* along with macrophages and fibroblasts (**Figure 4.3**). Macrophages were the major source of *Mmp12*, with neutrophils and fibroblasts also contributing to the expression profile.



IL-1 β induced the neutrophil signalome towards cytokine mediated inflammation.

For neutrophils stimulated with IL-1 β , there were 25 proteins differentially expressed in the two arrays; 22 were upregulated and 3 were downregulated. As a positive control, IL-1 β increased 18647-fold in the secretome ($p < 0.0001$). By fold change, next 4 proteins that increased by IL-1 β were IL-2 (127.5-fold, $p = 0.03$), IFN γ (15.2-fold, $p = 0.001$), IL-5 (11.2-fold, $p = 0.004$) and IL-6 (8.4-fold, $p = 0.01$). By volcano plot, top upregulated proteins included IFN γ , IL-5, CXCL1 (8.4-fold, $p = 0.005$), TNF α (3.7-fold, $p = 0.0006$), and phosphorylated serum response factor (SRF, 1.04-fold, $p = 0.003$). The three downregulated proteins were transforming growth factor receptor type 2 (TGFB2, 0.87-fold, $p = 0.047$), polo like kinase 1 (PLK1, 0.93-fold, $p = 0.034$), and cyclin dependent kinase 1 (CDK1, 0.97-fold, $p = 0.035$; **Figure 4.4A**).

Enrichment analysis of the upregulated genes showed that CCAAT enhancer binding protein beta (CEBPB) was the most enriched transcription factor, followed by promyelocytic leukemia nuclear body scaffold (PML), nuclear factor kappa beta subunit 1 (NFKB1), zinc Finger E-Box Binding Homeobox 1 (ZEB1) and Floricaula/leafy-like protein (FL1; **Figure 4.4B**). The heatmap shows the top 25 proteins changed in neutrophils with IL-1 β treatment (**Figure 4.4C**). The most enriched biological pathway by GO biological process was cytokine-mediated signaling pathway (**Figure 4.4D**). IL-1 β , therefore, stimulated a strong pro-inflammatory profile, as would be expected. IL-1 β treatment increased IL-10 release in neutrophils, a known anti-inflammatory molecule, which was unexpected and suggests activation of a negative feedback response. Overall, these results served as a positive control indicative of pro-inflammatory stimulation.

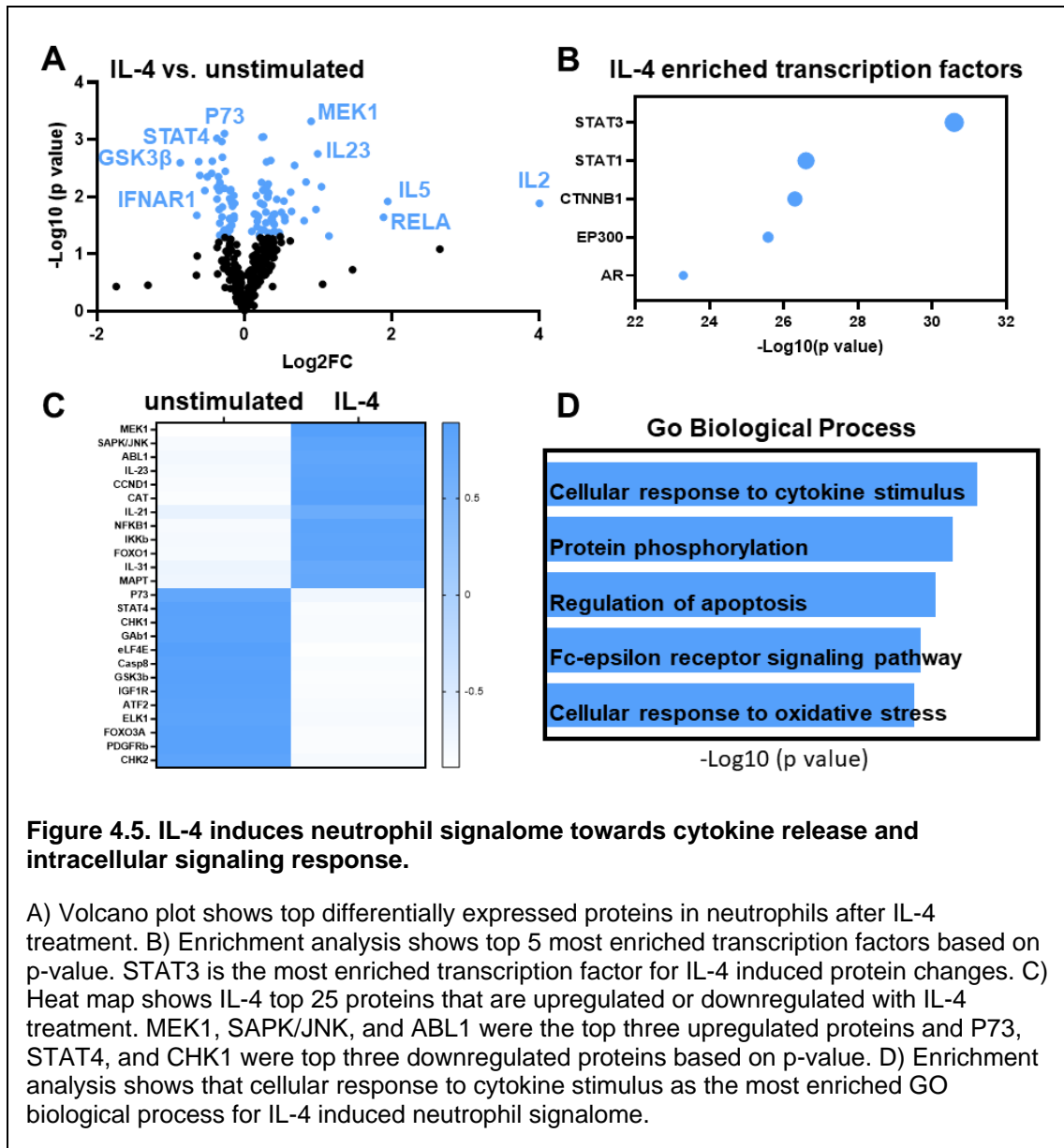


IL-4 induced the neutrophil signalome towards cytokine release and intracellular signaling response through protein phosphorylation.

For neutrophils stimulated with IL-4, there were 85 unique proteins differentially expressed in the two arrays; 49 were upregulated and 36 were downregulated. As a positive control, IL-4 was increased 63420-fold in the secretome (p=0.02). By fold change, next 4 factors increased were IL-2 (19.1-fold, p=0.01), IL-31 (8.0-fold, p=0.006), IL-5 (3.7-fold, p=0.01) and RELA/NFk β p65 (3.3-fold, p=0.02). By volcano plot, top

upregulated proteins included IL-4, mitogen-activated protein kinase kinase (MEK1, 1.9-fold, $p=0.0005$), stress activated protein kinases/ Jun amino-terminal kinases (SAPK/JNK, 1.2-fold, $p=0.0009$), ABL proto-oncogene 1 (Abl1, 1.04-fold, $p=0.0009$), IL-23 (2.0-fold, $p=0.001$), and cyclin dependent kinase 1 (CDK1, 1.3-fold increase, $p=0.002$). By volcano plot, top 5 downregulated genes were tumor protein p73 (P73, 0.83-fold, $p=0.0007$), signal transducer and activator of transcription 4 (STAT4, 0.77-fold, $p=0.001$), checkpoint kinase 1 (CHK1, 0.81-fold, $p=0.001$), GRB2 associated binding protein 1 (GAB1, 0.81-fold, $p=0.002$), and eukaryotic translation initiation factor 4E (eIF4E)-binding protein 1 (4E-BP1, 0.87-fold, $p=0.047$, **Figure 4.5A**).

Enrichment analysis showed that signal transducer and activator of transcription (STAT)3 was the most enriched transcription factor for all differentially expressed proteins, followed by STAT1, catenin beta 1 (CTNNB1), EA1 binding protein P300 (EP300), and androgen receptor (AR; **Figure 4.5B**). The heatmap in **Figure 4.5C** shows the top 25 proteins changed in neutrophils with IL-4 treatment. The most enriched biological process was cellular response to cytokine stimulus (**Figure 4.5D**). IL-4, therefore, stimulated a release of cytokine weaker than IL-1 β , as would be expected, along with regulation of cell cycle (CDK1, Cyclin D1) and apoptosis (FOXO1, P73). Of note, IL-4 maintained a basal inflammation activation in neutrophils, reflected by increased activation of the NF κ B pathway. Overall, these results served as a positive control for the anti-inflammatory stimulation in neutrophils.

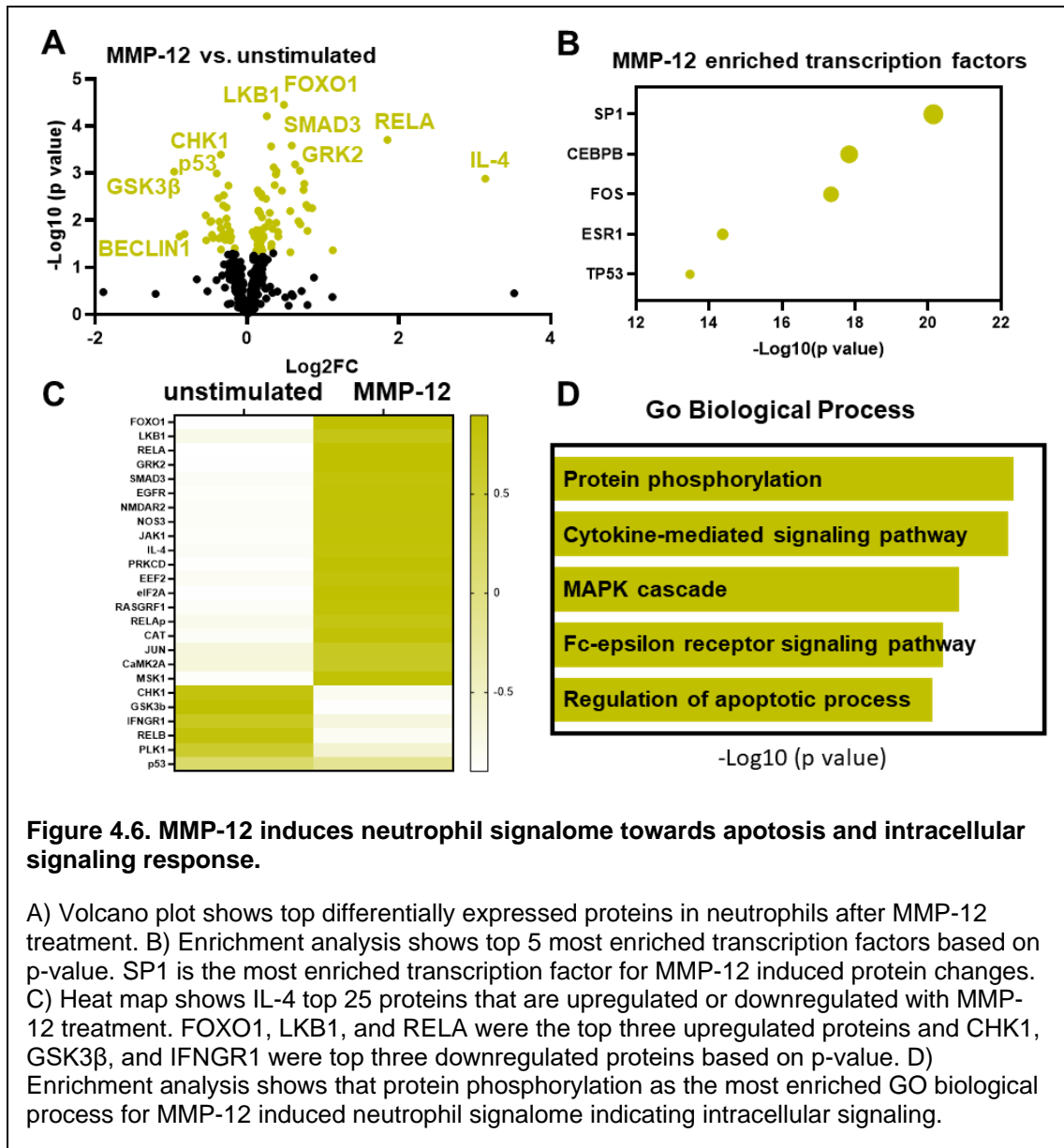


MMP-12 induced active intracellular signaling in neutrophil protein phosphorylation.

For neutrophils stimulated with MMP-12, there were 81 proteins differentially expressed; 55 were upregulated and 26 were downregulated. By fold change, IL-4 (20.0-fold, $p=0.001$), RELA/NF κ Bp65 (3.6-fold, $p=0.0001$), Macrophage inflammatory protein (MIP)-2 (2.0-fold, $p=0.04$), Syk (1.8-fold, $p=0.005$) and MIP-1 (1.7.3-fold, $p=0.01$). By volcano plot ranking, top 5 upregulated proteins were forkhead box O1 (FOXO1, 1.4-

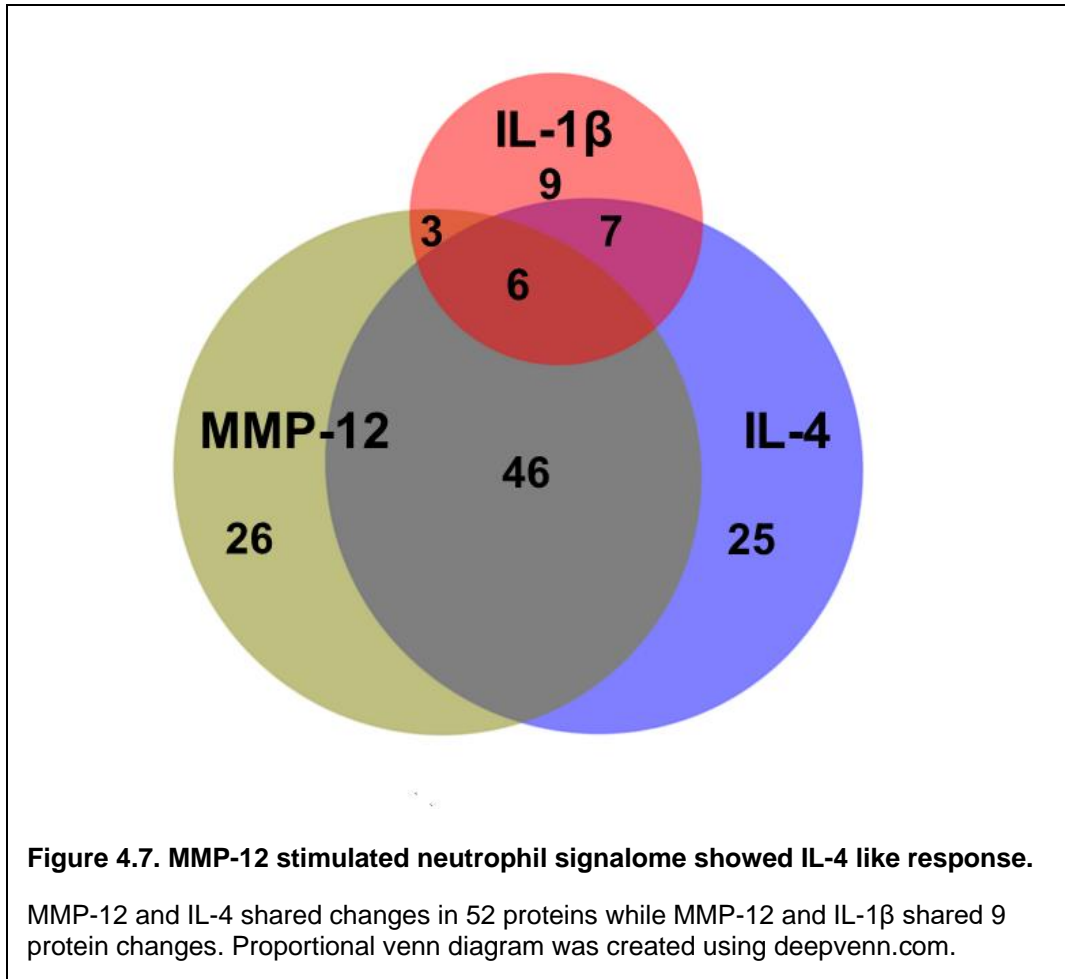
fold, $p < 0.0001$), liver kinase B1 (LKB1, 1.2-fold, $p < 0.0001$), RELA proto-oncogene, NF κ B subunit (RELA, 3.6-fold, $p = 0.0002$), G protein coupled receptor kinase 2 (GRK2, 1.5-fold, $p = 0.0003$), and Smad family member 3 (SMAD3, 1.3-fold, $p = 0.003$). By volcano plot, top 5 downregulated proteins were checkpoint kinase 1 (CHK1, 0.79-fold, $p = 0.0004$), glycogen synthase kinase 3 beta (GSK3 β , 0.50-fold, $p = 0.0009$) tumor protein p53 (P53, 0.76-fold, $p = 0.0001$), interferon gamma receptor alpha (IFNGR1, 0.84-fold, $p = 0.001$), and RELB proteo-oncogene, NF κ B subunit (GAB1, 0.80-fold, $p = 0.002$, **Figure 4.6A**).

Enrichment analysis showed that specificity protein 1 (SP1) was the most enriched transcription factor, followed by CEBPB, fos proto-oncogene (FOS), Estrogen receptor 1 (ESR1), and tumor protein 53 (TP53; **Figure 4.6B**). The heatmap in **Figure 4.6C** shows the top 25 proteins changed in neutrophils with MMP-12 treatment. The most enriched biological process by GO biological process was protein phosphorylation, indicating MMP-12 induces strong intracellular signaling (**Figure 4.6D**). MMP-12 stimulated a mixed pro-inflammatory and anti-inflammatory profile. MMP-12 stimulated a 3.6-fold increase in RELA indicative of pro-inflammation and a 20-fold increase in IL-4 indicative of anti-inflammation. The top pathways induced by MMP-12 intracellular signaling were associated with the regulation of cell cycle and apoptotic processes.



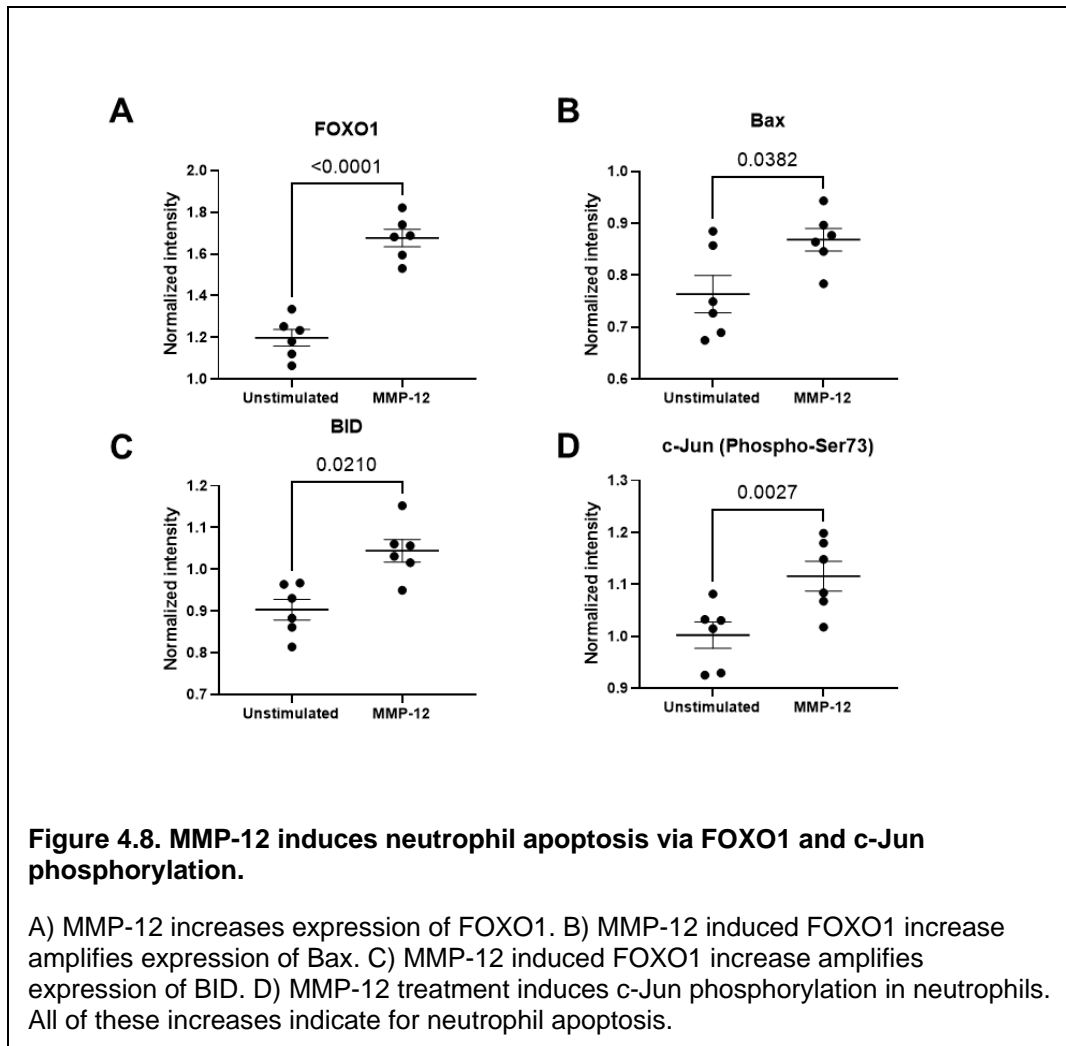
MMP-12 induced an IL-4-like neutrophil signalome.

Out of the 332 proteins evaluated (304 in the signaling array and 28 in the cytokine panel), the Venn diagram in **Figure 4.7** showed that compared to the unstimulated control, IL-1 β altered 25 proteins, IL-4 altered 84 proteins, and MMP-12 altered 81 proteins. MMP-12 shared 9 proteins with IL-1 β and 52 proteins with IL-4. A total of 26 proteins showed changes unique to MMP-12. Overall, the neutrophil signalome showed an overall higher resemblance towards neutrophils polarized by IL-4.



MMP-12 induced neutrophil apoptosis through upregulation of FOXO1 signaling.

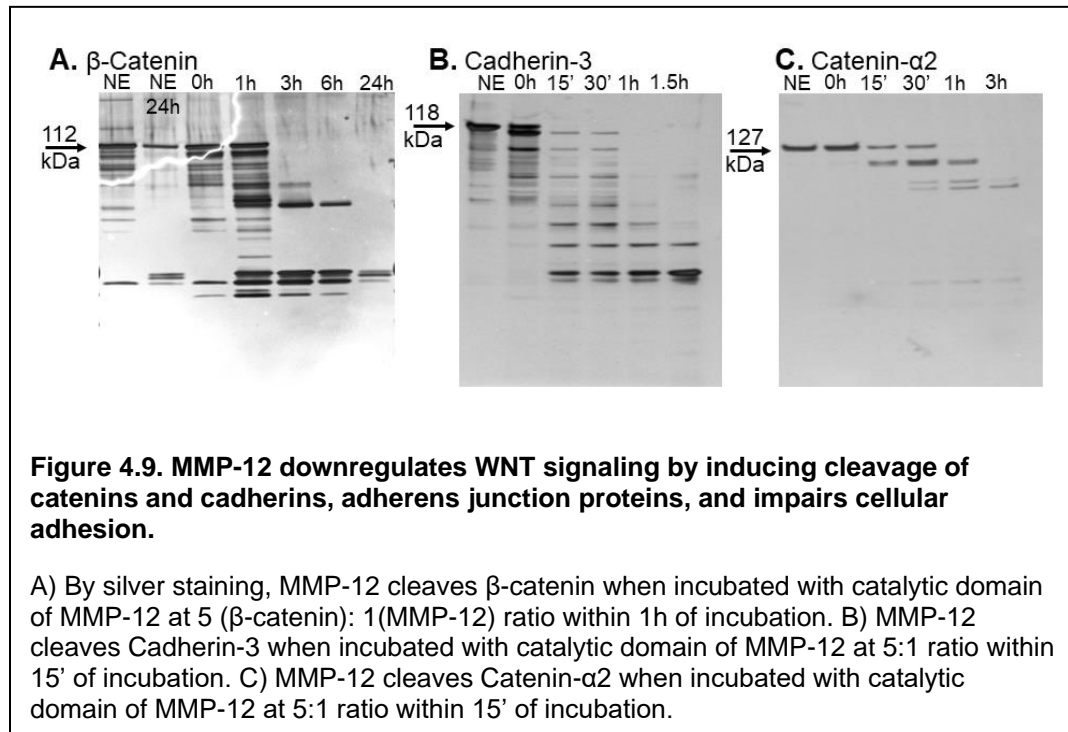
As FOXO1 was the highest ranked protein (**Figure 4.8A**) and apoptosis was one of the top-enriched pathways, we evaluated BH3 family protein expression in response to MMP-12. MMP-12 increased the pro-apoptotic proteins (1.1-fold, $p=0.038$, **Figure 4.8B**) and Bid (1.7-fold, $p=0.02$, **Figure 4.8C**). Along with FOXO1 signaling, phosphorylation of the proto-oncogene c-Jun (c-Jun) was increased 1.1-fold ($p=0.003$ **Figure 4.8D**) in neutrophils reflective of apoptotic signaling with MMP-12 stimulation. The FOXO1 mediated increase in Bcl2-family proteins was responsible for the apoptotic signature induced in the neutrophil signalome.



MMP-12 induced neutrophil adhesion through down regulation of WNT signaling.

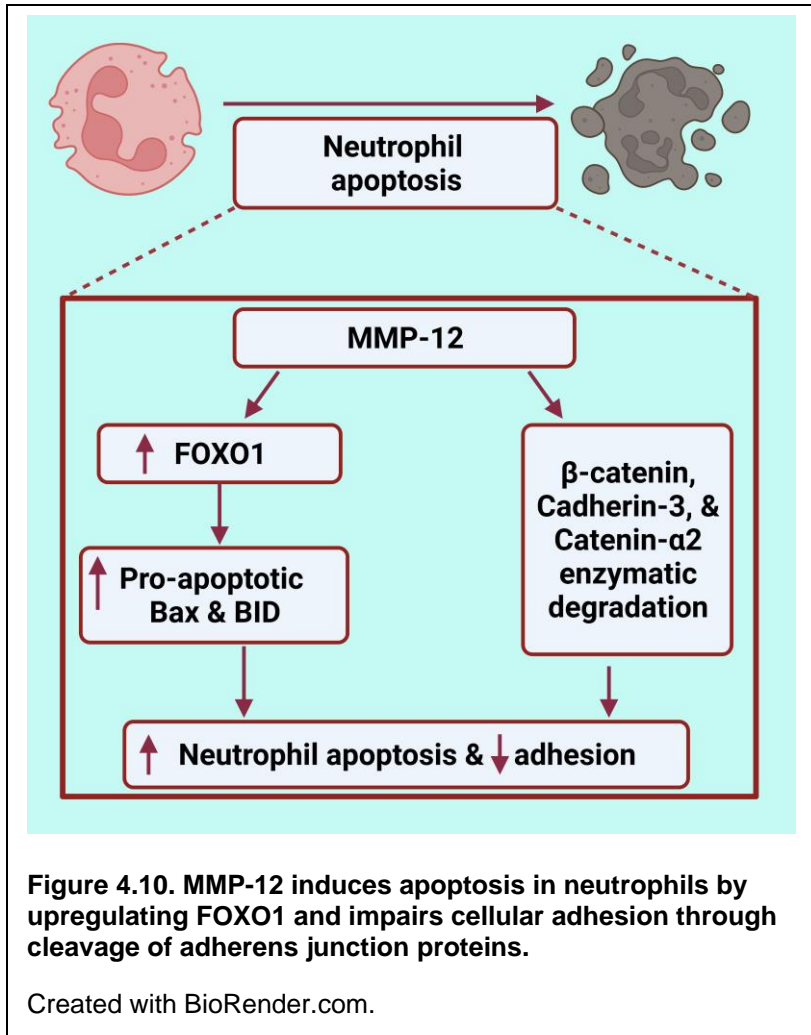
As GSK3 β was downregulated 50%, we looked at WNT signaling components that regulate cell adhesion. β -catenin was downregulated in MMP-12 stimulated neutrophils (0.84-fold, p=0.054) which suggested that MMP-12 might cleave β -catenin. We performed *in vitro* substrate analysis by incubating MMP-12 with β -catenin. MMP-12 proteolytically processed β -catenin within 3h of incubation (**Figure 4.9A**). As β -catenin is associated with adherens junctions and actin-cytoskeleton involved in cellular adhesion, we looked at cadherins -1 (CDH1) and -3 (CDH3) and catenin- α 2 (Ctnna2) to see if MMP-12 downregulated cellular adhesion through cleavage of these proteins. By enzymatic action, MMP-12 cleaved CDH3 (**Figure 4.9B**) and Ctnna2 (**Figure 4.9C**)

rapidly within 15 mins of incubation. CDH1 was not cleaved by MMP-12 by 24h of incubation. Overall, downregulation of WNT signaling through enzymatic cleavage of cadherins and catenin indicated that MMP-12 downregulated proteins involved in cellular adhesion.



4. Discussion

The goal of this project was to identify how the neutrophil responds to a range of stimuli. The major findings were: 1) Neutrophils shows unique polarization to specific stimulus; 2) MMP-12 induced neutrophil signalome shows higher closeness in response towards IL-4; and 3) MMP-12 polarizes neutrophil signalome towards apoptotic signature by upregulating FOXO1 and downregulating WNT signaling (**Figure 4.10**). Our results highlight neutrophils have a lot more plasticity than previously appreciated and shows the unique range of polarization response in neutrophils.



Historically, neutrophils have always been regarded as a proinflammatory cell type. Lately, various groups have shown phenotypic transition of neutrophils from pro-inflammatory to anti-inflammatory and tissue reparatory subtype over the course of wound healing in different disease environment, including myocardial infarction.(32, 171, 172, 222, 239-242) Neutrophils are the crucial element of myocardial infarction resolution as they initiate the early process of necrotic debris removal and later lay ground for ECM remodeling by secreting ECM proteins.(91) Steffens group have shown that neutrophils depletion impairs MI wound healing by decreased macrophage differentiation and downregulated debris clearance leading to fibrosis.(180) As neutrophil depletion does not yield favorable results, it is important to know how neutrophils are

modulated under different physiological stimuli in order to target detrimental effect elicited by neutrophils.

IL-1 β is a major pro-inflammatory signal present at day 1 and 3 of MI, which polarizes neutrophils to pro-inflammatory tissue degrading phenotype by activating them as they enter the infarct site. IL-4 is one of the anti-inflammatory signals prevalent later in MI, which is responsible for the change in tissue microenvironment to anti-inflammatory and change in cellular phenotype. Previously we have shown that MMP-12 increases after MI and remains elevated until day 7 of MI in the infarct region in mice.(36) MMP-12 elevation seen in human plasma after MI further validates that MMP-12 increases early in response to ischemic injury. We have also previously shown that neutrophils are early source of MMP-12 in the infarct. *In situ* hybridization strengthens the fact that neutrophils are one of the predominant sources of MMP-12 in the LV along with macrophages and fibroblasts, though it was previously thought macrophages are the only major source.(243, 244) Therefore, using specific MI specific polarization stimuli, we attempted to look at the polarization phenotype and compare neutrophil physiology changes with resolution promoting factor, MMP-12.(245)

IL-1 β stimulated neutrophils showed expected pro-inflammatory cytokine expression such as TNF α . We see an activation of inflammasome response with increase in Caspase 1 which further increases IL-1 β production.(246) Enrichment analysis for IL-1 β showed enrichment for cytokine production. CEBP is the major enriched transcription factor enriched which is associated with IL-6 production.(247) Previously, it has been shown that NF κ B and CEBP regulates IL-6 promoter.(247) CEBPB is associated with granulopoiesis and at day 1 of MI neutrophils have increased expression of CEBPB along with hypoxia induced factor alpha as recently shown by Vafadearnejad et al.(32) IL-1 β induced neutrophil physiology showed similar property to Lipopolysaccharide (LPS) response as indicated by enrichment analysis in GO biological

process. LPS stimulates neutrophils for IL-6 and TNF α production, which has been previously shown.(248, 249) IL-1 β was a great downstream effector for cytokine release that induces cellular migration such as CXCL1, which is also a LPS like response.(250) We see lesser change in cellular signaling molecule and robust effect on cytokine release.

IL-4 stimulation, on the other hand, had mixed response with which increased massive signaling changes. Enrichment analysis showed STAT3 as a major enriched transcription factor for IL-4 stimulated signaling changes, which entails for protective role of IL-4 in myocardial infarction. STAT3 has been shown to have protective role in myocardial infarction and ischemia reperfusion injury along with other cardiovascular diseases as it regulates ROS production in mitochondria and induces angiogenesis.(251-253) MEK1 upregulation seen with IL-4 treatment also strengthen protective role of IL-4 in MI signaling, as MEK1-ERK2 signaling pathway has protective role in ischemic injury mainly through cardiomyocyte action.(254) Though MEK1 is associated with delay in apoptosis in neutrophils, MEK1 signaling in cardiomyocyte impairs their apoptosis and hence cardiomyocyte death.(254-256) MEK1 impairs MI induced remodeling by increased phosphorylation of STAT3 and downregulation of MMP-9 in the infarct.(257) STAT4 downregulation could be responsible for anti-inflammatory action of IL-4 as STAT4 is required for IL-12 induced inflammation in neutrophils.(258, 259) IL-4 in overall promoted signaling that promotes MI wound healing.

MMP-12 stimulation of neutrophils showed unique phenotype which showed apoptotic changes. Interestingly, we see combined pro-inflammatory and anti-inflammatory changes with MMP-12 treatment. MMP-12 directly stimulates, both, IL-4 and NF κ B action through RELA bringing both IL-1 β and IL-4 like responses to neutrophil physiology. SP1 was the most enriched transcription factor in MMP-12, which when

inhibited is protective against myocardial ischemia injury through inhibition of cardiomyocytes cell death.(260-262) CBEPB enrichment is similar to IL-1 β . FOXO1 was the most upregulated signaling molecule in MMP-12 treated neutrophils, which is associated with apoptosis of various cell types.(263, 264) FOXO1 is associated with apoptosis due to increased oxidative stress and DNA damage.(265, 266) FOXO1 induces pro-apoptotic response through Bcl-2 family proteins.(263) We see an increased expression of Bcl-2 family proteins Bax and Bid which validates upregulation of neutrophil apoptosis through FOXO1. Reseveratrol and Cucurmin induces apoptotic response through FOXO1.(264, 267) Increase in RELA could also be a response to FOXO1 increase.(268) MMP-12 also increases phosphorylation of other apoptotic proteins such as c-Jun.(269, 270) We see downregulation of p53, which is also an important gene in apoptotic signaling. Literature suggests that p53 independent apoptosis is induced by reseveratrol through FOXO1 under oxidative stress which is similar to MMP-12.(271)

FOXO1 is also a member of WNT signaling which regulates cellular adhesion and migration.(272) We see downregulation of GSK3 β which is responsible for β -catenin degradation by phosphorylation of GSK3 β .(273) As, MMP-12 enzymatically cleaves β -catenin, downregulation of GSK3 β could be a potential negative feedback response. β -catenin is a component of adherens junction along with other cadherins, catenins and actin filaments.(274, 275) MMP-12 enzymatic degradation of adherens junction would suggest its role in cellular adhesion and migration along with cellular apoptosis. Overall lab has shown that MMP-12 degrades actin-filaments and impairs neutrophil infiltration in arthritis.(276) This corroborates with our finding that MMP-12 impairs cellular adhesion by action on adherent junction. Decreased cellular adhesion of neutrophils after MI would potentially limit inflammation in MI.

5. Conclusion

In summary, we used various stimuli to polarize neutrophils and map their signalome. We see strong cytokine-mediated inflammatory LPS-like signalome with IL-1 β . Similarly, with IL-4 we see subdued inflammation with IL-4 treatment. MMP-12 treatment induced a robust apoptotic neutrophil signalome. IL-1 β induces IL-10 and indicates that pro-inflammation is a necessary first step before you can get to anti-inflammation & that IL-4 induces pro-inflammation marker NF κ B, indicating that some pro-inflammatory signaling networks may serve dual purposes- therefore, blocking pro-inflammation has multiple negative consequences for downstream anti-inflammatory signaling. This is a key point why blocking pro-inflammation has not been a useful strategy for cardiac wound healing after MI.(277)

CHAPTER 5. Harnessing the plasma proteome to predict cardiac remodeling after myocardial infarction

1. Introduction

Myocardial infarction (MI) induces robust infarct wall thinning and dilation of the left ventricle (LV) over the first week in mice.(22, 34, 222, 278) In response to MI, cardiac wound healing involves the early initiation of inflammation to clear necrotic debris followed by fibroblast activation to secrete extracellular matrix needed to form the infarct scar. Cardiac remodeling starts with infarct wall thinning due to early cardiomyocyte necrosis, with the greatest change in wall thinning occurring over the first 24h of MI. Wall thinning is followed by LV dilation with reduced ejection fraction and volume overload.(119)

Several plasma markers have been previously identified that assess the inflammatory component of MI.(279) Early inflammation markers of MI include c reactive protein, matrix metalloproteinase (MMP)-9, myeloperoxidase, galectin-3, and neutrophil blood count; all have been shown, both in mice and in humans, to reflect the inflammatory component and predict adverse outcomes, namely progression to heart failure and death.(124, 176-178, 280-288) The early phase of inflammation is followed by consecutive phases of anti-inflammation and repair.(84, 278) As such, inflammatory markers that are transient in expression in plasma and may not hold predictive reliability at every timepoint of MI. Thus, examination of those markers needs to occur at an optimum snapshot in time that may not be easily translatable from mouse to human or may not be uniform across individual patients. Diagnostic or prognostic markers that continuously predict cardiac dysfunction over a range of times after MI is of high clinical significance.

Reliable biomarkers with uniform patterns will aid in better treatment for patients with MI by providing an easier way to develop a personalized medicine strategy.(289, 290) Identification of biomarkers that are functionally relevant also reveals signaling mechanisms, which potentially will uncover new therapeutic targets. Here, we used data from three different proteomics platforms in mice to identify plasma markers of adverse cardiac remodeling after MI. We hypothesized that the identified plasma markers could reflect cardiac physiology across an extended timepoint of MI. The hypothesis was tested in a second validation cohort to examine continued predictability at an extended timepoint of MI. We also examined by glycoprotein array human plasma from patients with MI to identify signaling associated with the identified biomarkers.

2. Methods

Experimental design

The experimental design included a retrospective study using a previously collected database and tissue bank, a prospective study using a new cohort of mice, and a human cohort (**Figure 5.1**).

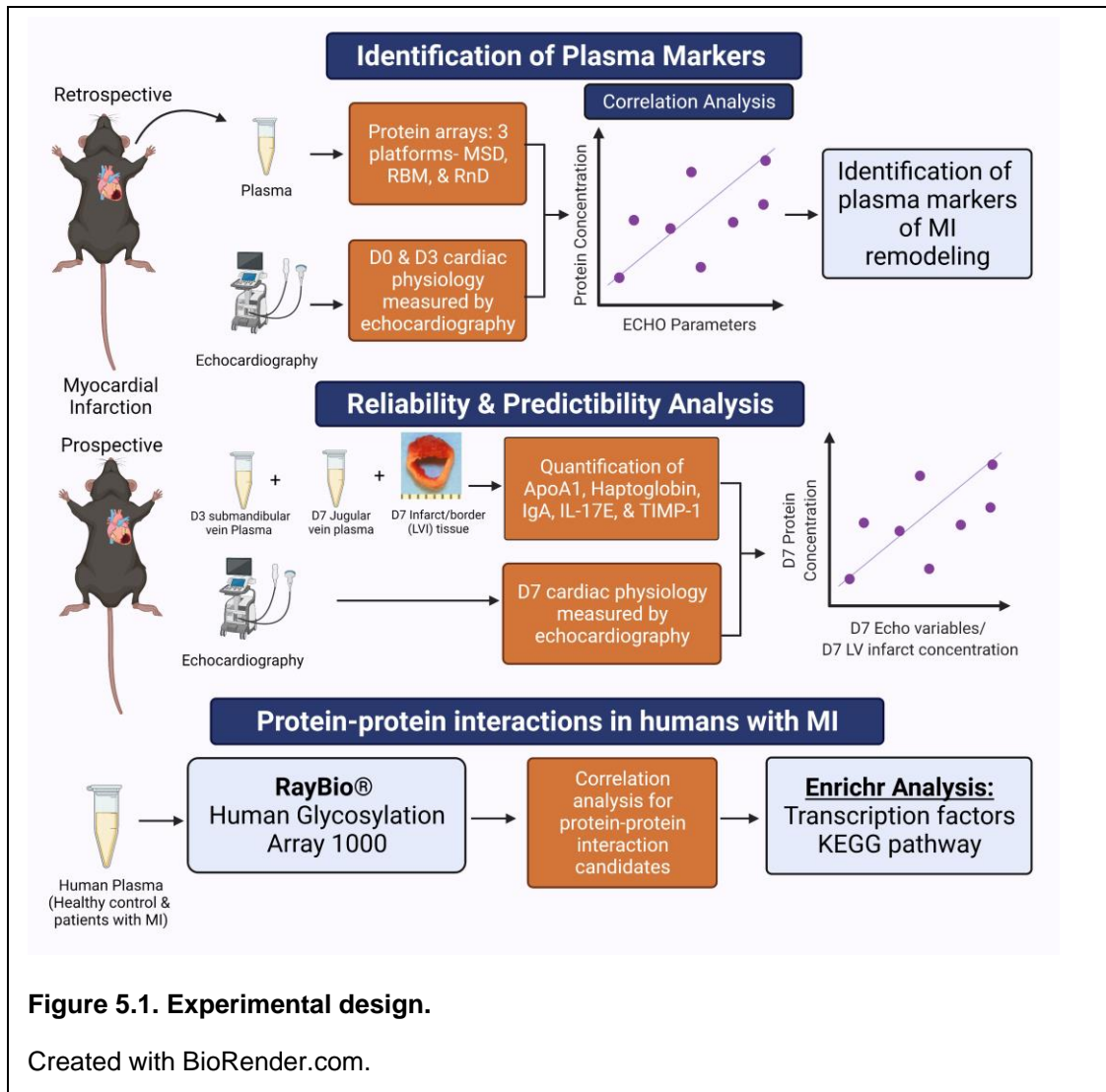


Figure 5.1. Experimental design.

Created with BioRender.com.

Retrospective study

All animal procedures were approved by the Institutional Animal Care and Use Committee and were conducted in accordance with the Guide for the Care and Use of Laboratory Animals published by the National Institutes of Health.(291) The mouse Heart Attack Research Tool (mHART) database and tissue bank consists of data combined from across MI projects published since 2007 under standard operating procedures from a single site lab.(292) For the retrospective analysis, we included data for male and female C57BL/6J mice (n=31) ranging from 3 to 6 months of age that were evaluated at day (D)0 (no MI) or MI D3. The database was accessed on May 2020 (by

UC). The plasma analysis was originally evaluated by multi-analyte profiling using a 60 protein array (Rules Based Medicine / Myriad). Echocardiography included examination of dimensions: end systolic dimension (ESD) and end diastolic dimension (EDD), volumes: end systolic volume (ESV) and end diastolic volume (EDV), and wall thickness: anterior wall thickness at systole (AWTs) and anterior wall thickness at diastole (AWTd). Infarct size was included to confirm MI. We additionally screened the banked plasma using two additional protein arrays- V-PLEX Plus Mouse Cytokine 29-plex Kit (Meso Scale Discovery (MSD), Cat. No. K15267G) and Proteome Profiler Mouse XL Cytokine Array (R&D Systems (R&D), Cat. No. ARY028) containing 111 proteins, both of which were performed according to manufacturer instructions. Combined, this yielded 165 unique plasma analytes and 6 variables of cardiac physiology.

Prospective study

A new cohort of mice (n=20) underwent surgery and cardiac physiology was assessed by echocardiography per established guidelines and standard operating procedures.(23, 26, 52, 293-295) At D3 of MI, the mice underwent echocardiography using the VEVO 3100 (Fujifilm) and blood was collected by submandibular vein collection in heparin to obtain plasma. At MI D7, the mice underwent echocardiography and were sacrificed. Blood was collected from the jugular vein to obtain D7 plasma, and the LV infarct region (infarct and border) was collected separate from the remote region.

Immunoblotting

Immunoblotting was performed according to the published guidelines.(296) LV infarct protein was homogenized in TPER™ tissue protein extraction buffer (Thermo Fisher, Cat. No. 78510, 16 ul/ 1 mg LVI). Protein was quantified using Nanodrop (Thermo Fisher, Cat. No. ND2000). A total of 0.1 uL plasma or 10 ug total LV protein for LV infarct was loaded onto 4–12% Criterion XT Bis-Tris precast gels (Bio-Rad, Cat. No. 345-0125) and transferred onto Trans-Blot Turbo Transfer Pack Nitrocellulose

Membranes (Bio-Rad, Cat. No. 170-4159). The membranes were stained with Pierce Reversible Protein Stain Kit for nitrocellulose membranes (Thermo Scientific, Rockford, IL) and densitometry was analyzed for normalization of LV samples.(52, 222, 297, 298) Membranes were blocked with Blotting Grade Blocker (Bio-Rad) in 5% triphosphate buffer solution and incubated overnight with primary antibody at 4°C followed by incubation at room temperature for 1h with secondary antibody. The antibodies used included ApoA1 (Abcam, Cat. No. ab227455, 1:1000), Haptoglobin (Thermo Fisher Scientific, Cat. No. MA5-32584,1:1000), and IL-17E/IL-25 (R&D systems, Cat. No. MAB1399, 1:1000). For ApoA1 and Haptoglobin primary antibodies, the blots were incubated with goat anti-rabbit IgG secondary antibody (Vector Laboratories, Cat. No. PI-1000, 1:5000). For IL-17E/IL25 primary antibody, the blot was incubated with goat anti-rat IgG secondary antibody (Vector Laboratories, Cat. No. PI-9400, 1:5000). For TIMP-1 assessment, we tried the following 4 antibodies, and none gave a specific band of the right molecular weight: Abcam Cat. No. ab38978, ab216432, and ab179580 (1:1000) and Epitomics Cat. No. 3346-1 (1:1000). Chemiluminescent images were captured using the iBright FL1000 imaging system (Thermo Fisher) and quantified using iBright analysis software 4.0.0. The blots were normalized to the total protein, and the data were presented as normalized arbitrary units.

IgA isotyping panel

Plasma and infarct homogenates were used to quantify IgA expression by a mouse isotyping panel (MSD, Cat. No. K15183B). The experiment was run as per manufacturer recommendations. The plate contained 7 antibody fixed spots in each well of the isotyping panel, and each spot was linked to electrodes for signal quantification. A sulpho-tagged antibody was used with appropriate read buffer after sample incubation and electrical signals were quantified. LV samples were normalized to total protein and reported as ng/μg, whereas plasma samples were volume loaded and reported as μg/μl

with appropriate dilution correction. Plasma samples were run at 1:10,000 dilution and LV infarct samples were run at 1:100 dilution.

Human evaluation

All participants gave written consent before participation in the study. The investigation conformed to the principles outlined in the Declaration of Helsinki. The human subject protocol was approved by the Institutional Review Board at the University of Mississippi Medical Center (IRB# 2013-0164). Plasma was collected at 48h after admission in patients with MI (n= 41) or from healthy controls (n=18). Patient characteristics are listed in **Table 5.1**.(298)

	Healthy controls (n=18)	MI (48 h; n=41)
Age (years)	48 (range 25-76)	56 (range 33-72)
Sex	14 Women, 4 Men	18 Women, 23 Men
Race	7 Black, 11 White	18 Black, 23 White

Table 5.1. Patient Characteristics.

Glycoprotein array

The Human Glycosylation Antibody Array 1000 (RayBio®, Cat. No. GAH-GCM-1000-4) contained pre-blocked glass slides coated with antibodies for 1000 glycosylated proteins. The array was performed according to manufacturer instructions. The slides were incubated with human plasma (1:5 dilution) and washed to remove unbound proteins. Five unique biotin-labeled lectins were incubated with the array. Each lectin bound their respective glycan moieties on the captured proteins present on the glass surface. Streptavidin-conjugated fluorescent dye (Cy3 equivalent) was added to the array which recognized the biotin attached to any bound lectin molecule. Chemidoc laser fluorescence scanning (Biorad laboratories) was used to visualize the signals. Signals were quantified and normalized to reference spots. CXCL4 concentrations were previously reported from this dataset.(298)

Statistical Analysis and Bioinformatics:

Statistical analyses were performed with GraphPad Prism 9, according to the guidelines outlined in Statistical Considerations in Reporting Cardiovascular Research.(299) For all analyses, $p < 0.05$ was considered significant. Pearson correlation was conducted between the 6 cardiac physiology variables and all 165 protein candidates. Multiple regression was used to increase stringency of the identified plasma markers to predict specific echocardiography variables. Multicollinearity among proteins was checked with Variance Inflation Factor (VIF) score > 5.0 . Protein candidates with $r > 0.60$ were accepted for further evaluation. An unpaired t-test was used for retrospective data with D0 and D3 plasma derived from different mice; and a paired t-test was used for the prospective data with D3 and D7 plasma derived from the same mouse. Bioinformatics tools provided in Metaboanalyst 5.0 were used for correlation analysis, partial least squares – discriminant analysis (PLS-DA) and volcano plotting. PLS-DA important features analysis was used to rank proteins based on Variable Importance in Projection (VIP) scores. The Enrichr bioinformatic platform was used for transcription factor enrichment assessment and associated Kyoto Encyclopedia of Genes and Genomes (KEGG) pathway enrichment analysis of the human glycoarray data.(191, 192, 300, 301)

3. Results

Five candidates in the MI D3 plasma proteome mirrored cardiac physiology

Out of 165 unique proteins, 46 proteins correlated with at least one of the 6 cardiac physiology variables across D0 and MI D3 (all $p < 0.05$; primary cardiac physiology data provided in **Table 5.2**). When we ranked significant proteins by r value, 24 proteins had $r > 0.5$ and 5 proteins had $r > 0.6$ for all 6 echocardiography variables. The 5 proteins were Apolipoprotein A1 (ApoA1), Interleukin (IL)-17E/IL-25 (IL-17E), Immunoglobulin (Ig)A, Haptoglobin, and Tissue Inhibitor of Metalloproteinase-1 (TIMP-

1). By multiple regression to further test the stringency of these markers, all 5 plasma markers remained significant ($p < 0.05$) for at least one of the 6 cardiac physiology variables (**Figure 5.2A**). **Figure 5.2B** shows the representative correlation where ApoA1 correlated with AWTs. These 5 proteins were further evaluated in a prospective study.

Table 5.3 contains cardiac physiology data for the prospective study.

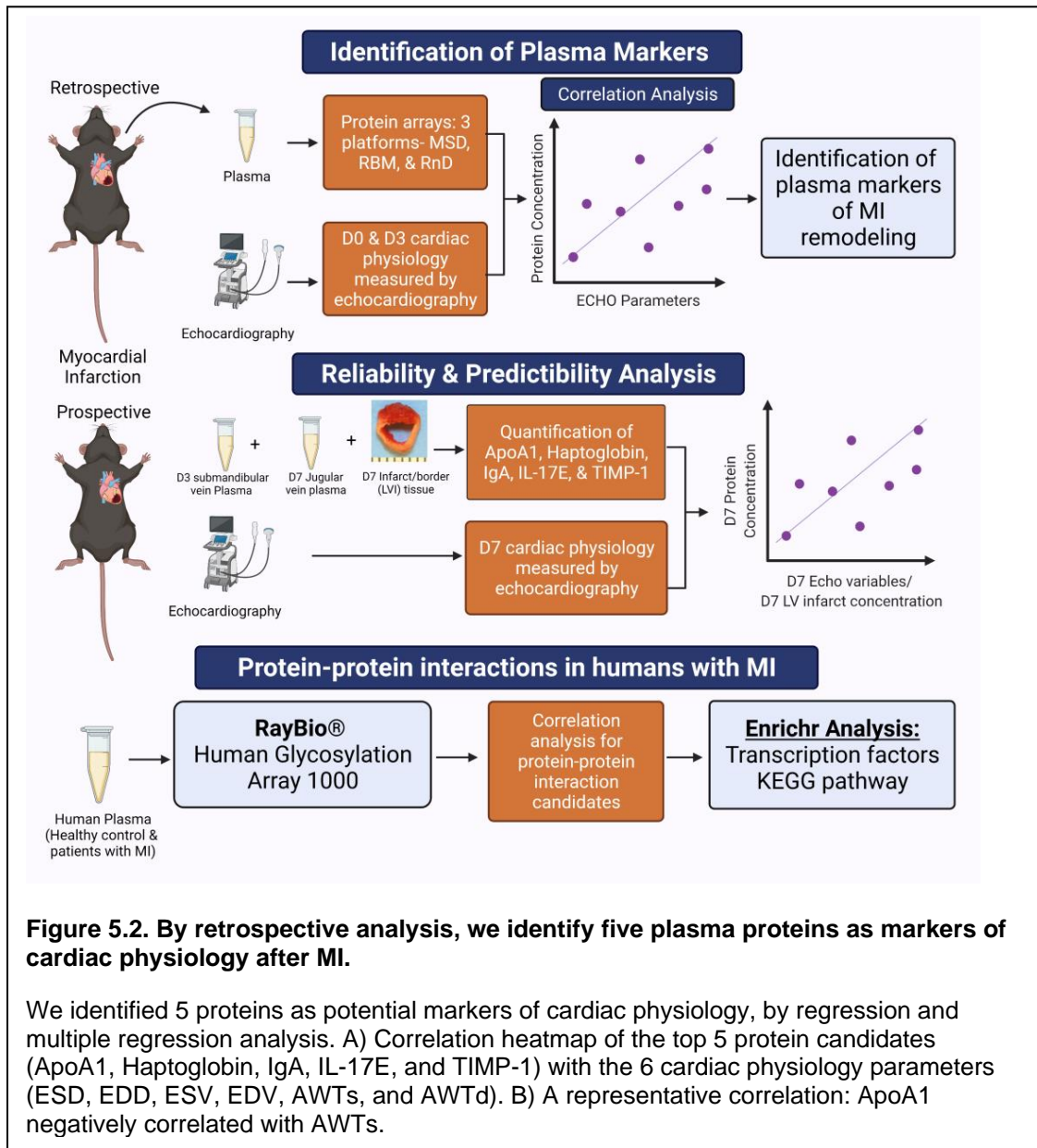


Table 5.2. Cardiac physiology data (Retrospective).

	D0	D3	p value
End Diastolic Dimension (EDD, mm)	3.52±0.10	4.54±0.10	3.06E-08
End Systolic Dimension (ESD, mm)	2.20±0.10	4.17±0.11	2.23E-14
End Diastolic Volume (EDV, µL)	58±3	95±5	7.97E-07
End Systolic Volume (ESV, µL)	19±1	78±5	4.54E-13
Septal Wall Thickness (Diastole) AWTd, mm	0.85±0.02	0.57±0.04	1.07E-07
Septal Wall Thickness (Systole) AWTs, mm	1.20±0.05	0.59±0.03	6.07E-12
Ejection Fraction (EF)	68±2	19±2	3.6E-18
Infarct size (%)	NA	49±2	NA

Table 5.3. Cardiac physiology data (Prospective).

	D0	D3	p value
End Diastolic Dimension (EDD, mm)	3.68±0.06	5.22±0.17	1.90266E-10
End Systolic Dimension (ESD, mm)	2.46±0.05	4.85±0.19	1.11715E-14
End Diastolic Volume (EDV, µL)	54±2	92±6	9.96225E-08
End Systolic Volume (ESV, µL)	20±1	76±6	1.91992E-11
Septal Wall Thickness (Diastole) AWTd, mm	0.77±0.02	0.48±0.02	1.33898E-12
Septal Wall Thickness (Systole) AWTs, mm	0.94±0.03	0.53±0.03	1.04089E-12
Ejection Fraction (EF)	64±2	19±2	5.4015E-22
Infarct size (%)	NA	51±2	NA

ApoA1 mirrored and predicted cardiac physiology.

In both the retrospective and prospective studies, plasma ApoA1 increased with MI (**Figure 5.3A top and bottom**). ApoA1 increased 1.5-fold from D0 to MI D3 in the retrospective study and increased 2.3-fold from D3 to D7 in the prospective study. In addition, the MI D3 plasma concentration of ApoA1 correlated with MI D7 plasma,

indicating predictive capability. ApoA1 in the MI D7 plasma correlated with MI D7 cardiac physiology, with the highest correlation being to AWTd and ESV (**Figure 5.3B**). In the human cohort, ApoA1 correlated with 89 other glycoproteins (all $p < 0.05$): Bone Morphogenetic protein-9 (BMP-9), BRG1 associated factor 57 (BAF57), Aldolase B, Focal Adhesion Kinase (FAK), and S100A6 being the top 5. By enrichment analysis, foxm1 was the most enriched transcription factor associated with ApoA1 protein-protein interactions. KEGG human pathway revealed that cytokine-cytokine receptor interaction was the most enriched pathway linked to ApoA1 and its associated proteins (**Figure 5.3C**).

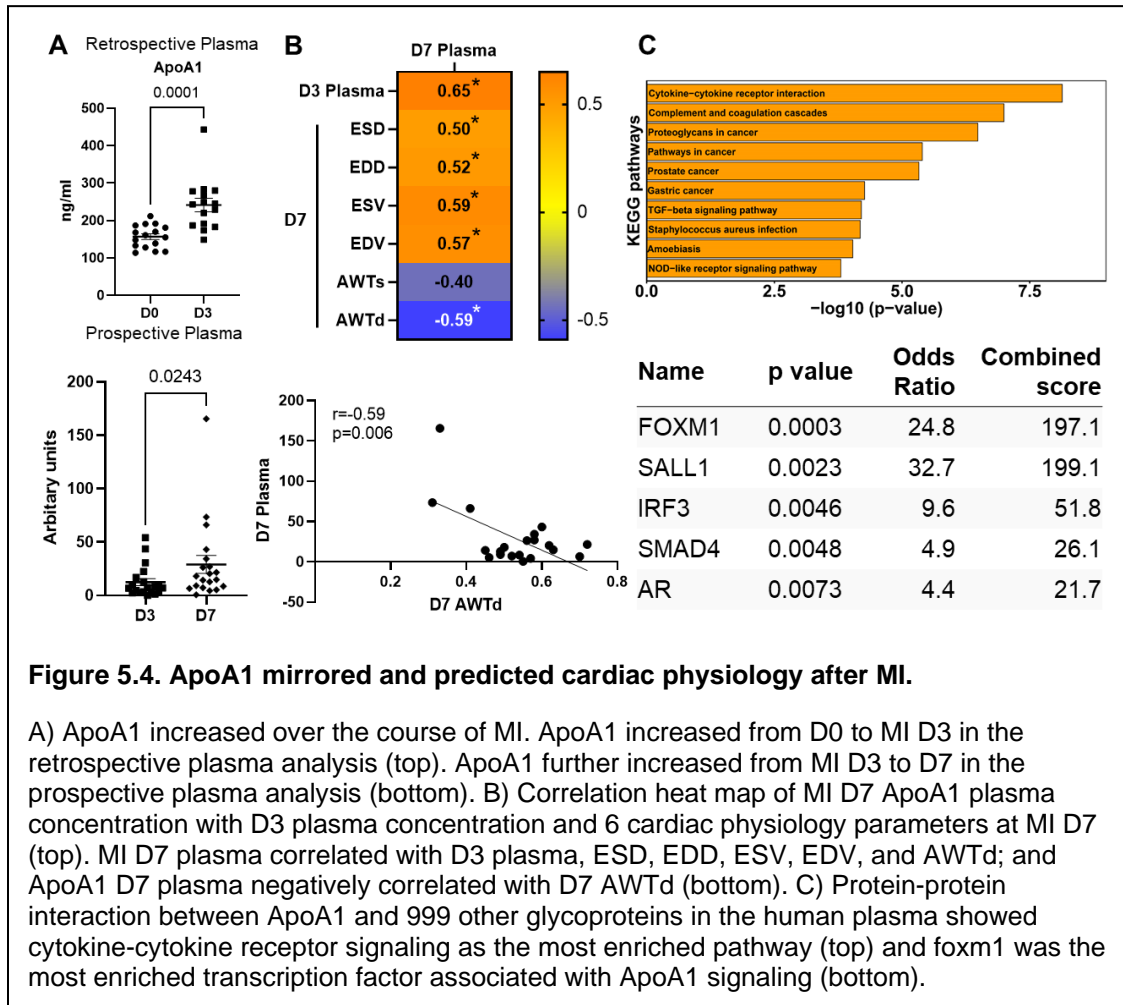


Figure 5.4. ApoA1 mirrored and predicted cardiac physiology after MI.

A) ApoA1 increased over the course of MI. ApoA1 increased from D0 to MI D3 in the retrospective plasma analysis (top). ApoA1 further increased from MI D3 to D7 in the prospective plasma analysis (bottom). B) Correlation heat map of MI D7 ApoA1 plasma concentration with D3 plasma concentration and 6 cardiac physiology parameters at MI D7 (top). MI D7 plasma correlated with D3 plasma, ESD, EDD, ESV, EDV, and AWTd; and ApoA1 D7 plasma negatively correlated with D7 AWTd (bottom). C) Protein-protein interaction between ApoA1 and 999 other glycoproteins in the human plasma showed cytokine-cytokine receptor signaling as the most enriched pathway (top) and foxm1 was the most enriched transcription factor associated with ApoA1 signaling (bottom).

IL-17E/IL-25 mirrored cardiac dilation after MI.

IL-17E/IL-25, similar to ApoA1, linearly increased after MI, showing 5.3-fold increase from D0 to MI D3 in the retrospective plasma and 1.8-fold increase from MI D3 to D7 in the prospective plasma (**Figure 5.4A top and bottom**). IL-17E correlated with cardiac physiology at the early timepoint of MI (D3) and showed extended prediction of LV dilation (both volumes and dimensions) at MI D7. At MI D7, plasma IL-17E/IL-25 had highest correlation with ESV (**Figure 5.4B**). From the human glycoarray expression, IL-17E showed protein-protein interaction (PPIs) with 180 glycoproteins (all $p < 0.05$). IL-12p40, IL-3 R alpha, IL-20R beta, IL-11, and Leptin (OB) were the top 5 glycoproteins positively correlating with IL-17E. Stat3 was the most enriched transcription factor and cytokine-cytokine receptor interaction was the most enriched pathway in KEGG human pathway (**Figure 5.4C**).

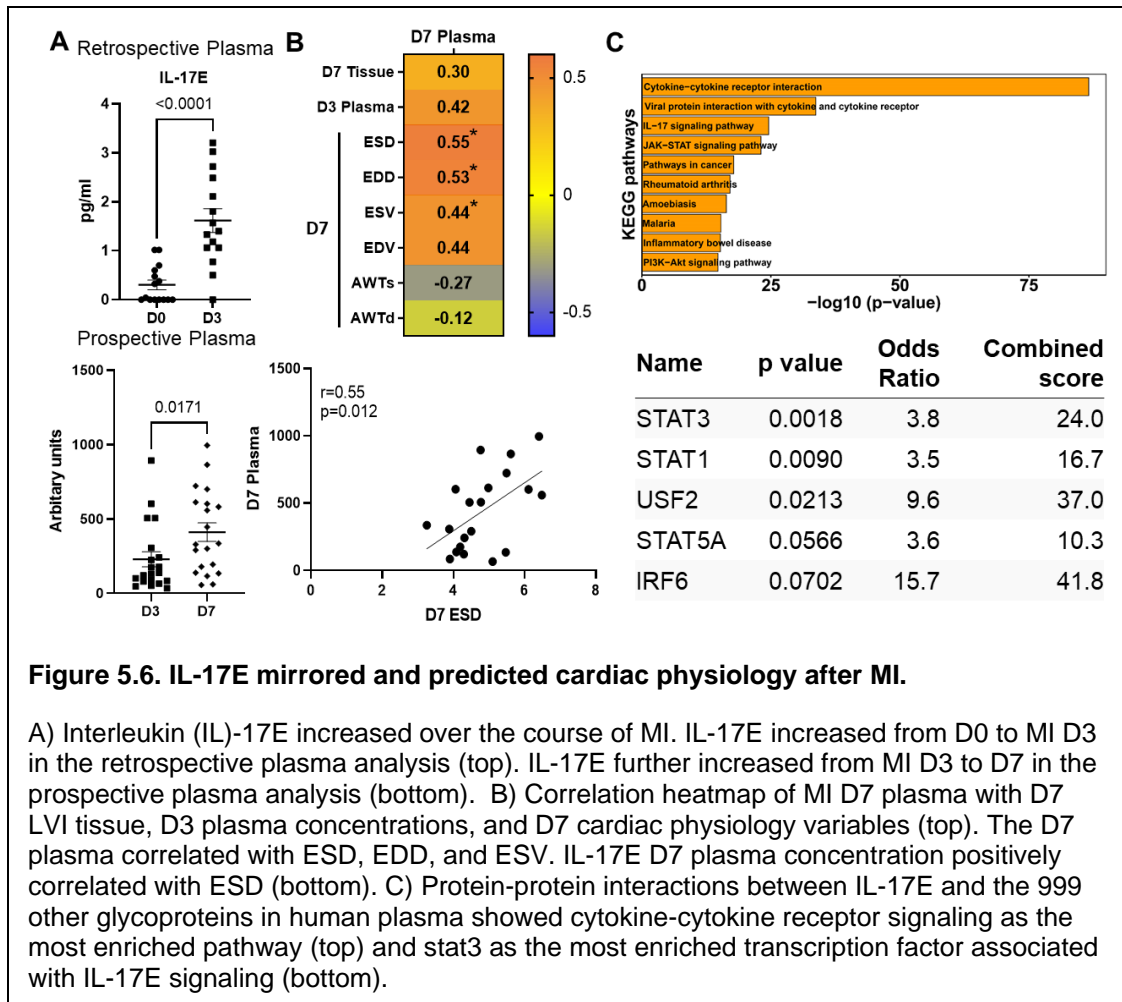
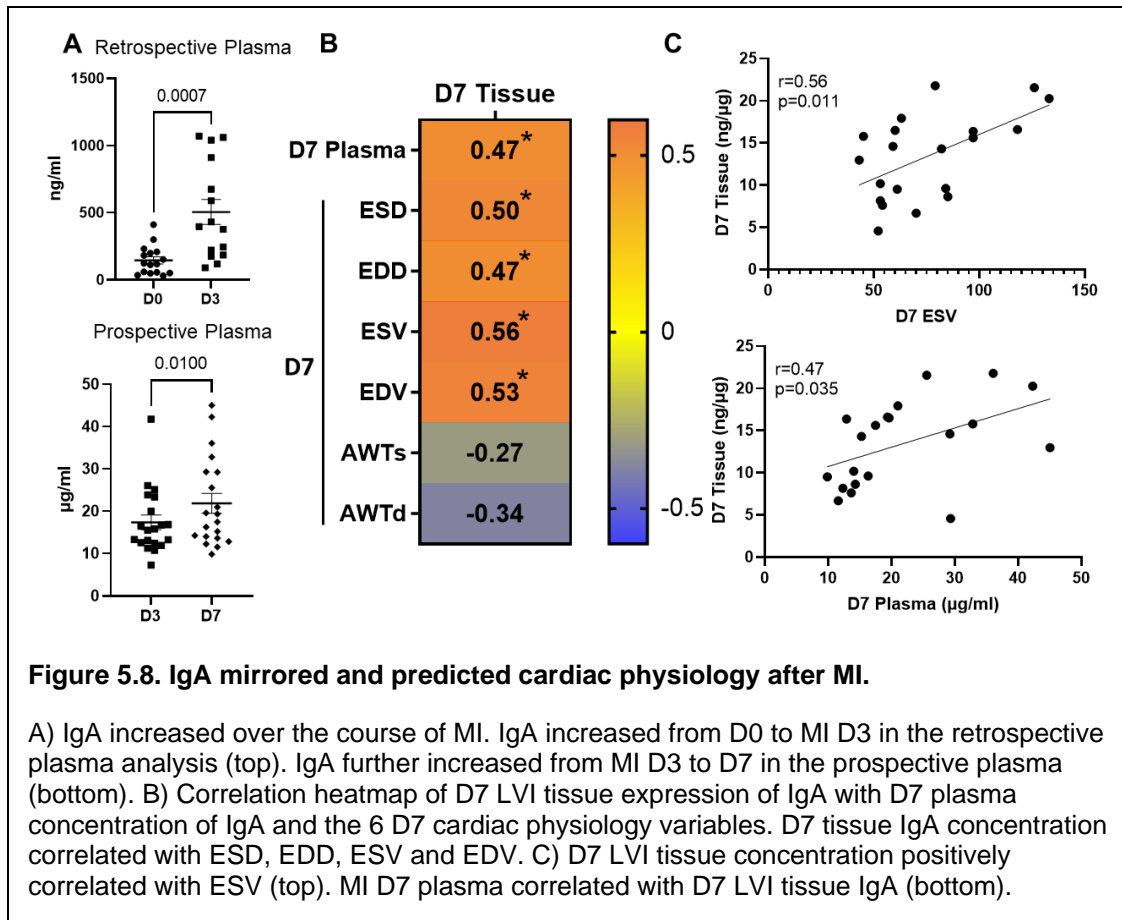


Figure 5.6. IL-17E mirrored and predicted cardiac physiology after MI.

A) Interleukin (IL)-17E increased over the course of MI. IL-17E increased from D0 to MI D3 in the retrospective plasma analysis (top). IL-17E further increased from MI D3 to D7 in the prospective plasma analysis (bottom). B) Correlation heatmap of MI D7 plasma with D7 LVI tissue, D3 plasma concentrations, and D7 cardiac physiology variables (top). The D7 plasma correlated with ESD, EDD, and ESV. IL-17E D7 plasma concentration positively correlated with ESD (bottom). C) Protein-protein interactions between IL-17E and the 999 other glycoproteins in human plasma showed cytokine-cytokine receptor signaling as the most enriched pathway (top) and stat3 as the most enriched transcription factor associated with IL-17E signaling (bottom).

IgA mirrored and predicted cardiac physiology

Plasma IgA also showed linearity in expression after MI, similar to ApoA1 and IL-17E, with the lowest expression at D0 and the highest expression at MI D7. Retrospective plasma showed a 3.5-fold increase from D0 to MI D3, while the prospective plasma showed an 1.3-fold increase from MI D3 to D7 (**Figure 5.5A top and bottom**). IgA in the LV infarct at MI D7 predicted cardiac physiology and also correlated with MI D7 plasma expression (**Figure 5.5B**). Like IL-17E/IL-25, LV infarct expression of IgA at D7 predicted LV dilation at D7, with the highest correlation being to ESV (**Figure 5.5C**). IgA was not among the proteins measured in the human glycoarray, thus the protein-protein interaction analysis for IgA was not performed.



Haptoglobin is an early marker of cardiac dysfunction after MI.

Haptoglobin expression peaked at MI D3, giving an inverted U-shaped expression curve. Haptoglobin increased 1.4-fold from D0 to MI D3 and decreased 3.0-fold from MI D3 to D7 (**Figure 5.6A top and bottom**). Plasma Haptoglobin expression correlated with cardiac physiology at MI D3 in the retrospective study, but not at D7 in the prospective study, indicating haptoglobin was a time specific marker of MI (**Figure 5.6B**). Human plasma expression of Haptoglobin correlated with 73 other glycoproteins (all $p < 0.05$), with the highest positive correlations being to IL-34, Fibronectin, Glucose-regulated protein (GRP75), Programmed cell death protein 1 (PD-1), and Proopiomelanocortin (POMC). Protein-protein interaction analysis indicated stat1 as the

most enriched transcription factor and cytokine-cytokine receptor interaction as the most enriched pathway in KEGG human pathway (Figure 5.6C).

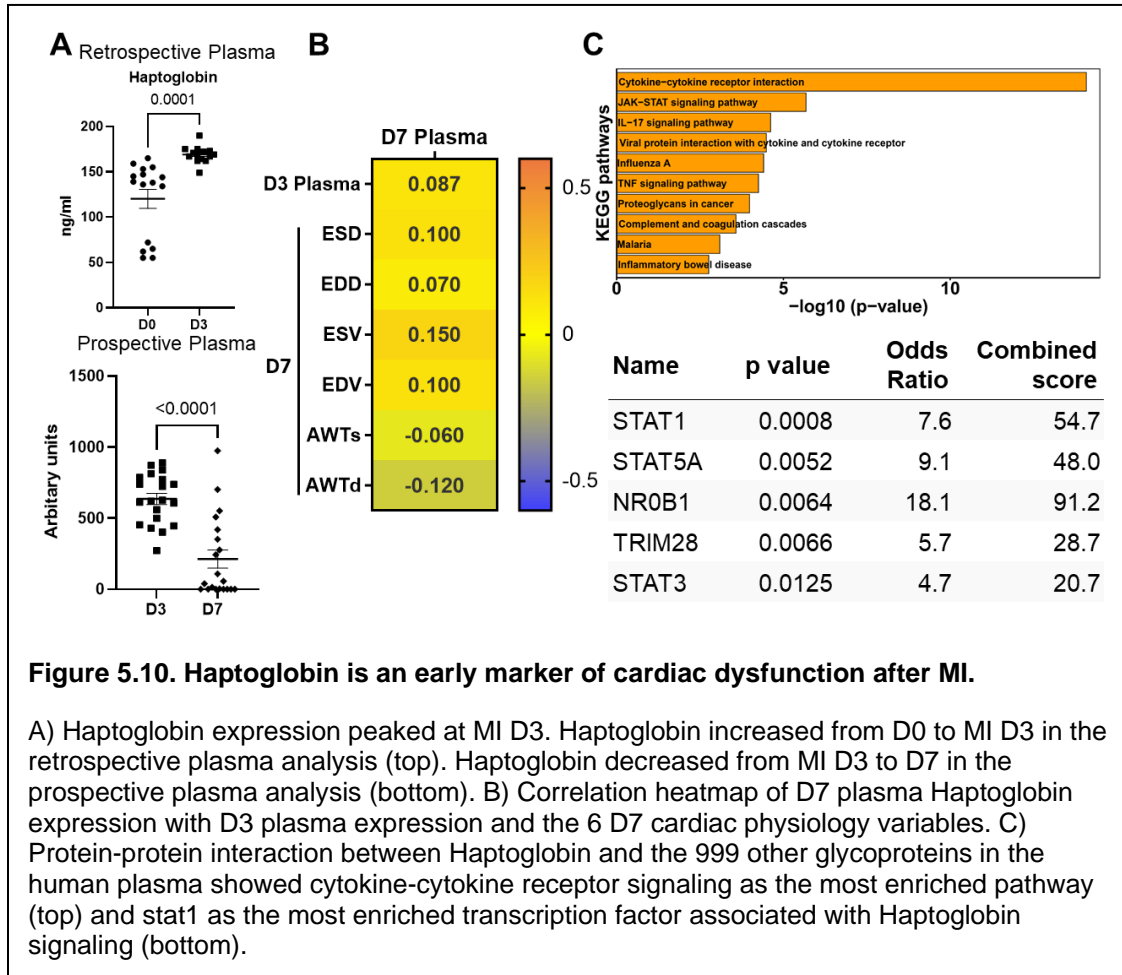


Figure 5.10. Haptoglobin is an early marker of cardiac dysfunction after MI.

A) Haptoglobin expression peaked at MI D3. Haptoglobin increased from D0 to MI D3 in the retrospective plasma analysis (top). Haptoglobin decreased from MI D3 to D7 in the prospective plasma analysis (bottom). B) Correlation heatmap of D7 plasma Haptoglobin expression with D3 plasma expression and the 6 D7 cardiac physiology variables. C) Protein-protein interaction between Haptoglobin and the 999 other glycoproteins in the human plasma showed cytokine-cytokine receptor signaling as the most enriched pathway (top) and stat1 as the most enriched transcription factor associated with Haptoglobin signaling (bottom).

TIMP-1 increased after MI and predicted cardiac physiology:

Plasma TIMP-1 linearly increased after MI, showing 4.2-fold in plasma from D0 to MI D3 in the retrospective plasma and 1.4-fold increase from MI D3 to D7 in the prospective plasma. (Figure 5.7A top and bottom) TIMP-1 correlated with cardiac physiology at the early timepoint of MI (D3) and showed extended prediction of LV dilation (end systolic and diastolic volumes) at MI D7. At MI D7, plasma TIMP-1 had highest correlation with ESV (Figure 5.4B). In human plasma glycoarray expression, TIMP-1 correlated with 37 out of 999 other glycoproteins (all $p < 0.05$), and the highest ranked were TIMP-4, TNF-related apoptosis-inducing ligand receptor 2 (Trail R2/CR5/T),

Transforming growth factor beta-2 (TGF-beta 2), Osteoactivin/GPN, and TNF-related apoptosis-inducing ligand (Trail/TNFSF10). TIMP-1 and its interactors were enriched for USF2 signaling and cytokine-cytokine receptor interaction was the most enriched KEGG pathway (**Figure 5.7C**).

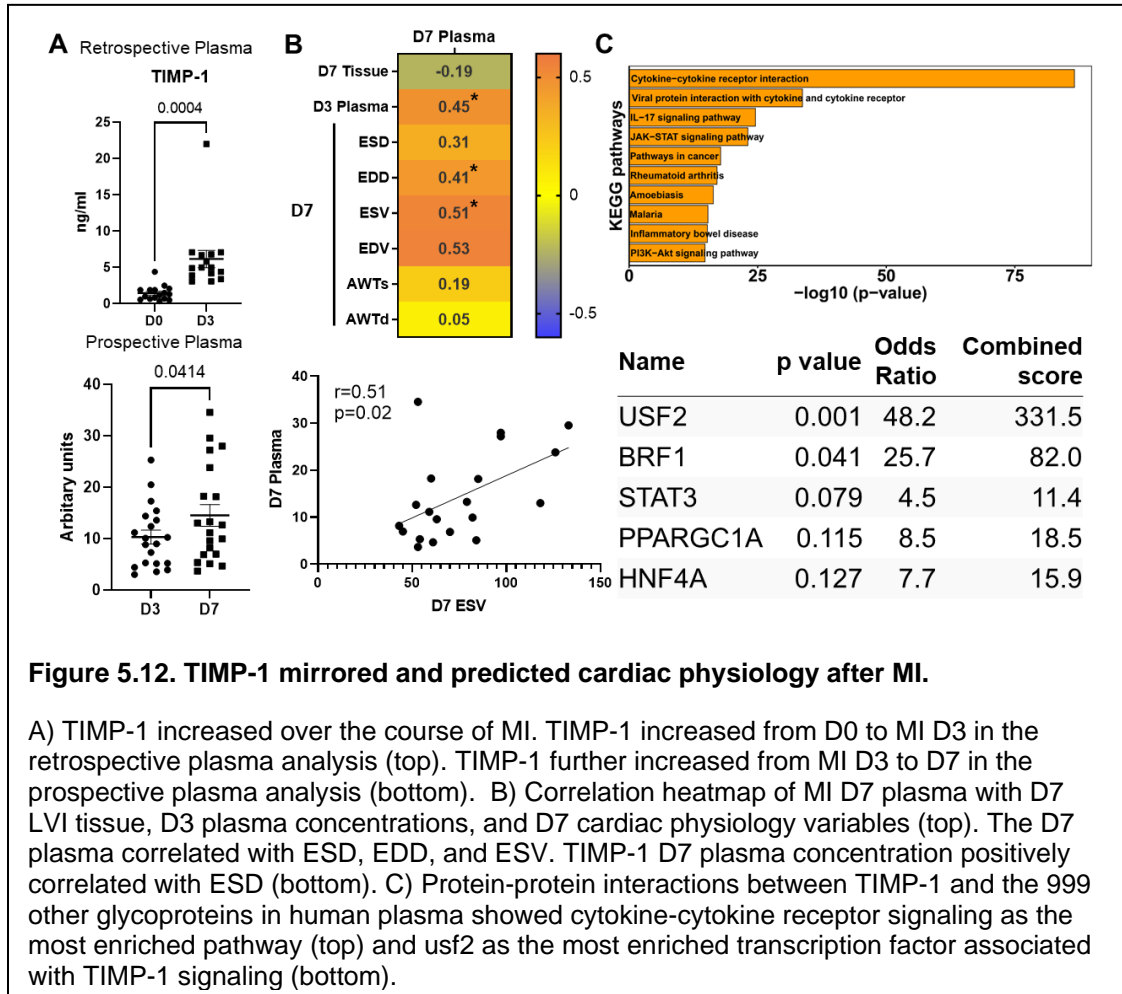


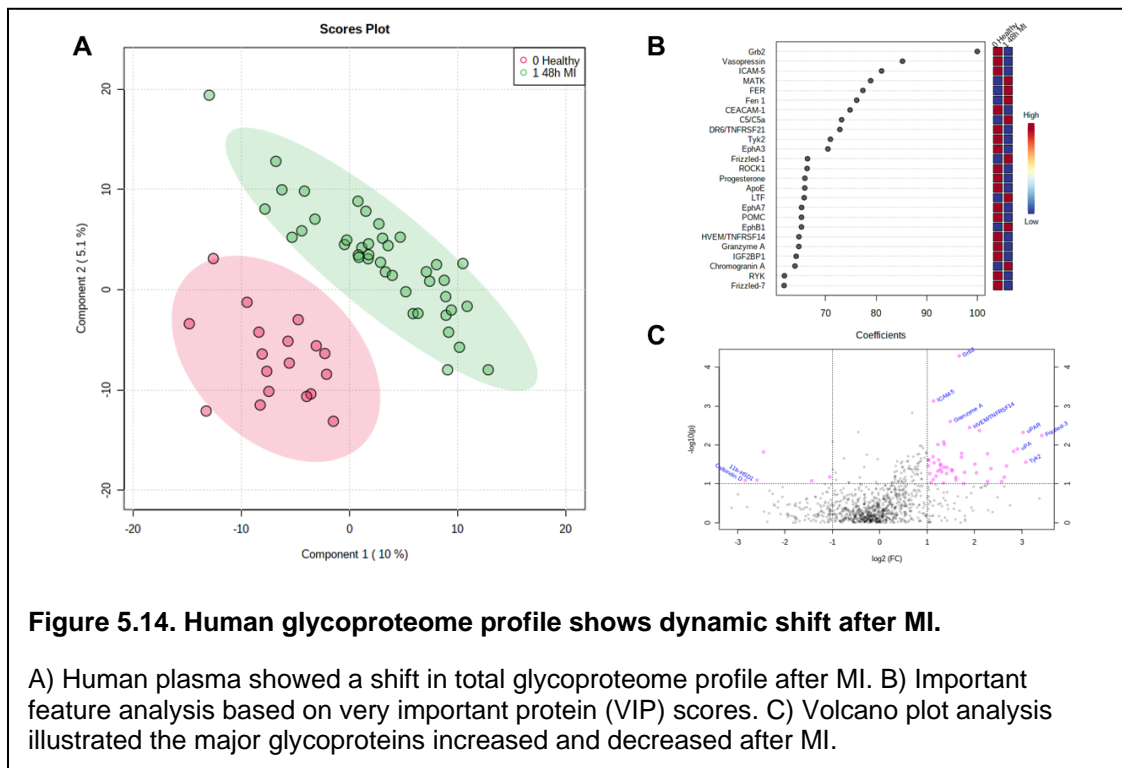
Figure 5.12. TIMP-1 mirrored and predicted cardiac physiology after MI.

A) TIMP-1 increased over the course of MI. TIMP-1 increased from D0 to MI D3 in the retrospective plasma analysis (top). TIMP-1 further increased from MI D3 to D7 in the prospective plasma analysis (bottom). B) Correlation heatmap of MI D7 plasma with D7 LVI tissue, D3 plasma concentrations, and D7 cardiac physiology variables (top). The D7 plasma correlated with ESD, EDD, and ESV. TIMP-1 D7 plasma concentration positively correlated with ESD (bottom). C) Protein-protein interactions between TIMP-1 and the 999 other glycoproteins in human plasma showed cytokine-cytokine receptor signaling as the most enriched pathway (top) and usf2 as the most enriched transcription factor associated with TIMP-1 signaling (bottom).

Human glycoarray analysis revealed a shift in plasma glycoproteome with MI.

The human plasma glycoproteome shifted with MI, as illustrated by partial least squares discriminant analysis (PLS-DA; **Figure 5.8A**). By unpaired t-test, 83 glycoproteins out of 999 increased or decreased after MI (all $p < 0.05$; **Figure 5.8B**). PLS-DA important feature analysis showed Megakaryocyte-associated tyrosine kinase (MATK), Tyrosine-protein kinase fer (FER), and Flap endonuclease 1 (Fen1) as the top

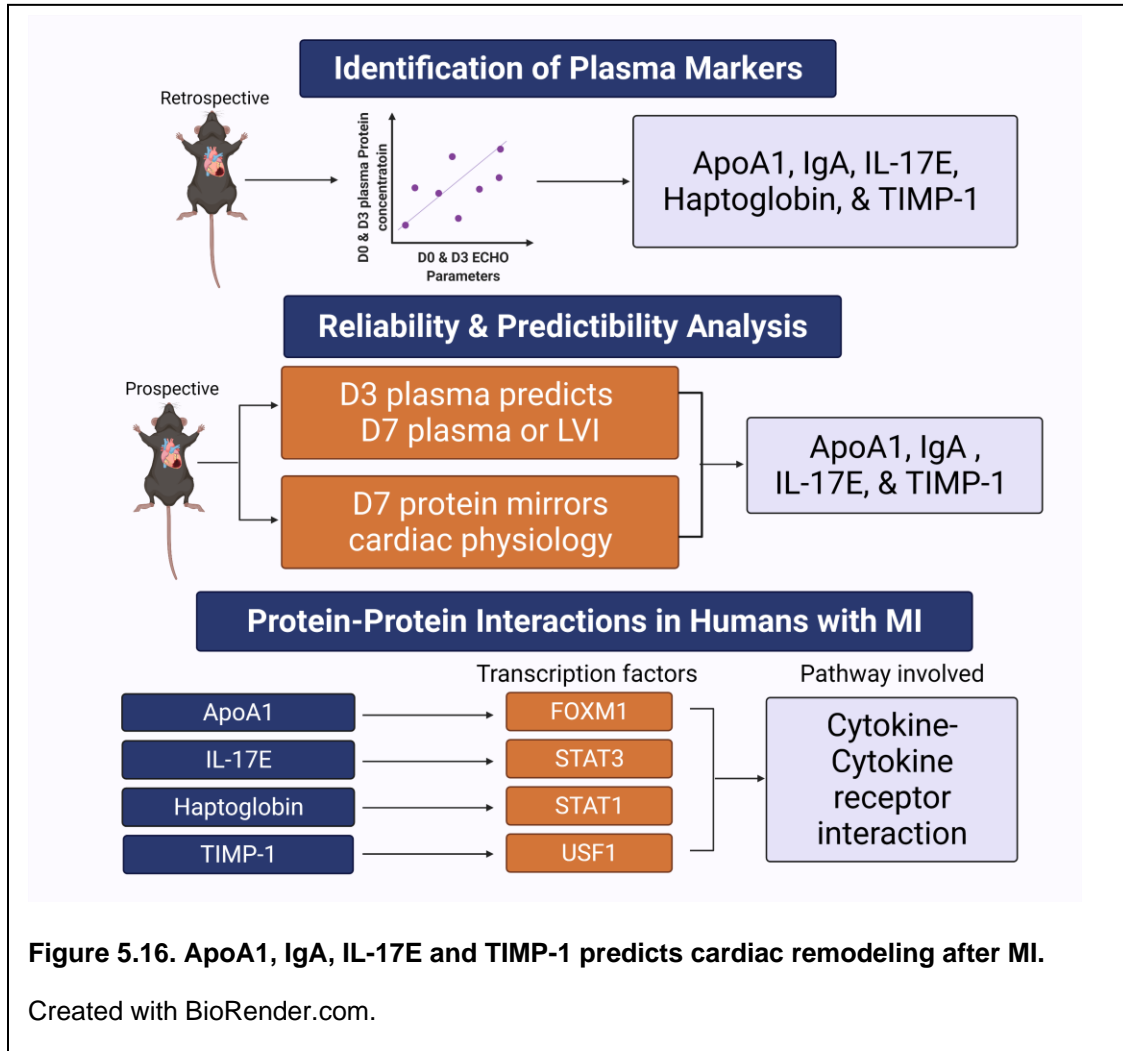
3 increased glycoproteins while Growth factor receptor bound protein 2 (Grb2), Vasopressin, and Intracellular adhesion molecule-5 (ICAM-5) were the top 3 decreased glycoproteins at 48h after MI compared to healthy controls. Volcano plotting showed Grb2 and ICAM-5 as the most increased glycoprotein while Calbindin D and 11 beta hydroxysteroid dehydrogenase type 1 (11b-HSD1) as the largest decreased glycoproteins by combined p-value and fold change (**Figure 5.8C**).



4. Discussion

The objectives of this study were to: 1) identify in a mouse model the plasma proteins at MI D3 that mirror LV wall thickness and dilation; 2) validate candidates in a second cohort for the ability to predict cardiac remodeling at MI D7; and 3) evaluate translation to humans with MI. Five proteins were identified in the MI D3 plasma that mirrored echocardiography: ApoA1, Haptoglobin, IgA, IL-17E, and TIMP-1. Of these proteins, ApoA1, IgA, and IL-17E mirrored current and predicted future adverse cardiac remodeling. In the human cohort, cytokine-cytokine receptor interaction was the most

enriched pathway, with foxm1, stat1, stat3, and usf1 being the most enriched transcription factors. Combined, our results revealed that the inflammatory status of the LV spilling into the plasma can be used to indicate both present and predict future LV infarct wall thinning and dilation (**Figure 5.9**).



ApoA1 is a major component of high-density lipoprotein (HDL) cholesterol, which transports excess cholesterol from peripheral tissues to the liver. ApoA1 was previously identified as a better predictor for ischemic heart disease and cardiovascular mortality than HDL, low-density lipoprotein, or apolipoprotein B.(302) ApoA1 positively correlates with HDL and negatively correlates with c-reactive protein. The Apolipoprotein-related

Mortality RiSk study (AMORIS) showed that increased risk of fatal MI strongly correlated with ApoB/ApoA1 ratio, indicating ApoA1 may serve protective roles prior to MI.(303) However, studies on role of ApoA1 after MI are lacking.

Similar to our observations in mice, increased IL-17E/IL-25 also associates with severity of coronary artery disease in humans.(304) Macrophages and T lymphocytes are the major sources of IL-17E, and both macrophages and T lymphocytes increase under a variety of ischemic conditions, including acute MI and unstable and stable angina pectoris.(304) IL-17E promotes TH2 cytokine responses, and inhibition of IL-17E in cancer increases macrophage and T lymphocyte numbers by inhibiting apoptosis and promoting cellular proliferation.(305, 306) IL-17E promotes angiogenesis by increasing vascular endothelial growth factor signaling in endothelial cells.(307) Our understanding of the role of IL-17E in MI is incomplete and needs further study.

In line with our findings, others have shown that IgA increases with MI.(308, 309) We extend these past observations to show linearity in the increase of plasma IgA level over the course of MI remodeling in mice. Elevated plasma IgA is a marker of previous MI, indicating temporal sustainability in humans.(309) Increased IgA in MI could be due to increased B-cell mediated inflammation. Targeted B-cell therapy has been suggested in atherosclerosis and various cardiovascular diseases.(310) B-cell depletion using monoclonal CD-20 antibody resulted in better MI remodeling through reduced monocyte recruitment.(311, 312)

Haptoglobin is a plasma protein that binds to hemoglobin, and increased binding occurs in response to immune activation. Haptoglobin increases after MI and elevated Haptoglobin is a known risk factor for MI and congestive heart failure.(313-315) The AMORIS study revealed that increased Haptoglobin correlated to higher risk ratio for MI, irrespective of total cholesterol levels.(313) We observed a time specific change in Haptoglobin expression, with an inverted U-shaped pattern in mice over the first week of

MI remodeling, which could be due to inflammation going down after MI D3 as Haptoglobin is a known positive acute phase protein.(316) As such, Haptoglobin is likely a better early diagnostic and prognostic marker of MI outcomes.

TIMP-1 is an endogenous inhibitor of MMPs, including MMP-9.(317) In a human study with 389 males undergoing coronary angiography, TIMP-1 was identified as the only biomarker that could independently predict all-cause mortality and MI.(318) In that study, lower plasma TIMP-1 after MI yielded improved survival rates. TIMP-1 and MMP-9 are documented indicators of cardiac remodeling after MI.(319) The biological function of TIMP-1 may have a U-shaped curve, as animal studies with overexpression of TIMP-1 also show protection.(320)

In the validation cohort, three identified markers, ApoA1, IgA, and IL-17E, extended from MI D3 to D7 in terms of ability of plasma concentrations to mirror current cardiac physiology status. This was important to assess because information on valid clinical equivalence for mouse MI timepoints are not available; and markers that can predict cardiac physiology across MI remodeling timepoints will be valuable for translation. In contrast, Haptoglobin has a small window of predictability, making it easy to miss the optimum evaluation time.

Bioinformatics analyses of the human cohort revealed cytokine-cytokine receptor pathway as the most enriched signaling pathway for all 4 proteins (IgA was not measured in the human cohort). Foxm1, stat3, stat1 and usf2 were the transcription factors associated with ApoA1, IL-17E, Haptoglobin, and TIMP-1. Foxm1 is required for cardiomyocyte development and has cardioprotective properties.(321, 322) Similar to foxm1, activation of stat3 signaling in MI has protective actions to inhibit inflammation.(83, 323) Rapamycin and Empagliflozin both attenuate MI remodeling through actions on cell death and both activating stat3 signaling.(324, 325) Stat1 inhibits autophagy and is detrimental in MI remodeling by promoting inflammation.(326, 327)

While information on usf2 roles in MI is limited, usf2 is one of the top 5 upregulated transcription factors with larger transcription regulator network associated with differentially expressed genes in myocardial infarction, along with stat3.(328) Usf2 is associated with iron overload and regulates hepcidin expression, which increases in the LV remote region after MI.(329) These transcription factors, therefore, are directly and indirectly connected with MI remodeling.

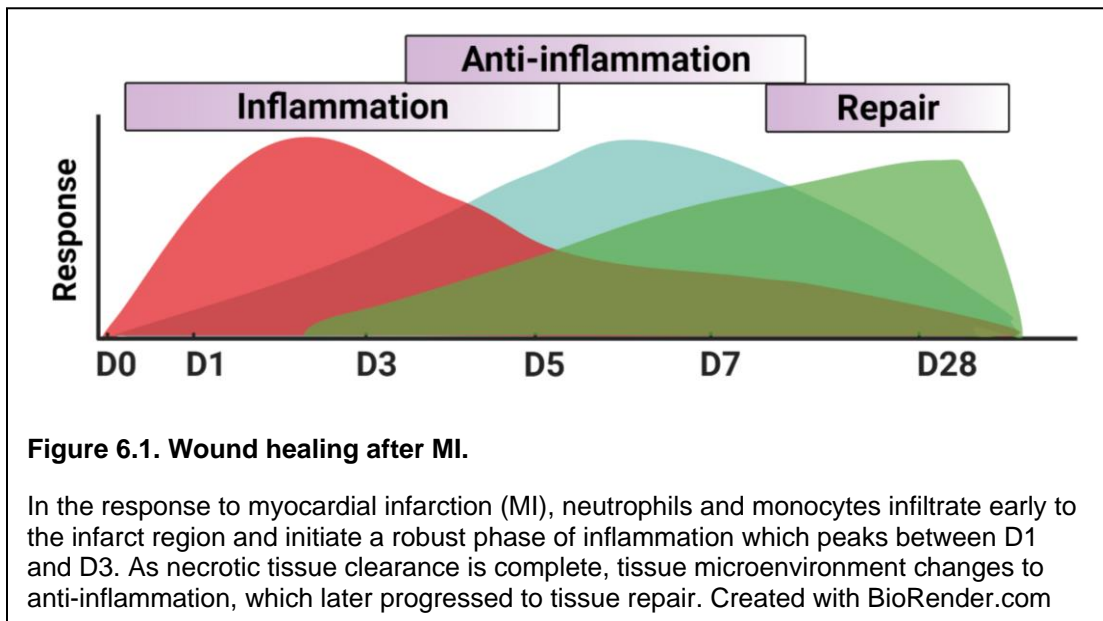
5. Conclusion

Our results revealed that MI shifts the plasma proteome, with ApoA1, IL-17E, IgA, Haptoglobin, and TIMP-1 serving as plasma mirrors of cardiac remodeling. ApoA1, IL-17E, and IgA have an extended window for predicting cardiac physiology after MI, while the window is narrow for Haptoglobin. All markers signal primarily through the cytokine-cytokine receptor interaction pathway. Clinical evaluation of these markers may help to improve early identification of patients vulnerable for later death or development of congestive heart failure.

CHAPTER 6. DISCUSSION

Neutrophil crosstalk during cardiac wound healing after myocardial infarction

When coronary ischemia extends past the point of reversibility, myocardial infarction (MI) ensues and cardiomyocytes undergo necrosis.(7, 330, 331) Myocardial ischemia initiates an early phase of inflammation, which later progresses to tissue repair over the course of MI with change in tissue microenvironment to anti-inflammation (Figure 6.1). Cardiac remodeling after MI is dependent of optimal timing of these phases as they ensure for timely healing of the infarcted myocardium.



Clinically, the current optimal therapy is reperfusion to restore blood flow through the occluded coronary artery.(2) Approximately 25% of patients will not be reperfused, due in part to patients not seeking medical attention early enough.(5, 332-335) In addition, up to 30% of those patients undergoing successful reperfusion therapy will experience no-reflow, a state of myocardial hypoperfusion due to impaired microvascular flow despite the presence of a patent epicardial coronary artery.(6) Combined, this contributes to a significant number of patients undergoing adverse cardiac remodeling

and progressing to heart failure after MI.(7) Heart failure affects over 20 million people worldwide,(336, 337) and MI is the underlying etiology for the majority of heart failure cases.(8, 338, 339) Despite research efforts to improve the clinical scenario, the 5 year mortality for heart failure has not changed over the past 50 years and remains at 50%.(337)

Cardiomyocyte death releases danger associated molecular patterns (DAMPs) and initiates the complement cascade that brings in inflammatory leukocytes from the circulation.(119, 340) The entry of leukocytes into the infarct region begins a series of wound healing events that transcend through pro-inflammation to anti-inflammation to tissue repair phases, culminating in the generation of an infarct scar that provides architectural and structural support to the infarcted left ventricle.(91) While macrophages are initially the first to infiltrate, neutrophils quickly overtake by numbers, and at MI day 1 in the mouse non-reperfused MI model are the predominant leukocytes in the infarct.(184, 341) Neutrophil numbers peak at MI days 1 and 3, slowly returning towards baseline numbers by day 7.(32, 158, 171, 342) During this period, the neutrophil interacts with the cardiomyocyte, macrophage, fibroblast, and endothelial cell to coordinate the wound healing response.(172) Neutrophil interactions with endothelial cells during diapedesis have been well studied.(173) A half of this thesis focused on the importance of neutrophils in MI wound healing, primarily focusing on their crosstalk with cardiomyocytes and macrophages in the MI heart to regulated wall thinning after MI **(Figure 6.2).**

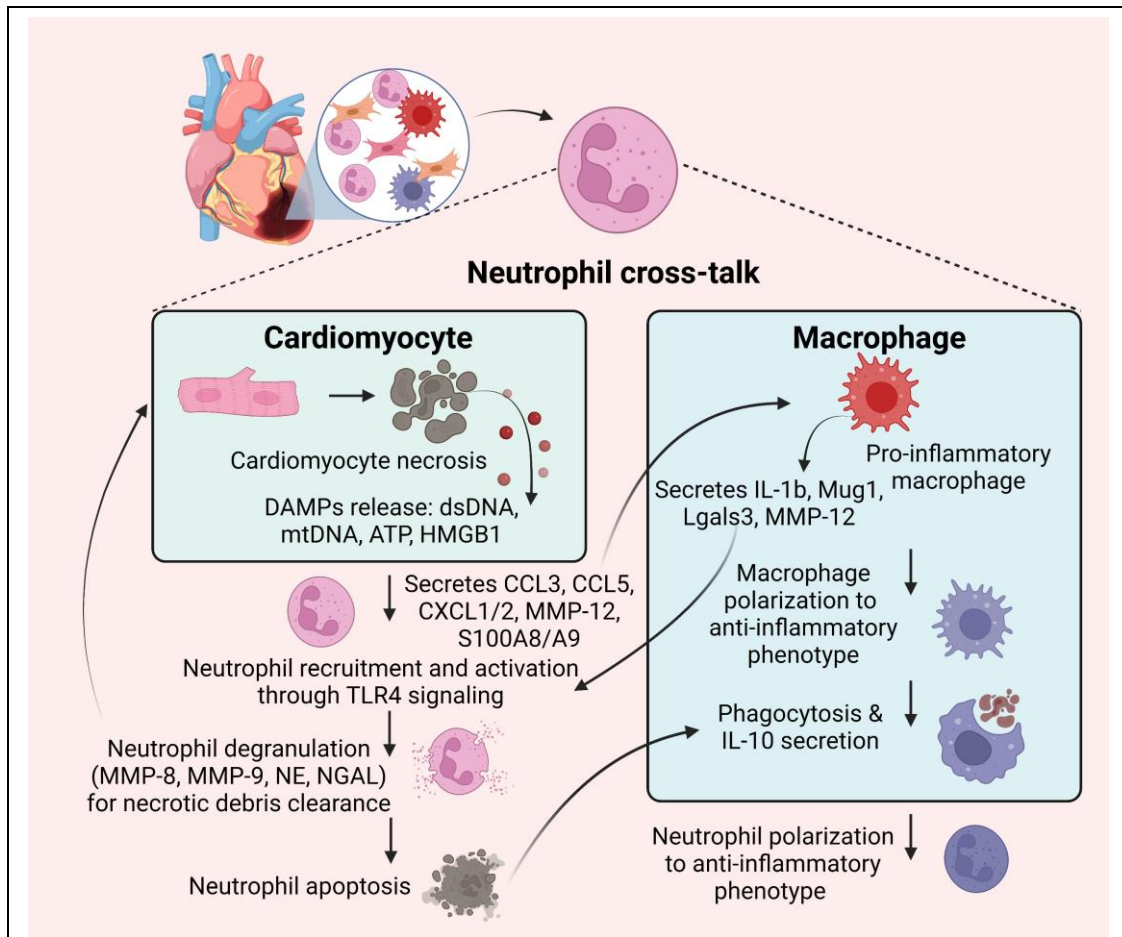


Figure 6.3. Neutrophil crosstalk after MI.

In the response to myocardial infarction (MI), neutrophils communicate with cardiomyocytes and macrophages. Necrotic cardiomyocytes release damage associated molecular patterns (DAMPs) that stimulate neutrophil infiltration. At the site of the infarct, neutrophils are pro-inflammatory and degranulate to release proteases such as matrix metalloproteinase (MMP)-8, MMP-9 and neutrophil elastase (NE) along with neutrophil gelatinase-associated lipocalin (NGAL) that break down the extracellular matrix to release necrotic cardiomyocytes. Pro-inflammatory neutrophils bring in pro-inflammatory macrophages to amplify the inflammatory response through secretion of interleukin (IL)-1 β , Mug1, Lgals3, and MMP-12. As wound healing progresses to the anti-inflammation phase, macrophages phagocytose apoptotic neutrophils and necrotic cardiomyocytes and secrete IL-10 to convert neutrophils and macrophages to an anti-inflammatory phenotype. Created with BioRender.com.

1. Neutrophil cross talk at MI day 1.

The pro-inflammatory neutrophil peaks at MI day 1.(171, 222) In response to MI, neutrophils are activated and infiltrate into the infarct region where they interact with the necrotic cardiomyocyte and other inflammatory cells. To infiltrate into the infarct, the

neutrophil interacts with endothelial cells within the coronary vasculature to promote its extravasation. Neutrophils recruited from the bone marrow to the circulation sheds L-selectin (CD-62L) upon activation. L-selectin and ICAM-1 interactions are required for adhesion, neutrophil rolling across endothelial cells and diapedesis.(173, 343) L-Selectin and ICAM-1 on the endothelial cell work in concert to mediate neutrophil diapedesis by regulating adhesion.(30) Cytokines such as IL-8 and TNF- α induces L-selectin shedding and neutrophil entry to the infarct.(30)

The MI day 1 neutrophil is a pro-inflammatory cell that promotes and amplifies the inflammatory response by working in concert with necrotic cardiomyocytes and activated resident fibroblasts to signal the further influx of leukocytes.(173, 344) Neutrophils release a number of chemotactic factors (i.e., CCL3/macrophage inflammatory protein (MIP)-1 α , CCL5/RANTES, CXCL1 and CXCL2) that drive the influx of pro-inflammatory macrophages in a positive feedback mechanism.(173, 345) Further, neutrophils also secrete endogeneous DAMPs such as S100A8 and S100A9 which induces further granulopoiesis through interleukin (IL)-1 β secretion and toll like receptor (TLR)4 activation.(142, 346) The pro-inflammatory MI microenvironment is maintained by infiltrating neutrophils through production of pro-inflammatory cytokines such as IL-1 β .(347) Reactive oxygen species (ROS) produced by neutrophils activates the inflammasome to further augment IL-1 β signaling.(348) IL-1 β prevents fibroblast proliferation and myofibroblast activation and increases production of MMP-3 and MMP-8 to increase collagen degradation.(344, 347, 349)

Another primary role of the pro-inflammatory neutrophil is to degranulate, releasing proteases that degrade the extracellular matrix (ECM) surrounding the necrotic cardiomyocyte.(22) This is a necessary step in the wound healing process to remove necrotic debris and provide space for the infarct scar. If there is too much degradation of existing ECM before new ECM can form, the result is excessive infarct wall thinning. In

the non-reperfused MI model in mice, this can lead to rupture.(66) In humans, while rupture is not as prevalent as it was before the advent of reperfusion, LV aneurysms can form, yielding a weakened ventricular architecture.(350) Excessive infarct wall thinning can amplify dilation of the left ventricle and stimulate the progression to heart failure.(22) The neutrophils also contain components that indirectly influence wall thinning, such as S100A9.(147) S100A9 forms a heterodimer with S100A8, *in vivo*. Short term blockade of S100A9 improves cardiac physiology after MI.(147) S100A9 has been discussed as a potential therapeutic target after MI that directly targets the immune cell population.(148, 156)

While depletion of pro-inflammatory neutrophils is in theory a logical therapeutic plan, the actual implementation has consistently been unsuccessful. Early attempts to block inflammation using methylprednisolone yielded promising results in animal models, followed by a clinical trial that yielded cardiac rupture and consequently was terminated early.(170, 351) Since that time, therapy has been more directly targeted at the neutrophil or particular neutrophil components, to similar results.(147, 186) Steffens and colleagues demonstrated that neutrophils release neutrophil gelatinase associated lipocalin (NGAL) that directly stimulates macrophages to convert to a reparative phenotype.(180, 198) Inhibiting neutrophils as a global strategy, therefore, prevents macrophage conversion.

2. Neutrophil cross talk at MI day 3.

The anti-inflammatory neutrophil peaks at MI day 3.(171, 222) The MI day 3 neutrophil is apoptotic, with high cathepsin activity and roles in ECM reorganization.(222) The anti-inflammatory neutrophil is characterized by high expression of Ly6G and CD206, which continue to increase until MI day 7.(171) Neutrophils cross-talk with macrophages at MI day 3 primarily by undergoing apoptosis and being phagocytosed by the macrophage.(184)

Rather than inhibiting the pro-inflammatory neutrophil, which is necessary for later anti-inflammation and repair, an effective strategy may be to promote early anti-inflammation instead. When IL-4 is endogenously administered by subcutaneous infusion beginning at MI day 1, the MI day 3 neutrophil shows less pro-inflammation (CCL3, IL-12a, TGF- β 1, and TNF- α) while the macrophage shows more anti-inflammation (ARG1 and YM1).(118) The IL-4 treatment showed increased phagocytosis of apoptotic neutrophils by MI day 3 macrophages, without a change in necrotic myocyte uptake, and this effect is mediated through FCGF2b, MERTK, and MRC1.(118)

Resolution promoting factors (RPFs) regulate inflammation and promote tissue repair after MI by targeting immune cell trafficking, their activation and cytokine production.(114, 352) Known resolution promoting factors include resolvin E1, lipoxin A4, MMP-12, and protectin-D1 which enhance MI wound repair by targeting neutrophils.(198, 277, 352, 353) Similarly, annexin A1, a neutrophil derived microvesicle protein is also known to inhibit inflammation by targeting leukocyte infiltration.(354, 355) Neutrophils at MI day 3 also secrete factors such as fibronectin and fibrinogen that stimulate fibroblasts to proliferate and help with ECM reorganization.(222) Therapeutically modifying the neutrophil at MI day 3 for optimum effect would include promoting apoptosis of lingering pro-inflammatory neutrophils and stimulating the conversion of anti-inflammatory and reparative neutrophils.

3. Neutrophils cross talk at MI days 5-7.

The reparative neutrophil peaks at MI days 5-7.(171, 222) At this time, the neutrophil is characterized by roles in repair and ECM reorganization.(222, 356) While the reparative neutrophil cross talks with macrophages, fibroblasts, and endothelial cells, the direct role of neutrophils in tissue repair has been understudied. Neutrophils at MI day 5 and 7 have increased protein expression of several reparative factors, including fibrinogen, cathepsin B, S100A4, fibronectin, thrombospondin-2, Igals3, MMP-2, tissue

inhibitor of metalloproteinase (TIMP)-2, and vitronectin.(222) Both neutrophil secreted fibronectin and Igals3 autoregulate MMP-9 release, as MMP-9 degrades fibronectin and Igals3. Neutrophil to fibroblast cross talk occurs in part through ECM mediators such as fibrinogen, which stimulates fibroblast proliferation.(50) The increase in TIMP-2 would prevent further ECM breakdown to turn off necrotic cardiomyocyte debris removal after it is no longer needed. At the same time, the increased expression of MMP-2 may indicate a neo-homeostatic role to help maintain the infarct scar, as MMP-2 is linked to cardiomyocyte homeostasis.(51)

The need for the neutrophil to convert to an anti-inflammatory and reparative phenotype is illustrated by studies that prevent conversion. When MMP-12 is inhibited using the specific inhibitor RXP 470.1 initiated at 3 hours after MI, neutrophils do not undergo apoptosis and cardiac remodeling is worsened at MI day 7 (more dilation, more remodeling, and lower ejection fraction).(36) Neutrophils both produce and respond to MMP-12, as MMP-12 itself directly stimulates neutrophils in vitro to undergo apoptosis by activating caspase 3.(36) Therapeutically stimulating the reparative neutrophil is a promising area that needs further investigation.(180, 186, 198)

4. Identifying therapeutic targets after myocardial infarction

Exploring disease proteomics has been an excellent method for recognition of therapeutic targets.(290, 357, 358) As my thesis focuses on identifying potential therapeutic targets, I used proteomics to study cellular specific protein targets and plasma-derived protein targets. As I discussed how neutrophil target mapping would be beneficial for modulating neutrophil physiology for therapeutic benefit in the previous section, harnessing plasma proteomics would be equally beneficial as it is a noninvasive and translational way for identifying prognostic, diagnostic and functional markers of cardiac remodeling.(359)

Plasma reflects the ECM changes in the heart after myocardial infarction.(360) Targeted proteomics allows to identify low abundance proteins in the plasma that reflects cardiac physiology changes.(361) Various factors has been previously identified that are helpful for diagnosis of myocardial infarction. However, identification of plasma markers that mirrors extent of adverse cardiac remodeling has been lacking. My study shows the possibility of using markers to predict future progression to heart failure and potential MI outcomes. This would be highly valuable for personalizing medicine and improving therapeutic precision.

One of the major findings of my study is that acute phase proteins such as Haptoglobin are good marker of diagnosis as it is a time-specific marker. Acute phase proteins do not mirror overall cardiac physiology after MI in a wholesome manner, as previously thought.(362) ApoA1 highlights the potential of targeting lipoproteins in MI, while IL-17E demands for further extensive study as it has not been explored. On the other hand, immunoglobulins mirroring cardiac dysfunction after myocardial infarction hints for humoral immunity component in MI which has not as equally been appreciates as innate immunity.(363) This suggests for B-cell having significant role in regulating wound healing phase and heart failure progression, in overall.(364) TIMP-1 is a strong ECM component which has complex and essential role in myocardial infarction.(364)

Integrated omics is one major component of my study as it links proteomics to previously studied and identified results to give a comprehensive result through bioinformatics application.(365, 366) Identification of potential pathway involved and enriched transcription factors further allows for delineation of potential targets for further research.

5. Future Directions and Conclusions

The knowledge of MI wound healing and the role of inflammation has been amplified over the last decade. While our knowledge has grown exponentially, question

remain on how to modify the neutrophil to allow optimal wound healing to occur in a controlled way. A crucial component to consider is the time and space of where in the MI remodeling continuum the response is when the intervention occurs. We know that excessive neutrophil function is detrimental, and amplified release of neutrophil components can extend the initial injury. At the same time, we know that early complete neutrophil depletion impairs wound healing, indicating that there is a need for neutrophils and the infarct to proceed through the pro-inflammatory phase before repair can be accomplished. The neutrophil has been the target of many interventions, all with a general lack of success, and we must glean information from those studies to identify new targets that temper rather than exclude components of the wound healing process.

Along these lines, there is a need to triangulate information when developing experimental designs that target the neutrophil and the overall MI wound healing.(367) With the information already obtained by the MI remodeling community, this area is ripe for evaluation using computational modeling approaches. Simulation experiments may provide a means to quickly test effects of interventions on neutrophil responses, and such approaches have been exploited for the understanding of complex cellular signaling and immune responses.(368) Computational modeling of the macrophage and fibroblast have yielded insights into their cell physiology in MI, and similar approaches would likely be fruitful for the neutrophil.(369, 370) These approaches may also improve the rigor and reproducibility of research targeting the neutrophil by unveiling connections that would not be observed using traditional *in vitro* and *in vivo* approaches, thus increasing odds of translating a novel therapy. Recent guidelines provide extensive information on how to use the MI model in mice to understand how the neutrophil regulates cardiac remodeling.(113) This can be used to further our research on identified predictors to study their functional predictability.

In conclusion, the neutrophil cross talks with several cell types, including cardiomyocytes and macrophages during MI wound healing to coordinate the cardiac remodeling process. The neutrophil remains a viable candidate for intervention if we can figure out the optimal conditions of modification to achieve a favorable and predictable outcome. Previous studies focusing on anti-inflammation alone has shown that pro-inflammation is extremely important in MI wound healing. A new challenge lies in identification of an optimum timeline to limit inflammation and promote anti-inflammation. Moderation of inflammation and modulation of the inflammatory phase might take us to the next avenue in myocardial infarction research.

BIBLIOGRAPHY

1. Thygesen K, Alpert JS, White HD, Joint ESCAAHAWHFTFftRoMI, Jaffe AS, Apple FS, Galvani M, Katus HA, Newby LK, Ravkilde J, Chaitman B, Clemmensen PM, Dellborg M, Hod H, Porela P, Underwood R, Bax JJ, Beller GA, Bonow R, Van der Wall EE, Bassand JP, Wijns W, Ferguson TB, Steg PG, Uretsky BF, Williams DO, Armstrong PW, Antman EM, Fox KA, Hamm CW, Ohman EM, Simoons ML, Poole-Wilson PA, Gurfinkel EP, Lopez-Sendon JL, Pais P, Mendis S, Zhu JR, Wallentin LC, Fernandez-Aviles F, Fox KM, Parkhomenko AN, Priori SG, Tendera M, Voipio-Pulkki LM, Vahanian A, Camm AJ, De Caterina R, Dean V, Dickstein K, Filippatos G, Funck-Brentano C, Hellemans I, Kristensen SD, McGregor K, Sechtem U, Silber S, Tendera M, Widimsky P, Zamorano JL, Morais J, Brener S, Harrington R, Morrow D, Lim M, Martinez-Rios MA, Steinhubl S, Levine GN, Gibler WB, Goff D, Tubaro M, Dudek D, and Al-Attar N. Universal definition of myocardial infarction. *Circulation* 116: 2634-2653, 2007.
2. Ibanez B, James S, Agewall S, Antunes MJ, Bucciarelli-Ducci C, Bueno H, Caforio AL, Crea F, Goudevenos JA, and Halvorsen S. 2017 ESC Guidelines for the management of acute myocardial infarction in patients presenting with ST-segment elevation: The Task Force for the management of acute myocardial infarction in patients presenting with ST-segment elevation of the European Society of Cardiology (ESC). *European heart journal* 39: 119-177, 2018.
3. Roe MT, Parsons LS, Pollack CV, Canto JG, Barron HV, Every NR, Rogers WJ, Peterson ED, and Investigators NRoMI. Quality of care by classification of myocardial infarction: treatment patterns for ST-segment elevation vs non-ST-segment elevation myocardial infarction. *Archives of internal medicine* 165: 1630-1636, 2005.
4. Members C, Ryan TJ, Anderson JL, Antman EM, Braniff BA, Brooks NH, Califf RM, Hillis LD, Hiratzka LF, and Rapaport E. ACC/AHA guidelines for the management of patients with acute myocardial infarction: a report of the American College of Cardiology/American Heart Association Task Force on Practice Guidelines (Committee on Management of Acute Myocardial Infarction). *Journal of the American College of Cardiology* 28: 1328-1419, 1996.
5. Lindsey ML, Brás LE, DeLeon-Pennell KY, Frangogiannis NG, Halade GV, O'Meara CC, Spinale FG, Kassiri Z, Kirk JA, Kleinbongard P, Ripplinger CM, and Brunt KR. Reperused vs. nonreperused myocardial infarction: when to use which model. *American Journal of Physiology-Heart and Circulatory Physiology* 321: H208-H213, 2021.
6. Rezkalla SH, and Kloner RA. No-reflow phenomenon. *Circulation* 105: 656-662, 2002.
7. Reed GW, Rossi JE, and Cannon CP. Acute myocardial infarction. *Lancet* 389: 197-210, 2017.
8. Roger VL. Epidemiology of heart failure. *Circ Res* 113: 646-659, 2013.
9. Cahill TJ, and Kharbanda RK. Heart failure after myocardial infarction in the era of primary percutaneous coronary intervention: mechanisms, incidence and identification of patients at risk. *World journal of cardiology* 9: 407, 2017.
10. Ho JE, Lyass A, Lee DS, Vasan RS, Kannel WB, Larson MG, and Levy D. Predictors of new-onset heart failure: differences in preserved versus reduced ejection fraction. *Circulation: heart failure* 6: 279-286, 2013.
11. Mouton AJ, Rivera OJ, and Lindsey ML. Myocardial infarction remodeling that progresses to heart failure: A signaling misunderstanding. *American Journal of Physiology - Heart and Circulatory Physiology* 315: H71-H79, 2018.
12. Guo Y, Flaherty MP, Wu WJ, Tan W, Zhu X, Li Q, and Bolli R. Genetic background, gender, age, body temperature, and arterial blood pH have a major impact on myocardial infarct size in the mouse and need to be carefully measured and/or taken into account: results of a comprehensive analysis of determinants of infarct size in 1,074 mice. *Basic Res Cardiol* 107: 288, 2012.
13. Yeap XY, Dehn S, Adelman J, Lipsitz J, and Thorp EB. Quantitation of acute necrosis after experimental myocardial infarction. *Methods Mol Biol* 1004: 115-133, 2013.
14. Frangogiannis NG. The inflammatory response in myocardial injury, repair, and remodelling. *Nat Rev Cardiol* 11: 255-265, 2014.

15. **Dewald O, Ren G, Duerr GD, Zoerlein M, Klemm C, Gersch C, Tincey S, Michael LH, Entman ML, and Frangogiannis NG.** Of mice and dogs: species-specific differences in the inflammatory response following myocardial infarction. *Am J Pathol* 164: 665-677, 2004.
16. **Dobaczewski M, Bujak M, Zymek P, Ren G, Entman ML, and Frangogiannis NG.** Extracellular matrix remodeling in canine and mouse myocardial infarcts. *Cell Tissue Res* 324: 475-488, 2006.
17. **Dutta P, Hoyer FF, Grigoryeva LS, Sager HB, Leuschner F, Courties G, Borodovsky A, Novobrantseva T, Ruda VM, Fitzgerald K, Iwamoto Y, Wojtkiewicz G, Sun Y, Da Silva N, Libby P, Anderson DG, Swirski FK, Weissleder R, and Nahrendorf M.** Macrophages retain hematopoietic stem cells in the spleen via VCAM-1. *J Exp Med* 212: 497-512, 2015.
18. **S BG, Gowda D, Kain V, Chiba H, Hui SP, Chalfant CE, Parcha V, Arora P, and Halade GV.** Sphingosine-1-phosphate interactions in the spleen and heart reflect extent of cardiac repair in mice and failing human hearts. *Am J Physiol Heart Circ Physiol* 321: H599-h611, 2021.
19. **Kain V, and Halade GV.** Role of neutrophils in ischemic heart failure. *Pharmacology & therapeutics* 205: 107424, 2020.
20. **Halade GV, Kain V, and Ingle KA.** Heart functional and structural compendium of cardiopleuric and cardiorenal networks in acute and chronic heart failure pathology. *Am J Physiol Heart Circ Physiol* 314: H255-h267, 2018.
21. **Ma Y, Yabluchanskiy A, Iyer RP, Cannon PL, Flynn ER, Jung M, Henry J, Cates CA, DeLeon-Pennell KY, and Lindsey ML.** Temporal neutrophil polarization following myocardial infarction. *Cardiovascular research* 110: 51-61, 2016.
22. **Daseke MJ, 2nd, Chalise U, Becirovic-Agic M, Salomon JD, Cook LM, Case AJ, and Lindsey ML.** Neutrophil signaling during myocardial infarction wound repair. *Cell Signal* 77: 109816, 2021.
23. **Mouton AJ, DeLeon-Pennell KY, Rivera Gonzalez OJ, Flynn ER, Freeman TC, Saucerman JJ, Garrett MR, Ma Y, Harmancey R, and Lindsey ML.** Mapping macrophage polarization over the myocardial infarction time continuum. *Basic Res Cardiol* 113: 26, 2018.
24. **Zaidi Y, Corker A, Vasileva VY, Oviedo K, Graham C, Wilson K, Martino J, Troncoso M, Broughton P, Ilatovskaya DV, Lindsey ML, and DeLeon-Pennell KY.** Chronic *Porphyromonas gingivalis* lipopolysaccharide induces adverse myocardial infarction wound healing through activation of CD8(+) T cells. *Am J Physiol Heart Circ Physiol* 321: H948-h962, 2021.
25. **Zaidi Y, Aguilar EG, Troncoso M, Ilatovskaya DV, and DeLeon-Pennell KY.** Immune regulation of cardiac fibrosis post myocardial infarction. *Cell Signal* 77: 109837, 2021.
26. **Mouton AJ, Ma Y, Rivera Gonzalez OJ, Daseke MJ, 2nd, Flynn ER, Freeman TC, Garrett MR, DeLeon-Pennell KY, and Lindsey ML.** Fibroblast polarization over the myocardial infarction time continuum shifts roles from inflammation to angiogenesis. *Basic Res Cardiol* 114: 6, 2019.
27. **Christopher MJ, Liu F, Hilton MJ, Long F, and Link DC.** Suppression of CXCL12 production by bone marrow osteoblasts is a common and critical pathway for cytokine-induced mobilization. *Blood, The Journal of the American Society of Hematology* 114: 1331-1339, 2009.
28. **Wang Y, Dembowski K, Chevalier E, Stüve P, Korf-Klingebiel M, Lochner M, Napp LC, Frank H, Brinkmann E, and Kanwischer A.** CXC motif chemokine receptor 4 blockade promotes tissue repair after myocardial infarction by enhancing regulatory T cell mobilization and immune-regulatory function. *Circulation* 139: 1798-1812, 2019.
29. **Hess A, Derlin T, Koenig T, Diekmann J, Wittneben A, Wang Y, Wester H-J, Ross TL, Wollert KC, and Bauersachs J.** Molecular imaging-guided repair after acute myocardial infarction by targeting the chemokine receptor CXCR4. *European Heart Journal* 41: 3564-3575, 2020.
30. **Hafezi-Moghadam A, Thomas KL, Prorock AJ, Huo Y, and Ley K.** L-selectin shedding regulates leukocyte recruitment. *The Journal of experimental medicine* 193: 863-872, 2001.
31. **Deniset JF, and Kubes P.** Recent advances in understanding neutrophils. *F1000Research* 5: 2016.

32. **Vafadarnejad E, Rizzo G, Krampert L, Arampatzi P, Arias-Loza A-P, Nazzal Y, Rizakou A, Knochenhauer T, Bandi SR, and Nugroho VA.** Dynamics of cardiac neutrophil diversity in murine myocardial infarction. *Circulation research* 127: e232-e249, 2020.
33. **Faxon DP, Gibbons RJ, Chronos NA, Gurbel PA, Sheehan F, and Investigators H-M.** The effect of blockade of the CD11/CD18 integrin receptor on infarct size in patients with acute myocardial infarction treated with direct angioplasty: the results of the HALT-MI study. *Journal of the American College of Cardiology* 40: 1199-1204, 2002.
34. **Becirovic-Agic M, Chalise U, Daseke MJ, 2nd, Konfrst S, Salomon JD, Mishra PK, and Lindsey ML.** Infarct in the Heart: What's MMP-9 Got to Do with It? *Biomolecules* 11: 2021.
35. **Horckmans M, Ring L, Duchene J, Santovito D, Schloss MJ, Drechsler M, Weber C, Soehnlein O, and Steffens S.** Neutrophils orchestrate post-myocardial infarction healing by polarizing macrophages towards a reparative phenotype. *European heart journal* 38: 187-197, 2017.
36. **Iyer RP, Patterson NL, Zouein FA, Ma Y, Dive V, de Castro Brás LE, and Lindsey ML.** Early matrix metalloproteinase-12 inhibition worsens post-myocardial infarction cardiac dysfunction by delaying inflammation resolution. *Int J Cardiol* 185: 198-208, 2015.
37. **Mouton AJ, Rivera Gonzalez OJ, Kaminski AR, Moore ET, and Lindsey ML.** Matrix metalloproteinase-12 as an endogenous resolution promoting factor following myocardial infarction. *Pharmacol Res* 137: 252-258, 2018.
38. **Daseke MJ, Valerio FM, Kalusche WJ, Ma Y, DeLeon-Pennell KY, and Lindsey ML.** Neutrophil proteome shifts over the myocardial infarction time continuum. *Basic research in cardiology* 114: 1-13, 2019.
39. **Prince LR, Prosseda SD, Higgins K, Carlring J, Prestwich EC, Ogryzko NV, Rahman A, Basran A, Falciani F, and Taylor P.** NR4A orphan nuclear receptor family members, NR4A2 and NR4A3, regulate neutrophil number and survival. *Blood, The Journal of the American Society of Hematology* 130: 1014-1025, 2017.
40. **Gopalkrishna S, Johnson J, Jaggars RM, Dahdah A, Murphy AJ, Hanssen NM, and Nagareddy PR.** Neutrophils in cardiovascular disease: Warmongers, peacemakers or both? *Cardiovascular Research* 2021.
41. **Jin F, Zhai Q, Qiu L, Meng H, Zou D, Wang Y, Li Q, Yu Z, Han J, Li Q, and Zhou B.** Degradation of BM SDF-1 by MMP-9: the role in G-CSF-induced hematopoietic stem/progenitor cell mobilization. *Bone Marrow Transplant* 42: 581-588, 2008.
42. **Kumar KP, Nicholls AJ, and Wong CH.** Partners in crime: neutrophils and monocytes/macrophages in inflammation and disease. *Cell and tissue research* 371: 551-565, 2018.
43. **Ma Y.** Role of Neutrophils in Cardiac Injury and Repair Following Myocardial Infarction. *Cells* 10: 2021.
44. **Hofbauer TM, Mangold A, Scherz T, Seidl V, Panzenböck A, Ondracek AS, Müller J, Schneider M, Binder T, and Hell L.** Neutrophil extracellular traps and fibrocytes in ST-segment elevation myocardial infarction. *Basic research in cardiology* 114: 1-15, 2019.
45. **DeLeon-Pennell KY, Tian Y, Zhang B, Cates CA, Iyer RP, Cannon P, Shah P, Aiyetan P, Halade GV, Ma Y, Flynn E, Zhang Z, Jin Y-F, Zhang H, and Lindsey ML.** CD36 Is a Matrix Metalloproteinase-9 Substrate That Stimulates Neutrophil Apoptosis and Removal During Cardiac Remodeling. *Circ Cardiovasc Genet* 9: 14-25, 2016.
46. **Chwieralski CE, Welte T, and Bühling F.** Cathepsin-regulated apoptosis. *Apoptosis* 11: 143-149, 2006.
47. **Conus S, Pop C, Snipas SJ, Salvesen GS, and Simon HU.** Cathepsin D primes caspase-8 activation by multiple intra-chain proteolysis. *J Biol Chem* 287: 21142-21151, 2012.
48. **Kettritz R, Xu Y-X, Kerren T, Quass P, Klein J, Luft FC, and Haller H.** Extracellular matrix regulates apoptosis in human neutrophils. *Kidney International* 55: 562-571, 1999.
49. **McCutcheon JC, Hart SP, Canning M, Ross K, Humphries MJ, and Dransfield I.** Regulation of macrophage phagocytosis of apoptotic neutrophils by adhesion to fibronectin. *J Leukoc Biol* 64: 600-607, 1998.
50. **Gray AJ, Bishop JE, Reeves JT, and Laurent GJ.** A alpha and B beta chains of fibrinogen stimulate proliferation of human fibroblasts. *J Cell Sci* 104 (Pt 2): 409-413, 1993.

51. **DeCoux A, Lindsey ML, Villarreal F, Garcia RA, and Schulz R.** Myocardial matrix metalloproteinase-2: inside out and upside down. *J Mol Cell Cardiol* 77: 64-72, 2014.
52. **Daseke MJ, 2nd, Tenkorang-Impraim MAA, Ma Y, Chalise U, Konfrst SR, Garrett MR, DeLeon-Pennell KY, and Lindsey ML.** Exogenous IL-4 shuts off pro-inflammation in neutrophils while stimulating anti-inflammation in macrophages to induce neutrophil phagocytosis following myocardial infarction. *J Mol Cell Cardiol* 145: 112-121, 2020.
53. **Liu X, Zhang J, Zeigler AC, Nelson AR, Lindsey ML, and Saucerman JJ.** Network Analysis Reveals a Distinct Axis of Macrophage Activation in Response to Conflicting Inflammatory Cues. *J Immunol* 206: 883-891, 2021.
54. **Kalafati L, Kourtzelis I, Schulte-Schrepping J, Li X, Hatzioannou A, Grinenko T, Hagag E, Sinha A, Has C, and Dietz S.** Innate immune training of granulopoiesis promotes anti-tumor activity. *Cell* 183: 771-785. e712, 2020.
55. **Zhao B, Lu R, Chen J, Xie M, Zhao X, and Kong L.** S100A9 blockade prevents lipopolysaccharide-induced lung injury via suppressing the NLRP3 pathway. *Respiratory Research* 22: 1-11, 2021.
56. **Gebhardt C, Németh J, Angel P, and Hess J.** S100A8 and S100A9 in inflammation and cancer. *Biochemical pharmacology* 72: 1622-1631, 2006.
57. **Volz HC, Laohachewin D, Seidel C, Lasitschka F, Keilbach K, Wienbrandt AR, Andrassy J, Bierhaus A, Kaya Z, and Katus HA.** S100A8/A9 aggravates post-ischemic heart failure through activation of RAGE-dependent NF- κ B signaling. *Basic research in cardiology* 107: 250, 2012.
58. **Pullen AB, Kain V, Serhan CN, and Halade GV.** Molecular and Cellular Differences in Cardiac Repair of Male and Female Mice. *J Am Heart Assoc* 9: e015672, 2020.
59. **Tourki B, Kain V, Pullen AB, Norris PC, Patel N, Arora P, Leroy X, Serhan CN, and Halade GV.** Lack of resolution sensor drives age-related cardiometabolic and cardiorenal defects and impedes inflammation-resolution in heart failure. *Mol Metab* 31: 138-149, 2020.
60. **DeLeon-Pennell KY, and Lindsey ML.** Somewhere over the sex differences rainbow of myocardial infarction remodeling: hormones, chromosomes, inflammasome, oh my. *Expert Rev Proteomics* 16: 933-940, 2019.
61. **DeLeon-Pennell KY, Mouton AJ, Ero OK, Ma Y, Padmanabhan Iyer R, Flynn ER, Espinoza I, Musani SK, Vasan RS, Hall ME, Fox ER, and Lindsey ML.** LXR/RXR signaling and neutrophil phenotype following myocardial infarction classify sex differences in remodeling. *Basic Res Cardiol* 113: 40, 2018.
62. **Zhao M, Wang DD, Liu X, and Tian R.** Metabolic Modulation of Macrophage Function Post Myocardial Infarction. *Front Physiol* 11: 674, 2020.
63. **Zhang S, Bories G, Lantz C, Emmons R, Becker A, Liu E, Abecassis MM, Yvan-Charvet L, and Thorp EB.** Immunometabolism of Phagocytes and Relationships to Cardiac Repair. *Front Cardiovasc Med* 6: 42, 2019.
64. **Tsujioka H, Imanishi T, Ikejima H, Kuroi A, Takarada S, Tanimoto T, Kitabata H, Okochi K, Arita Y, and Ishibashi K.** Impact of heterogeneity of human peripheral blood monocyte subsets on myocardial salvage in patients with primary acute myocardial infarction. *Journal of the American College of Cardiology* 54: 130-138, 2009.
65. **Maekawa Y, Anzai T, Yoshikawa T, Asakura Y, Takahashi T, Ishikawa S, Mitamura H, and Ogawa S.** Prognostic significance of peripheral monocytes after reperfused acute myocardial infarction: a possible role for left ventricular remodeling. *Journal of the American College of Cardiology* 39: 241-246, 2002.
66. **Hanna A, Shinde AV, and Frangogiannis NG.** Validation of diagnostic criteria and histopathological characterization of cardiac rupture in the mouse model of nonreperfused myocardial infarction. *American Journal of Physiology-Heart and Circulatory Physiology* 319: H948-H964, 2020.
67. **Panizzi P, Swirski FK, Figueiredo J-L, Waterman P, Sosnovik DE, Aikawa E, Libby P, Pittet M, Weissleder R, and Nahrendorf M.** Impaired infarct healing in atherosclerotic mice with Ly-6Chi Monocytosis. *Journal of the American College of Cardiology* 55: 1629-1638, 2010.
68. **Alvarez-Argote S, and O'Meara CC.** The Evolving Roles of Cardiac Macrophages in Homeostasis, Regeneration, and Repair. *Int J Mol Sci* 22: 2021.

69. **de Couto G, Jaghatspanyan E, DeBerge M, Liu W, Luther K, Wang Y, Tang J, Thorp EB, and Marbán E.** Mechanism of Enhanced MerTK-Dependent Macrophage Efferocytosis by Extracellular Vesicles. *Arterioscler Thromb Vasc Biol* 39: 2082-2096, 2019.
70. **DeBerge M, Zhang S, Ginton K, Grigoryeva L, Hussein I, Vorovich E, Ho K, Luo X, and Thorp EB.** Efferocytosis and Outside-In Signaling by Cardiac Phagocytes. Links to Repair, Cellular Programming, and Intercellular Crosstalk in Heart. *Front Immunol* 8: 1428, 2017.
71. **Zhang S, Yeap XY, DeBerge M, Naresh NK, Wang K, Jiang Z, Wilcox JE, White SM, Morrow JP, Burrige PW, Procissi D, Scott EA, Frazier W, and Thorp EB.** Acute CD47 Blockade During Ischemic Myocardial Reperfusion Enhances Phagocytosis-Associated Cardiac Repair. *JACC Basic Transl Sci* 2: 386-397, 2017.
72. **Rosales C.** Neutrophil: A Cell with Many Roles in Inflammation or Several Cell Types? *Front Physiol* 9: 113, 2018.
73. **Hanna A, and Frangogiannis NG.** The Role of the TGF- β Superfamily in Myocardial Infarction. *Front Cardiovasc Med* 6: 140, 2019.
74. **Humeres C, and Frangogiannis NG.** Fibroblasts in the Infarcted, Remodeling, and Failing Heart. *JACC Basic Transl Sci* 4: 449-467, 2019.
75. **Frantz S, Hofmann U, Fraccarollo D, Schäfer A, Kranepuhl S, Hagedorn I, Nieswandt B, Nahrendorf M, Wagner H, and Bayer B.** Monocytes/macrophages prevent healing defects and left ventricular thrombus formation after myocardial infarction. *The FASEB Journal* 27: 871-881, 2013.
76. **Ben-Mordechai T, Holbova R, Landa-Rouben N, Harel-Adar T, Feinberg MS, Abd Elrahman I, Blum G, Epstein FH, Silman Z, and Cohen S.** Macrophage subpopulations are essential for infarct repair with and without stem cell therapy. *Journal of the American College of Cardiology* 62: 1890-1901, 2013.
77. **Peet C, Ivetic A, Bromage DI, and Shah AM.** Cardiac monocytes and macrophages after myocardial infarction. *Cardiovasc Res* 116: 1101-1112, 2020.
78. **Morimoto H, Takahashi M, Shiba Y, Izawa A, Ise H, Hongo M, Hatake K, Motoyoshi K, and Ikeda U.** Bone marrow-derived CXCR4+ cells mobilized by macrophage colony-stimulating factor participate in the reduction of infarct area and improvement of cardiac remodeling after myocardial infarction in mice. *The American journal of pathology* 171: 755-766, 2007.
79. **Maekawa Y, Anzai T, Yoshikawa T, Sugano Y, Mahara K, Kohno T, Takahashi T, and Ogawa S.** Effect of granulocyte-macrophage colony-stimulating factor inducer on left ventricular remodeling after acute myocardial infarction. *Journal of the American College of Cardiology* 44: 1510-1520, 2004.
80. **Wynn TA, and Vannella KM.** Macrophages in Tissue Repair, Regeneration, and Fibrosis. *Immunity* 44: 450-462, 2016.
81. **Jung M, Ma Y, Iyer RP, DeLeon-Pennell KY, Yabluchanskiy A, Garrett MR, and Lindsey ML.** IL-10 improves cardiac remodeling after myocardial infarction by stimulating M2 macrophage polarization and fibroblast activation. *Basic research in cardiology* 112: 33, 2017.
82. **Shirakawa K, Endo J, Kataoka M, Katsumata Y, Yoshida N, Yamamoto T, Isobe S, Moriyama H, Goto S, Kitakata H, Hiraide T, Fukuda K, and Sano M.** IL (Interleukin)-10-STAT3-Galectin-3 Axis Is Essential for Osteopontin-Producing Reparative Macrophage Polarization After Myocardial Infarction. *Circulation* 138: 2021-2035, 2018.
83. **Shirakawa K, Endo J, Kataoka M, Katsumata Y, Yoshida N, Yamamoto T, Isobe S, Moriyama H, Goto S, and Kitakata H.** IL (interleukin)-10-STAT3-galectin-3 axis is essential for osteopontin-producing reparative macrophage polarization after myocardial infarction. *Circulation* 138: 2021-2035, 2018.
84. **Daseke MJ, 2nd, Tenkorang MAA, Chalise U, Konfrst SR, and Lindsey ML.** Cardiac fibroblast activation during myocardial infarction wound healing: Fibroblast polarization after MI. *Matrix Biol* 91-92: 109-116, 2020.
85. **Camelliti P, Borg TK, and Kohl P.** Structural and functional characterisation of cardiac fibroblasts. *Cardiovasc Res* 65: 40-51, 2005.
86. **Miragoli M, Salvarani N, and Rohr S.** Myofibroblasts induce ectopic activity in cardiac tissue. *Circ Res* 101: 755-758, 2007.

87. **Vasquez C, Benamer N, and Morley GE.** The cardiac fibroblast: functional and electrophysiological considerations in healthy and diseased hearts. *J Cardiovasc Pharmacol* 57: 380-388, 2011.
88. **Baudino TA, Carver W, Giles W, and Borg TK.** Cardiac fibroblasts: friend or foe? *Am J Physiol Heart Circ Physiol* 291: H1015-1026, 2006.
89. **Gaudesius G, Miragoli M, Thomas SP, and Rohr S.** Coupling of cardiac electrical activity over extended distances by fibroblasts of cardiac origin. *Circ Res* 93: 421-428, 2003.
90. **Nielsen SH, Mouton AJ, DeLeon-Pennell KY, Genovese F, Karsdal M, and Lindsey ML.** Understanding cardiac extracellular matrix remodeling to develop biomarkers of myocardial infarction outcomes. *Matrix Biol* 75-76: 43-57, 2019.
91. **Tenkorang MA, Chalise U, Daseke I, Michael J, Konfrst SR, and Lindsey ML.** Understanding the mechanisms that determine extracellular matrix remodeling in the infarcted myocardium. *Biochemical Society Transactions* 47: 1679-1687, 2019.
92. **Wu Y, Li Y, Zhang C, A X, Wang Y, Cui W, Li H, and Du J.** S100a8/a9 released by CD11b+Gr1+ neutrophils activates cardiac fibroblasts to initiate angiotensin II-induced cardiac inflammation and injury. *Hypertension* 63: 1241-1250, 2014.
93. **Li Z, Nguyen TT, and Valaperti A.** Human cardiac fibroblasts produce pro-inflammatory cytokines upon TLRs and RLRs stimulation. *Mol Cell Biochem* 476: 3241-3252, 2021.
94. **Turner NA.** Inflammatory and fibrotic responses of cardiac fibroblasts to myocardial damage associated molecular patterns (DAMPs). *J Mol Cell Cardiol* 94: 189-200, 2016.
95. **Mouton AJ, DeLeon-Pennell KY, Gonzalez OJR, Flynn ER, Freeman TC, Saucerman JJ, Garrett MR, Ma Y, Harmancey R, and Lindsey ML.** Mapping macrophage polarization over the myocardial infarction time continuum. *Basic research in cardiology* 113: 1-18, 2018.
96. **Wu CL, Yin R, Wang SN, and Ying R.** A Review of CXCL1 in Cardiac Fibrosis. *Front Cardiovasc Med* 8: 674498, 2021.
97. **Mylonas KJ, Turner NA, Bageghni SA, Kenyon CJ, White CI, McGregor K, Kimmitt RA, Sulston R, Kelly V, Walker BR, Porter KE, Chapman KE, and Gray GA.** 11 β -HSD1 suppresses cardiac fibroblast CXCL2, CXCL5 and neutrophil recruitment to the heart post MI. *J Endocrinol* 233: 315-327, 2017.
98. **Altara R, Mallat Z, Booz GW, and Zouein FA.** The CXCL10/CXCR3 Axis and Cardiac Inflammation: Implications for Immunotherapy to Treat Infectious and Noninfectious Diseases of the Heart. *J Immunol Res* 2016: 4396368, 2016.
99. **Dewald O, Zymek P, Winkelmann K, Koerting A, Ren G, Abou-Khamis T, Michael LH, Rollins BJ, Entman ML, and Frangogiannis NG.** CCL2/Monocyte Chemoattractant Protein-1 regulates inflammatory responses critical to healing myocardial infarcts. *Circ Res* 96: 881-889, 2005.
100. **Montecucco F, Braunersreuther V, Lenglet S, Delattre BM, Pelli G, Buatois V, Guilhot F, Galan K, Vuilleumier N, Ferlin W, Fischer N, Vallée JP, Kosco-Vilbois M, and Mach F.** CC chemokine CCL5 plays a central role impacting infarct size and post-infarction heart failure in mice. *Eur Heart J* 33: 1964-1974, 2012.
101. **Frangogiannis NG.** Interleukin-1 in cardiac injury, repair, and remodeling: pathophysiological and translational concepts. *Discoveries (Craiova)* 3: 2015.
102. **Pappritz K, Savvatis K, Koschel A, Miteva K, Tschöpe C, and Van Linthout S.** Cardiac (myo)fibroblasts modulate the migration of monocyte subsets. *Sci Rep* 8: 5575, 2018.
103. **Turner NA, Mughal RS, Warburton P, O'Regan DJ, Ball SG, and Porter KE.** Mechanism of TNF α -induced IL-1 α , IL-1 β and IL-6 expression in human cardiac fibroblasts: effects of statins and thiazolidinediones. *Cardiovasc Res* 76: 81-90, 2007.
104. **de Boer RA, De Keulenaer G, Bauersachs J, Brutsaert D, Cleland JG, Diez J, Du XJ, Ford P, Heinzl FR, Lipson KE, McDonagh T, Lopez-Andres N, Lunde IG, Lyon AR, Pollesello P, Prasad SK, Tocchetti CG, Mayr M, Sluijter JPG, Thum T, Tschöpe C, Zannad F, Zimmermann WH, Ruschitzka F, Filippatos G, Lindsey ML, Maack C, and Heymans S.** Towards better definition, quantification and treatment of fibrosis in heart failure. A scientific roadmap by the Committee of Translational Research of the Heart Failure Association (HFA) of the European Society of Cardiology. *Eur J Heart Fail* 21: 272-285, 2019.
105. **Ma Y, Iyer RP, Jung M, Czubyrt MP, and Lindsey ML.** Cardiac Fibroblast Activation Post-Myocardial Infarction: Current Knowledge Gaps. *Trends Pharmacol Sci* 38: 448-458, 2017.

106. **Mitchell MD, Laird RE, Brown RD, and Long CS.** IL-1beta stimulates rat cardiac fibroblast migration via MAP kinase pathways. *Am J Physiol Heart Circ Physiol* 292: H1139-1147, 2007.
107. **Dobaczewski M, Bujak M, Li N, Gonzalez-Quesada C, Mendoza LH, Wang XF, and Frangogiannis NG.** Smad3 signaling critically regulates fibroblast phenotype and function in healing myocardial infarction. *Circ Res* 107: 418-428, 2010.
108. **Freed DH, Chilton L, Li Y, Dangerfield AL, Raizman JE, Rattan SG, Visen N, Hryshko LV, and Dixon IM.** Role of myosin light chain kinase in cardiotrophin-1-induced cardiac myofibroblast cell migration. *Am J Physiol Heart Circ Physiol* 301: H514-522, 2011.
109. **Virag JI, and Murry CE.** Myofibroblast and endothelial cell proliferation during murine myocardial infarct repair. *Am J Pathol* 163: 2433-2440, 2003.
110. **Gourdie RG, Dimmeler S, and Kohl P.** Novel therapeutic strategies targeting fibroblasts and fibrosis in heart disease. *Nat Rev Drug Discov* 15: 620-638, 2016.
111. **Prabhu SD, and Frangogiannis NG.** The Biological Basis for Cardiac Repair After Myocardial Infarction: From Inflammation to Fibrosis. *Circ Res* 119: 91-112, 2016.
112. **Zamilpa R, and Lindsey ML.** Extracellular matrix turnover and signaling during cardiac remodeling following MI: causes and consequences. *J Mol Cell Cardiol* 48: 558-563, 2010.
113. **Lindsey ML, Brunt KR, Kirk JA, Kleinbongard P, Calvert JW, de Castro Brás LE, DeLeon-Pennell KY, Del Re DP, Frangogiannis NG, Frantz S, Gumina RJ, Halade GV, Jones SP, Ritchie RH, Spinale FG, Thorp EB, Ripplinger CM, and Kassiri Z.** Guidelines for in vivo mouse models of myocardial infarction. *Am J Physiol Heart Circ Physiol* 321: H1056-h1073, 2021.
114. **Kain V, Prabhu SD, and Halade GV.** Inflammation revisited: inflammation versus resolution of inflammation following myocardial infarction. *Basic research in cardiology* 109: 444, 2014.
115. **Gong T, Liu L, Jiang W, and Zhou R.** DAMP-sensing receptors in sterile inflammation and inflammatory diseases. *Nature Reviews Immunology* 20: 95-112, 2020.
116. **Frangogiannis NG.** The inflammatory response in myocardial injury, repair, and remodelling. *Nature Reviews Cardiology* 11: 255-265, 2014.
117. **Daseke II MJ, Tenkorang MA, Chalise U, Konfrst SR, and Lindsey ML.** Cardiac fibroblast activation during myocardial infarction wound healing: Fibroblast polarization after MI. *Matrix Biology* 91: 109-116, 2020.
118. **Daseke II MJ, Tenkorang-Impraim MA, Ma Y, Chalise U, Konfrst SR, Garrett MR, DeLeon-Pennell KY, and Lindsey ML.** Exogenous IL-4 shuts off pro-inflammation in neutrophils while stimulating anti-inflammation in macrophages to induce neutrophil phagocytosis following myocardial infarction. *Journal of molecular and cellular cardiology* 145: 112-121, 2020.
119. **Prabhu SD, and Frangogiannis NG.** The biological basis for cardiac repair after myocardial infarction: from inflammation to fibrosis. *Circulation research* 119: 91-112, 2016.
120. **Aikawa T, Kariya T, Yamada KP, Miyashita S, Bikou O, Tharakan S, Fish K, and Ishikawa K.** Impaired left ventricular global longitudinal strain is associated with elevated left ventricular filling pressure after myocardial infarction. *American Journal of Physiology-Heart and Circulatory Physiology* 319: H1474-H1481, 2020.
121. **van den Borne SW, Cleutjens JP, Hanemaaijer R, Creemers EE, Smits JF, Daemen MJ, and Blankesteyn WM.** Increased matrix metalloproteinase-8 and-9 activity in patients with infarct rupture after myocardial infarction. *Cardiovascular Pathology* 18: 37-43, 2009.
122. **Lindsey ML, de Castro Bras LE, DeLeon-Pennell KY, Frangogiannis NG, Halade GV, O'Meara CC, Spinale FG, Kassiri Z, Kirk JA, and Kleinbongard P.** Reperfused vs. nonreperfused myocardial infarction: when to use which model. American Physiological Society Rockville, MD, 2021.
123. **Lindsey ML, Brunt KR, Kirk JA, Kleinbongard P, Calvert JW, de Castro Brás LE, DeLeon-Pennell KY, Del Re DP, Frangogiannis NG, and Frantz S.** Guidelines for in vivo mouse models of myocardial infarction. *American Journal of Physiology-Heart and Circulatory Physiology* 2021.
124. **Arruda-Olson AM, Reeder GS, Bell MR, Weston SA, and Roger VL.** Neutrophilia predicts death and heart failure after myocardial infarction: a community-based study. *Circulation: Cardiovascular Quality and Outcomes* 2: 656-662, 2009.

125. **Daseke II MJ, Chalise U, Becirovic-Agic M, Salomon JD, Cook LM, Case AJ, and Lindsey ML.** Neutrophil signaling during myocardial infarction wound repair. *Cellular signalling* 109816, 2020.
126. **Tanindi A, Sahinarslan A, Elbeg S, and Cemri M.** Relationship between MMP-1, MMP-9, TIMP-1, IL-6 and risk factors, clinical presentation, extent and severity of atherosclerotic coronary artery disease. *The open cardiovascular medicine journal* 5: 110, 2011.
127. **Webb CS, Bonnema DD, Ahmed SH, Leonardi AH, McClure CD, Clark LL, Stroud RE, Corn WC, Finklea L, and Zile MR.** Specific temporal profile of matrix metalloproteinase release occurs in patients after myocardial infarction. *Circulation* 114: 1020-1027, 2006.
128. **Becirovic-Agic M, Chalise U, Daseke MJ, Konfrst S, Salomon JD, Mishra PK, and Lindsey ML.** Infarct in the Heart: What's MMP-9 Got to Do with It? *Biomolecules* 11: 491, 2021.
129. **Wang S, Song R, Wang Z, Jing Z, Wang S, and Ma J.** S100A8/A9 in Inflammation. *Frontiers in immunology* 9: 1298, 2018.
130. **Xia C, Braunstein Z, Toomey AC, Zhong J, and Rao X.** S100 proteins as an important regulator of macrophage inflammation. *Frontiers in immunology* 8: 1908, 2018.
131. **Health Nlo.** *Guide for the care and use of laboratory animals.* National Academies, 1985.
132. **Lindsey ML, Bolli R, Canty Jr JM, Du X-J, Frangogiannis NG, Frantz S, Gourdie RG, Holmes JW, Jones SP, and Kloner RA.** Guidelines for experimental models of myocardial ischemia and infarction. *American Journal of Physiology-Heart and Circulatory Physiology* 314: H812-H838, 2018.
133. **Mouton AJ, DeLeon-Pennell KY, Gonzalez OJR, Flynn ER, Freeman TC, Saucerman JJ, Garrett MR, Ma Y, Harmancey R, and Lindsey ML.** Mapping macrophage polarization over the myocardial infarction time continuum. *Basic research in cardiology* 113: 26, 2018.
134. **Zaidi Y, Corker A, Vasileva VY, Oviedo K, Graham C, Wilson K, Martino J, Troncoso M, Broughton P, and Ilatovskaya DV.** Chronic Porphyromonas gingivalis lipopolysaccharide induces adverse myocardial infarction wound healing through activation of CD8+ T cells. *American Journal of Physiology-Heart and Circulatory Physiology* 321: H948-H962, 2021.
135. **Hibino T, Sakaguchi M, Miyamoto S, Yamamoto M, Motoyama A, Hosoi J, Shimokata T, Ito T, Tsuboi R, and Huh N-h.** S100A9 is a novel ligand of EMMPRIN that promotes melanoma metastasis. *Cancer research* 73: 172-183, 2013.
136. **Lindsey ML, Kassiri Z, Virag JA, de Castro Brás LE, and Scherrer-Crosbie M.** Guidelines for measuring cardiac physiology in mice. *American Journal of Physiology-Heart and Circulatory Physiology* 314: H733-H752, 2018.
137. **Brooks HL, and Lindsey ML.** Guidelines for authors and reviewers on antibody use in physiology studies. *American Journal of Physiology-Heart and Circulatory Physiology* 314: H724-H732, 2018.
138. **Lindsey ML, Gray GA, Wood SK, and Curran-Everett D.** Statistical considerations in reporting cardiovascular research. *American Journal of Physiology-Heart and Circulatory Physiology* 315: H303-H313, 2018.
139. **Brinkmann V, and Zychlinsky A.** Neutrophil extracellular traps: is immunity the second function of chromatin? *Journal of cell biology* 198: 773-783, 2012.
140. **Mauracher LM, Posch F, Martinod K, Grilz E, Däullary T, Hell L, Brostjan C, Zielinski C, Ay C, and Wagner D.** Citrullinated histone H3, a biomarker of neutrophil extracellular trap formation, predicts the risk of venous thromboembolism in cancer patients. *Journal of Thrombosis and Haemostasis* 16: 508-518, 2018.
141. **Grilz E, Mauracher LM, Posch F, Königsbrügge O, Zöchbauer-Müller S, Marosi C, Lang I, Pabinger I, and Ay C.** Citrullinated histone H3, a biomarker for neutrophil extracellular trap formation, predicts the risk of mortality in patients with cancer. *British journal of haematology* 186: 311-320, 2019.
142. **Sreejit G, Abdel-Latif A, Athmanathan B, Annabathula R, Dhyani A, Noothi SK, Quaife-Ryan GA, Al-Sharea A, Pernes G, and Dragoljevic D.** Neutrophil-Derived S100A8/A9 amplify granulopoiesis after myocardial infarction. *Circulation* 141: 1080-1094, 2020.
143. **Vogl T, Stratis A, Wixler V, Völler T, Thurainayagam S, Jorch SK, Zenker S, Dreiling A, Chakraborty D, and Fröhling M.** Autoinhibitory regulation of S100A8/S100A9 alarmin activity locally restricts sterile inflammation. *The Journal of clinical investigation* 128: 1852-1866, 2018.

144. **Cai Z, Xie Q, Hu T, Yao Q, Zhao J, Wu Q, and Tang Q.** S100A8/A9 in Myocardial Infarction: A Promising Biomarker and Therapeutic Target. *Frontiers in Cell and Developmental Biology* 8: 1310, 2020.
145. **Nagareddy PR, Sreejit G, Abo-Aly M, Jagggers RM, Chelvarajan L, Johnson J, Pernes G, Athmanathan B, Abdel-Latif A, and Murphy AJ.** NETosis Is Required for S100A8/A9-Induced Granulopoiesis After Myocardial Infarction. *Arteriosclerosis, Thrombosis, and Vascular Biology* 40: 2805-2807, 2020.
146. **Simard J-C, Cesaro A, Chapeton-Montes J, Tardif M, Antoine F, Girard D, and Tessier PA.** S100A8 and S100A9 induce cytokine expression and regulate the NLRP3 inflammasome via ROS-dependent activation of NF- κ B1. *PLoS one* 8: e72138, 2013.
147. **Marinković G, Grauen Larsen H, Yndigegn T, Szabo IA, Mares RG, de Camp L, Weiland M, Tomas L, Goncalves I, and Nilsson J.** Inhibition of pro-inflammatory myeloid cell responses by short-term S100A9 blockade improves cardiac function after myocardial infarction. *European heart journal* 40: 2713-2723, 2019.
148. **Frangogiannis NG.** S100A8/A9 as a therapeutic target in myocardial infarction: cellular mechanisms, molecular interactions, and translational challenges. *European heart journal* 40: 2724-2726, 2019.
149. **Iyer RP, de Castro Brás LE, Cannon PL, Ma Y, DeLeon-Pennell KY, Jung M, Flynn ER, Henry JB, Bratton DR, and White JA.** Defining the sham environment for post-myocardial infarction studies in mice. *American Journal of Physiology-Heart and Circulatory Physiology* 311: H822-H836, 2016.
150. **Boyd JH, Kan B, Roberts H, Wang Y, and Walley KR.** S100A8 and S100A9 mediate endotoxin-induced cardiomyocyte dysfunction via the receptor for advanced glycation end products. *Circulation research* 102: 1239-1246, 2008.
151. **Ryckman C, Vandal K, Rouleau P, Talbot M, and Tessier PA.** Proinflammatory activities of S100: proteins S100A8, S100A9, and S100A8/A9 induce neutrophil chemotaxis and adhesion. *The Journal of Immunology* 170: 3233-3242, 2003.
152. **Averill MM, Barnhart S, Becker L, Li X, Heinecke JW, LeBoeuf RC, Hamerman JA, Sorg C, Kerkhoff C, and Bornfeldt KE.** S100A9 differentially modifies phenotypic states of neutrophils, macrophages, and dendritic cells: implications for atherosclerosis and adipose tissue inflammation. *Circulation* 123: 1216-1226, 2011.
153. **Li Y, Chen B, Yang X, Zhang C, Jiao Y, Li P, Liu Y, Li Z, Qiao B, and Bond Lau W.** S100a8/a9 signaling causes mitochondrial dysfunction and cardiomyocyte death in response to ischemic/reperfusion injury. *Circulation* 140: 751-764, 2019.
154. **Han X, Shi H, Sun Y, Shang C, Luan T, Wang D, Ba X, and Zeng X.** CXCR2 expression on granulocyte and macrophage progenitors under tumor conditions contributes to mo-MDSC generation via SAP18/ERK/STAT3. *Cell death & disease* 10: 1-15, 2019.
155. **van den Bosch MH, Blom AB, Schelbergen RF, Koenders MI, van de Loo FA, van den Berg WB, Vogl T, Roth J, van der Kraan PM, and van Lent PL.** Alarmin S100A9 induces proinflammatory and catabolic effects predominantly in the M1 macrophages of human osteoarthritic synovium. *The Journal of rheumatology* 43: 1874-1884, 2016.
156. **Marinković G, Koenis DS, de Camp L, Jablonowski R, Graber N, de Waard V, de Vries CJ, Goncalves I, Nilsson J, and Jovinge S.** S100A9 links inflammation and repair in myocardial infarction. *Circulation Research* 127: 664-676, 2020.
157. **Soehnlein O, Zernecke A, Eriksson EE, Rothfuchs AG, Pham CT, Herwald H, Bidzhekov K, Rottenberg ME, Weber C, and Lindbom L.** Neutrophil secretion products pave the way for inflammatory monocytes. *Blood, The Journal of the American Society of Hematology* 112: 1461-1471, 2008.
158. **Frodermann V, and Nahrendorf M.** Neutrophil-macrophage cross-talk in acute myocardial infarction. Oxford University Press, 2017.
159. **B. Gowda S, Gowda D, Kain V, Chiba H, Hui S-P, Chalfant CE, Parcha V, Arora P, and Halade GV.** Sphingosine-1-phosphate interactions in the spleen and heart reflect extent of cardiac repair in mice and failing human hearts. *American Journal of Physiology-Heart and Circulatory Physiology* 321: H599-H611, 2021.

160. **Zhou J, Chen R, Liu C, Zhou P, Li J, Wang Y, Zhao X, Zhao H, Song L, and Yan H.** Associations of NETs with inflammatory risk and atherosclerotic severity in ST-segment elevation myocardial infarction. *Thrombosis Research* 2021.
161. **Liu J, Yang D, Wang X, Zhu Z, Wang T, Ma A, and Liu P.** Neutrophil extracellular traps and dsDNA predict outcomes among patients with ST-elevation myocardial infarction. *Scientific reports* 9: 1-9, 2019.
162. **Du M, Yang W, Schull S, Gu J, and Xue S.** Inhibition of peptidyl arginine deiminase-4 protects against myocardial infarction induced cardiac dysfunction. *International immunopharmacology* 78: 106055, 2020.
163. **Zhou Z, Zhang S, Ding S, Abudupataer M, Zhang Z, Zhu X, Zhang W, Zou Y, Yang X, and Ge J.** Excessive neutrophil extracellular trap formation aggravates acute myocardial infarction injury in apolipoprotein E deficiency mice via the ROS-dependent pathway. *Oxidative medicine and cellular longevity* 2019: 2019.
164. **Frangogiannis NG.** The extracellular matrix in myocardial injury, repair, and remodeling. *The Journal of clinical investigation* 127: 1600-1612, 2017.
165. **Sörensen I, Susnik N, Inhester T, Degen JL, Melk A, Haller H, and Schmitt R.** Fibrinogen, acting as a mitogen for tubulointerstitial fibroblasts, promotes renal fibrosis. *Kidney international* 80: 1035-1044, 2011.
166. **Maresca G, Di Blasio A, Marchioli R, and Di Minno G.** Measuring plasma fibrinogen to predict stroke and myocardial infarction: an update. *Arteriosclerosis, thrombosis, and vascular biology* 19: 1368-1377, 1999.
167. **Di Minno G, and Mancini M.** Measuring plasma fibrinogen to predict stroke and myocardial infarction. *Arteriosclerosis: An Official Journal of the American Heart Association, Inc* 10: 1-7, 1990.
168. **Shojaie M, Pourahmad M, Eshraghian A, Izadi HR, and Naghshvar F.** Fibrinogen as a risk factor for premature myocardial infarction in Iranian patients: a case control study. *Vascular health and risk management* 5: 673, 2009.
169. **Tousoulis D, Papageorgiou N, Androulakis E, Briasoulis A, Antoniadis C, and Stefanadis C.** Fibrinogen and cardiovascular disease: genetics and biomarkers. *Blood reviews* 25: 239-245, 2011.
170. **Frangogiannis NG, Smith CW, and Entman ML.** The inflammatory response in myocardial infarction. *Cardiovascular research* 53: 31-47, 2002.
171. **Ma Y, Yabluchanskiy A, Iyer RP, Cannon PL, Flynn ER, Jung M, Henry J, Cates CA, Deleon-Pennell KY, and Lindsey ML.** Temporal neutrophil polarization following myocardial infarction. *Cardiovasc Res* 110: 51-61, 2016.
172. **Calcagno DM, Zhang C, Toomu A, Huang K, Ninh VK, Miyamoto S, Aguirre AD, Fu Z, Heller Brown J, and King KR.** SiglecF (HI) Marks Late-Stage Neutrophils of the Infarcted Heart: A Single-Cell Transcriptomic Analysis of Neutrophil Diversification. *Journal of the American Heart Association* 10: e019019, 2021.
173. **Daseke II MJ, Chalise U, Becirovic-Agic M, Salomon JD, Cook LM, Case AJ, and Lindsey ML.** Neutrophil signaling during myocardial infarction wound repair. *Cellular signalling* 77: 109816, 2021.
174. **Goldmann BU, Rudolph V, Rudolph TK, Holle A-K, Hillebrandt M, Meinertz T, and Baldus S.** Neutrophil activation precedes myocardial injury in patients with acute myocardial infarction. *Free Radical Biology and Medicine* 47: 79-83, 2009.
175. **Mauler M, Herr N, Schoenichen C, Witsch T, Marchini T, Härdtner C, Koentges C, Kienle K, Ollivier V, and Schell M.** Platelet serotonin aggravates myocardial ischemia/reperfusion injury via neutrophil degranulation. *Circulation* 139: 918-931, 2019.
176. **Halade GV, Jin Y-F, and Lindsey ML.** Matrix metalloproteinase (MMP)-9: a proximal biomarker for cardiac remodeling and a distal biomarker for inflammation. *Pharmacology & therapeutics* 139: 32-40, 2013.
177. **Hansson J, Vasan RS, Ärnlov J, Ingelsson E, Lind L, Larsson A, Michaëlsson K, and Sundström J.** Biomarkers of extracellular matrix metabolism (MMP-9 and TIMP-1) and risk of stroke, myocardial infarction, and cause-specific mortality: cohort study. *PLoS one* 6: e16185, 2011.

178. **Mocatta TJ, Pilbrow AP, Cameron VA, Senthilmohan R, Frampton CM, Richards AM, and Winterbourn CC.** Plasma concentrations of myeloperoxidase predict mortality after myocardial infarction. *Journal of the American College of Cardiology* 49: 1993-2000, 2007.
179. **Shah AD, Denaxas S, Nicholas O, Hingorani AD, and Hemingway H.** Neutrophil counts and initial presentation of 12 cardiovascular diseases: a CALIBER cohort study. *Journal of the American College of Cardiology* 69: 1160-1169, 2017.
180. **Horckmans M, Ring L, Duchene J, Santovito D, Schloss MJ, Drechsler M, Weber C, Soehnlein O, and Steffens S.** Neutrophils orchestrate post-myocardial infarction healing by polarizing macrophages towards a reparative phenotype. *Eur Heart J* 38: 187-197, 2017.
181. **Hammerman H, Kloner RA, Hale S, Schoen FJ, and Braunwald E.** Dose-dependent effects of short-term methylprednisolone on myocardial infarct extent, scar formation, and ventricular function. *Circulation* 68: 446-452, 1983.
182. **Liu S, Ngo DT, Chong CR, Amarasekera AT, Procter NE, Licari G, Dautov RF, Stewart S, Chirkov YY, and Horowitz JD.** Suppression of neutrophil superoxide generation by BNP is attenuated in acute heart failure: a case for 'BNP resistance'. *European journal of heart failure* 17: 475-483, 2015.
183. **Peterson AL, Siddiqui G, Sloan EK, and Creek DJ.** β -Adrenoceptor regulation of metabolism in U937 derived macrophages. *Molecular Omics* 2021.
184. **Peet C, Ivetic A, Bromage DI, and Shah AM.** Cardiac monocytes and macrophages after myocardial infarction. *Cardiovascular research* 116: 1101-1112, 2020.
185. **Frodermann V, and Nahrendorf M.** Neutrophil-macrophage cross-talk in acute myocardial infarction. *Eur Heart J* 38: 198-200, 2017.
186. **Puhl S-L, and Steffens S.** Neutrophils in post-myocardial infarction inflammation: damage vs. resolution? *Frontiers in cardiovascular medicine* 6: 25, 2019.
187. **Lambert JM, Lopez EF, and Lindsey ML.** Macrophage roles following myocardial infarction. *International journal of cardiology* 130: 147-158, 2008.
188. **Albus U.** Guide for the Care and Use of Laboratory Animals (8th edn). SAGE Publications Sage UK: London, England, 2012.
189. **Vizcaíno JA, Csordas A, Del-Toro N, Dienes JA, Griss J, Lavidas I, Mayer G, Perez-Riverol Y, Reisinger F, and Ternent T.** 2016 update of the PRIDE database and its related tools. *Nucleic acids research* 44: D447-D456, 2016.
190. **Lim K, Kim T-h, Trzeciak A, Amitrano AM, Reilly EC, Prizant H, Fowell DJ, Topham DJ, and Kim M.** In situ neutrophil efferocytosis shapes T cell immunity to influenza infection. *Nature immunology* 21: 1046-1057, 2020.
191. **Pang Z, Chong J, Zhou G, de Lima Morais DA, Chang L, Barrette M, Gauthier C, Jacques P-É, Li S, and Xia J.** MetaboAnalyst 5.0: narrowing the gap between raw spectra and functional insights. *Nucleic acids research* 2021.
192. **Xie Z, Bailey A, Kuleshov MV, Clarke DJ, Evangelista JE, Jenkins SL, Lachmann A, Wojciechowicz ML, Kropiwnicki E, and Jagodnik KM.** Gene set knowledge discovery with Enrichr. *Current protocols* 1: e90, 2021.
193. **Graw S, Chappell K, Washam CL, Gies A, Bird J, Robeson MS, and Byrum SD.** Multi-omics data integration considerations and study design for biological systems and disease. *Molecular Omics* 2021.
194. **Kim M, and Tagkopoulos I.** Data integration and predictive modeling methods for multi-omics datasets. *Molecular omics* 14: 8-25, 2018.
195. **Fernández GC, Ilarregui JM, Rubel CJ, Toscano MA, Gómez SA, Beigier Bompadre M, Isturiz MA, Rabinovich GA, and Palermo MS.** Galectin-3 and soluble fibrinogen act in concert to modulate neutrophil activation and survival: involvement of alternative MAPK pathways. *Glycobiology* 15: 519-527, 2005.
196. **Chalise U, Becirovic-Agic M, Daseke II MJ, Konfrst SR, Rodriguez-Paar JR, Feng D, Salomon JD, Anderson DR, Cook LM, and Lindsey ML.** S100A9 is a functional effector of infarct wall thinning after myocardial infarction. *Am J Physiol Heart Circ Physiol* 2021.
197. **Cederfur C, Salomonsson E, Nilsson J, Halim A, Öberg CT, Larson G, Nilsson UJ, and Leffler H.** Different affinity of galectins for human serum glycoproteins: galectin-3 binds many protease inhibitors and acute phase proteins. *Glycobiology* 18: 384-394, 2008.

198. **Soehnlein O, Steffens S, Hidalgo A, and Weber C.** Neutrophils as protagonists and targets in chronic inflammation. *Nature Reviews Immunology* 17: 248-261, 2017.
199. **Amano Y, Takayama M, and Kumita S.** Magnetic resonance imaging of apical left ventricular aneurysm and thinning associated with hypertrophic cardiomyopathy. *Journal of computer assisted tomography* 32: 259-264, 2008.
200. **Piamsiri C, Maneechote C, Siri-Angkul N, Chattipakorn SC, and Chattipakorn N.** Targeting necroptosis as therapeutic potential in chronic myocardial infarction. *Journal of biomedical science* 28: 1-13, 2021.
201. **Lacy P.** Mechanisms of degranulation in neutrophils. *Allergy, Asthma & Clinical Immunology* 2: 1-11, 2006.
202. **Wang S, Dougherty EJ, and Danner RL.** PPAR γ signaling and emerging opportunities for improved therapeutics. *Pharmacological research* 111: 76-85, 2016.
203. **Zhao Y-B, Zhao J, Zhang L-J, Shan R-G, Sun Z-Z, Wang K, Chen J-Q, and Mu J-X.** MicroRNA-370 protects against myocardial ischemia/reperfusion injury in mice following sevoflurane anesthetic preconditioning through PLIN5-dependent PPAR signaling pathway. *Biomedicine & Pharmacotherapy* 113: 108697, 2019.
204. **Lotz C, Lazariotto M, Redel A, Smul TM, Stumpner J, Blomeyer C, Tischer-Zeit T, Schmidt J, Pocij J, and Roewer N.** Activation of peroxisome-proliferator-activated receptors α and γ mediates remote ischemic preconditioning against myocardial infarction in vivo. *Experimental Biology and Medicine* 236: 113-122, 2011.
205. **DeLeon-Pennell KY, Mouton AJ, Ero OK, Ma Y, Iyer RP, Flynn ER, Espinoza I, Musani SK, Vasan RS, and Hall ME.** LXR/RXR signaling and neutrophil phenotype following myocardial infarction classify sex differences in remodeling. *Basic research in cardiology* 113: 1-19, 2018.
206. **Overbergh L, Torrekens S, Van Leuven F, and Van den Berghe H.** Molecular characterization of the murinoglobulins. *Journal of Biological Chemistry* 266: 16903-16910, 1991.
207. **Borth W.** Alpha 2-macroglobulin, a multifunctional binding protein with targeting characteristics. *Faseb j* 6: 3345-3353, 1992.
208. **Abe K, Yamamoto K, and Sinohara H.** Proteinase inhibitory spectrum of mouse murinoglobulin and α -macroglobulin. *The Journal of Biochemistry* 106: 564-568, 1989.
209. **Umans L, Serneels L, Overbergh L, Stas L, and Van Leuven F.** α 2-Macroglobulin- and Murinoglobulin-1- Deficient Mice: A Mouse Model for Acute Pancreatitis. *The American Journal of Pathology* 155: 983-993, 1999.
210. **Krause K, Azouz F, Nakano E, Nerurkar VR, and Kumar M.** Deletion of Pregnancy Zone Protein and Murinoglobulin-1 Restricts the Pathogenesis of West Nile Virus Infection in Mice. *Frontiers in Microbiology* 10: 2019.
211. **Margadant C, van den Bout I, van Boxel AL, Thijssen VL, and Sonnenberg A.** Epigenetic regulation of galectin-3 expression by β 1 integrins promotes cell adhesion and migration. *Journal of Biological Chemistry* 287: 44684-44693, 2012.
212. **Li M, Yuan Y, Guo K, Lao Y, Huang X, and Feng L.** Value of Galectin-3 in acute myocardial infarction. *American Journal of Cardiovascular Drugs* 20: 333-342, 2020.
213. **Frunza O, Russo I, Saxena A, Shinde AV, Humeres C, Hanif W, Rai V, Su Y, and Frangogiannis NG.** Myocardial galectin-3 expression is associated with remodeling of the pressure-overloaded heart and may delay the hypertrophic response without affecting survival, dysfunction, and cardiac fibrosis. *The American journal of pathology* 186: 1114-1127, 2016.
214. **Besler C, Lang D, Urban D, Rommel K-P, von Roeder M, Fengler K, Blazek S, Kandolf R, Klingel K, and Thiele H.** Plasma and cardiac galectin-3 in patients with heart failure reflects both inflammation and fibrosis: implications for its use as a biomarker. *Circulation: heart failure* 10: e003804, 2017.
215. **I. Lala R, Puschita M, Darabantiu D, and Pilat L.** Galectin-3 in heart failure pathology—“another brick in the wall”? *Acta cardiologica* 70: 323-331, 2015.
216. **Yancy CW, Jessup M, Bozkurt B, Butler J, Casey DE, Drazner MH, Fonarow GC, Geraci SA, Horwich T, and Januzzi JL.** 2013 ACCF/AHA guideline for the management of heart failure: a report of the American College of Cardiology Foundation/American Heart Association Task Force on Practice Guidelines. *Journal of the American College of Cardiology* 62: e147-e239, 2013.

217. **Asleh R, Enriquez-Sarano M, Jaffe AS, Manemann SM, Weston SA, Jiang R, and Roger VL.** Galectin-3 levels and outcomes after myocardial infarction: a population-based study. *Journal of the American College of Cardiology* 73: 2286-2295, 2019.
218. **Liu F-T, Hsu DK, Zuberi RI, Kuwabara I, Chi EY, and Henderson Jr WR.** Expression and function of galectin-3, a beta-galactoside-binding lectin, in human monocytes and macrophages. *The American journal of pathology* 147: 1016, 1995.
219. **Henderson NC, Mackinnon AC, Farnworth SL, Kipari T, Haslett C, Iredale JP, Liu F-T, Hughes J, and Sethi T.** Galectin-3 expression and secretion links macrophages to the promotion of renal fibrosis. *The American journal of pathology* 172: 288-298, 2008.
220. **Henderson NC, Mackinnon AC, Farnworth SL, Poirier F, Russo FP, Iredale JP, Haslett C, Simpson KJ, and Sethi T.** Galectin-3 regulates myofibroblast activation and hepatic fibrosis. *Proceedings of the National Academy of Sciences* 103: 5060-5065, 2006.
221. **Ochieng J, Fridman R, Nangia-Makker P, Kleiner DE, Liotta LA, Stetler-Stevenson WG, and Raz A.** Galectin-3 is a novel substrate for human matrix metalloproteinases-2 and-9. *Biochemistry* 33: 14109-14114, 1994.
222. **Daseke MJ, 2nd, Valerio FM, Kalusche WJ, Ma Y, DeLeon-Pennell KY, and Lindsey ML.** Neutrophil proteome shifts over the myocardial infarction time continuum. *Basic Res Cardiol* 114: 37, 2019.
223. **Ortega N, Behonick DJ, Colnot C, Cooper DN, and Werb Z.** Galectin-3 is a downstream regulator of matrix metalloproteinase-9 function during endochondral bone formation. *Molecular biology of the cell* 16: 3028-3039, 2005.
224. **Wright RD, Souza PR, Flak MB, Thedchanamoorthy P, Norling LV, and Cooper D.** Galectin-3-null mice display defective neutrophil clearance during acute inflammation. *Journal of Leukocyte Biology* 101: 717-726, 2017.
225. **Cassaglia P, Penas F, Betazza C, Estevez FF, Miksztowicz V, Naya NM, Llamosas MC, Truant SN, Wilensky L, and Volberg V.** Genetic Deletion of Galectin-3 Alters the Temporal Evolution of Macrophage Infiltration and Healing Affecting the Cardiac Remodeling and Function after Myocardial Infarction in Mice. *The American Journal of Pathology* 190: 1789-1800, 2020.
226. **Sica A, and Mantovani A.** Macrophage plasticity and polarization: in vivo veritas. *The Journal of clinical investigation* 122: 787-795, 2012.
227. **Orecchioni M, Ghosheh Y, Pramod AB, and Ley K.** Macrophage polarization: different gene signatures in M1 (LPS+) vs. classically and M2 (LPS-) vs. alternatively activated macrophages. *Frontiers in immunology* 10: 1084, 2019.
228. **Yu T, Zhao L, Huang X, Ma C, Wang Y, Zhang J, and Xuan D.** Enhanced activity of the macrophage M1/M2 phenotypes and phenotypic switch to M1 in periodontal infection. *Journal of periodontology* 87: 1092-1102, 2016.
229. **Hart PH, Bonder CS, Balogh J, Dickensheets HL, Donnelly RP, and Finlay-Jones JJ.** Differential responses of human monocytes and macrophages to IL-4 and IL-13. *Journal of leukocyte biology* 66: 575-578, 1999.
230. **Mayadas TN, Cullere X, and Lowell CA.** The multifaceted functions of neutrophils. *Annual Review of Pathology: Mechanisms of Disease* 9: 181-218, 2014.
231. **Borregaard N.** Neutrophils, from marrow to microbes. *Immunity* 33: 657-670, 2010.
232. **Ohms M, Möller S, and Laskay T.** An attempt to polarize human neutrophils toward N1 and N2 phenotypes in vitro. *Frontiers in immunology* 11: 532, 2020.
233. **Fox S, Leitch AE, Duffin R, Haslett C, and Rossi AG.** Neutrophil apoptosis: relevance to the innate immune response and inflammatory disease. *Journal of innate immunity* 2: 216-227, 2010.
234. **Carta S, Castellani P, Delfino L, Tassi S, Vene R, and Rubartelli A.** DAMPs and inflammatory processes: the role of redox in the different outcomes. *Journal of leukocyte biology* 86: 549-555, 2009.
235. **Bonecchi R, Garlanda C, Mantovani A, and Riva F.** Cytokine decoy and scavenger receptors as key regulators of immunity and inflammation. *Cytokine* 87: 37-45, 2016.
236. **Garlichs C, Eskafi S, Cicha I, Schmeisser A, Walzog B, Raaz D, Stumpf C, Yilmaz A, Bremer J, and Ludwig J.** Delay of neutrophil apoptosis in acute coronary syndromes. *Journal of leukocyte biology* 75: 828-835, 2004.

237. **Lee JW, Devanarayan V, Barrett YC, Weiner R, Allinson J, Fountain S, Keller S, Weinryb I, Green M, and Duan L.** Fit-for-purpose method development and validation for successful biomarker measurement. *Pharmaceutical research* 23: 312-328, 2006.
238. **Hulsen T, de Vlieg J, and Alkema W.** BioVenn—a web application for the comparison and visualization of biological lists using area-proportional Venn diagrams. *BMC genomics* 9: 1-6, 2008.
239. **Liu K, Wang F-S, and Xu R.** Neutrophils in liver diseases: pathogenesis and therapeutic targets. *Cellular & molecular immunology* 18: 38-44, 2021.
240. **Giese MA, Hind LE, and Huttenlocher A.** Neutrophil plasticity in the tumor microenvironment. *Blood, The Journal of the American Society of Hematology* 133: 2159-2167, 2019.
241. **García-Culebras A, Durán-Laforet V, Peña-Martínez C, Moraga A, Ballesteros I, Cuartero MI, de la Parra J, Palma-Tortosa S, Hidalgo A, and Corbí AL.** Role of TLR4 (toll-like receptor 4) in N1/N2 neutrophil programming after stroke. *Stroke* 50: 2922-2932, 2019.
242. **Bird L.** Neutrophil plasticity. *Nature Reviews Immunology* 9: 673-673, 2009.
243. **Khalil RA.** *Matrix metalloproteinases and tissue remodeling in health and disease: cardiovascular remodeling.* Academic press, 2017.
244. **Aristorena M, Gallardo-Vara E, Vicen M, de Las Casas-Engel M, Ojeda-Fernandez L, Nieto C, Blanco FJ, Valbuena-Diez AC, Botella LM, and Nachtigal P.** MMP-12, secreted by pro-inflammatory macrophages, targets endoglin in human macrophages and endothelial cells. *International journal of molecular sciences* 20: 3107, 2019.
245. **Mouton AJ, Gonzalez OJR, Kaminski AR, Moore ET, and Lindsey ML.** Matrix metalloproteinase-12 as an endogenous resolution promoting factor following myocardial infarction. *Pharmacological research* 137: 252-258, 2018.
246. **Mankan AK, Dau T, Jenne D, and Hornung V.** The NLRP3/ASC/Caspase-1 axis regulates IL-1 β processing in neutrophils. *European journal of immunology* 42: 710-715, 2012.
247. **Xiao W, Hodge DR, Wang L, Yang X, Zhang X, and Farrar WL.** Co-operative functions between nuclear factors NF κ B and CCAT/enhancer-binding protein- β (C/EBP- β) regulate the IL-6 promoter in autocrine human prostate cancer cells. *The Prostate* 61: 354-370, 2004.
248. **Nick JA, Avdi NJ, Young SK, Lehman LA, McDonald PP, Frasch SC, Billstrom MA, Henson PM, Johnson GL, and Worthen GS.** Selective activation and functional significance of p38 α mitogen-activated protein kinase in lipopolysaccharide-stimulated neutrophils. *The Journal of clinical investigation* 103: 851-858, 1999.
249. **Liu J, Li X, Yue Y, Li J, He T, and He Y.** The inhibitory effect of quercetin on IL-6 production by LPS-stimulated neutrophils. *Cell Mol Immunol* 2: 455-460, 2005.
250. **Guijarro-Muñoz I, Compte M, Álvarez-Cienfuegos A, Álvarez-Vallina L, and Sanz L.** Lipopolysaccharide activates Toll-like receptor 4 (TLR4)-mediated NF- κ B signaling pathway and proinflammatory response in human pericytes. *Journal of Biological Chemistry* 289: 2457-2468, 2014.
251. **Szczepanek K, Xu A, Hu Y, Thompson J, He J, Lerner AC, Salloum FN, Chen Q, and Lesnfsky EJ.** Cardioprotective function of mitochondrial-targeted and transcriptionally inactive STAT3 against ischemia and reperfusion injury. *Basic research in cardiology* 110: 1-10, 2015.
252. **Wu L, Tan J-L, Chen Z-Y, and Huang G.** Cardioprotection of post-ischemic moderate ROS against ischemia/reperfusion via STAT3-induced the inhibition of MCU opening. *Basic research in cardiology* 114: 1-15, 2019.
253. **Harhous Z, Booz GW, Ovize M, Bidaux G, and Kurdi M.** An update on the multifaceted roles of STAT3 in the heart. *Frontiers in cardiovascular medicine* 6: 150, 2019.
254. **Lips DJ, Bueno OF, Wilkins BJ, Purcell NH, Kaiser RA, Lorenz JN, Voisin L, Saba-EI-Leil MK, Meloche S, and Pouysségur J.** MEK1-ERK2 signaling pathway protects myocardium from ischemic injury in vivo. *Circulation* 109: 1938-1941, 2004.
255. **Simard FA, Cloutier A, Ear T, Vardhan H, and McDonald PP.** MEK-independent ERK activation in human neutrophils and its impact on functional responses. *Journal of leukocyte biology* 98: 565-573, 2015.
256. **Downey GP, Butler JR, Tapper H, Fialkow L, Saltiel AR, Rubin BB, and Grinstein S.** Importance of MEK in neutrophil microbicidal responsiveness. *The Journal of Immunology* 160: 434-443, 1998.

257. **Yeh CC, Malhotra D, Yang YL, Xu Y, Fan Y, Li H, and Mann MJ.** MEK1-induced physiological hypertrophy inhibits chronic post-myocardial infarction remodeling in mice. *Journal of cellular biochemistry* 114: 47-55, 2013.
258. **Mehrpouya-Bahrami P, Moriarty AK, De Melo P, Keeter WC, Alakhras NS, Nelson AS, Hoover M, Barrios MS, Nadler JL, and Serezani CH.** STAT4 is expressed in neutrophils and promotes antimicrobial immunity. *JCI insight* 2021.
259. **Lentsch AB, Kato A, Davis B, Wang W, Chao C, and Edwards MJ.** STAT4 and STAT6 regulate systemic inflammation and protect against lethal endotoxemia. *The Journal of clinical investigation* 108: 1475-1482, 2001.
260. **Xu Y, Wang B, Liu X, Deng Y, Zhu Y, Zhu F, Liang Y, and Li H.** Sp1 targeted PARP1 inhibition protects cardiomyocytes from myocardial ischemia–reperfusion injury via downregulation of autophagy. *Frontiers in Cell and Developmental Biology* 9: 2021.
261. **Geng H, Su Y, Huang R, Fan M, Li X, Lu X, and Sheng H.** Specific protein 1 inhibitor mithramycin A protects cardiomyocytes from myocardial infarction via interacting with PARP. *In Vitro Cellular & Developmental Biology-Animal* 57: 315-323, 2021.
262. **Li R, Geng H-h, Xiao J, Qin X-t, Wang F, Xing J-h, Xia Y-f, Mao Y, Liang J-w, and Ji X-p.** miR-7a/b attenuates post-myocardial infarction remodeling and protects H9c2 cardiomyoblast against hypoxia-induced apoptosis involving Sp1 and PARP-1. *Scientific reports* 6: 1-11, 2016.
263. **McLoughlin TJ, Smith SM, DeLong AD, Wang H, Unterman TG, and Esser KA.** FoxO1 induces apoptosis in skeletal myotubes in a DNA-binding-dependent manner. *American Journal of Physiology-Cell Physiology* 297: C548-C555, 2009.
264. **Liu X, Zhao H, Jin Q, You W, Cheng H, Liu Y, Song E, Liu G, Tan X, and Zhang X.** Resveratrol induces apoptosis and inhibits adipogenesis by stimulating the SIRT1-AMPK α -FOXO1 signalling pathway in bovine intramuscular adipocytes. *Molecular and cellular biochemistry* 439: 213-223, 2018.
265. **Shen M, Lin F, Zhang J, Tang Y, Chen W-K, and Liu H.** Involvement of the up-regulated FoxO1 expression in follicular granulosa cell apoptosis induced by oxidative stress. *Journal of Biological Chemistry* 287: 25727-25740, 2012.
266. **Shao D, Zhai P, Del Re DP, Sciarretta S, Yabuta N, Nojima H, Lim D-S, Pan D, and Sadoshima J.** A functional interaction between Hippo-YAP signalling and FoxO1 mediates the oxidative stress response. *Nature communications* 5: 1-10, 2014.
267. **Zhao Z, Li C, Xi H, Gao Y, and Xu D.** Curcumin induces apoptosis in pancreatic cancer cells through the induction of forkhead box O1 and inhibition of the PI3K/Akt pathway. *Molecular medicine reports* 12: 5415-5422, 2015.
268. **Kim DH, Kim JY, Yu BP, and Chung HY.** The activation of NF- κ B through Akt-induced FOXO1 phosphorylation during aging and its modulation by calorie restriction. *Biogerontology* 9: 33-47, 2008.
269. **Watson A, Eilers A, Lallemand D, Kyriakis J, Rubin LL, and Ham J.** Phosphorylation of c-Jun is necessary for apoptosis induced by survival signal withdrawal in cerebellar granule neurons. *Journal of Neuroscience* 18: 751-762, 1998.
270. **Behrens A, Sibilina M, and Wagner EF.** Amino-terminal phosphorylation of c-Jun regulates stress-induced apoptosis and cellular proliferation. *Nature genetics* 21: 326-329, 1999.
271. **Hori YS, Kuno A, Hosoda R, and Horio Y.** Regulation of FOXOs and p53 by SIRT1 modulators under oxidative stress. *PLoS One* 8: e73875, 2013.
272. **Dejana E.** The role of wnt signaling in physiological and pathological angiogenesis. *Circulation research* 107: 943-952, 2010.
273. **Huang H, and He X.** Wnt/ β -catenin signaling: new (and old) players and new insights. *Current opinion in cell biology* 20: 119-125, 2008.
274. **Niessen CM, and Gottardi CJ.** Molecular components of the adherens junction. *Biochimica et Biophysica Acta (BBA)-Biomembranes* 1778: 562-571, 2008.
275. **Meng W, and Takeichi M.** Adherens junction: molecular architecture and regulation. *Cold Spring Harbor perspectives in biology* 1: a002899, 2009.
276. **Bellac CL, Dufour A, Krisinger MJ, Loonchanta A, Starr AE, auf dem Keller U, Lange PF, Goebeler V, Kappelhoff R, and Butler GS.** Macrophage matrix metalloproteinase-12 dampens inflammation and neutrophil influx in arthritis. *Cell reports* 9: 618-632, 2014.

277. **Saxena A, Russo I, and Frangogiannis NG.** Inflammation as a therapeutic target in myocardial infarction: learning from past failures to meet future challenges. *Translational Research* 167: 152-166, 2016.
278. **Tenkorang MAA, Chalise U, Daseke li MJ, Konfrst SR, and Lindsey ML.** Understanding the mechanisms that determine extracellular matrix remodeling in the infarcted myocardium. *Biochem Soc Trans* 47: 1679-1687, 2019.
279. **Lindsey ML, Ma Y, Flynn ER, Winniford MD, Hall ME, and DeLeon-Pennell KY.** Identifying the molecular and cellular signature of cardiac dilation following myocardial infarction. *Biochimica et Biophysica Acta (BBA)-Molecular Basis of Disease* 1865: 1845-1852, 2019.
280. **Somuncu MU, Pusuroglu H, Karakurt H, Bolat İ, Karakurt ST, Demir AR, Isiksacan N, Akgul O, and Surgit O.** The prognostic value of elevated matrix metalloproteinase-9 in patients undergoing primary percutaneous coronary intervention for ST-elevation myocardial infarction: A two-year prospective study. *Revista Portuguesa de Cardiologia* 2020.
281. **Kelly D, Cockerill G, Ng LL, Thompson M, Khan S, Samani NJ, and Squire IB.** Plasma matrix metalloproteinase-9 and left ventricular remodelling after acute myocardial infarction in man: a prospective cohort study. *European heart journal* 28: 711-718, 2007.
282. **Bhat T, Teli S, Rijal J, Bhat H, Raza M, Khoueiry G, Meghani M, Akhtar M, and Costantino T.** Neutrophil to lymphocyte ratio and cardiovascular diseases: a review. *Expert review of cardiovascular therapy* 11: 55-59, 2013.
283. **Arbel Y, Finkelstein A, Halkin A, Birati EY, Revivo M, Zuzut M, Shevach A, Berliner S, Herz I, and Keren G.** Neutrophil/lymphocyte ratio is related to the severity of coronary artery disease and clinical outcome in patients undergoing angiography. *Atherosclerosis* 225: 456-460, 2012.
284. **Schindhelm RK, van der Zwan LP, Teerlink T, and Scheffer PG.** Myeloperoxidase: a useful biomarker for cardiovascular disease risk stratification? *Clinical chemistry* 55: 1462-1470, 2009.
285. **Heslop CL, Frohlich JJ, and Hill JS.** Myeloperoxidase and C-reactive protein have combined utility for long-term prediction of cardiovascular mortality after coronary angiography. *Journal of the American College of Cardiology* 55: 1102-1109, 2010.
286. **Lobbes M, Kooi M, Lutgens E, Ruiters A, Lima Passos V, Braat S, Rousch M, Ten Cate H, van Engelshoven J, and Daemen M.** Leukocyte counts, myeloperoxidase, and pregnancy-associated plasma protein a as biomarkers for cardiovascular disease: towards a multi-biomarker approach. *International journal of vascular medicine* 2010: 2010.
287. **Meijers WC, van der Velde AR, Pascual-Figal DA, and de Boer RA.** Galectin-3 and post-myocardial infarction cardiac remodeling. *European journal of pharmacology* 763: 115-121, 2015.
288. **Du W, Piek A, Schouten EM, van de Kolk CW, Mueller C, Mebazaa A, Voors AA, de Boer RA, and Silljé HH.** Plasma levels of heart failure biomarkers are primarily a reflection of extracardiac production. *Theranostics* 8: 4155, 2018.
289. **Chan D, and Ng LL.** Biomarkers in acute myocardial infarction. *BMC medicine* 8: 1-11, 2010.
290. **Arab S, Gramolini AO, Ping P, Kislinger T, Stanley B, van Eyk J, Ouzounian M, MacLennan DH, Emili A, and Liu PP.** Cardiovascular proteomics: tools to develop novel biomarkers and potential applications. *Journal of the American College of Cardiology* 48: 1733-1741, 2006.
291. **Council NR.** Guide for the care and use of laboratory animals. *National Academies Press* 2011.
292. **DeLeon-Pennell KY, Iyer RP, Ma Y, Yabluchanskiy A, Zamilpa R, Chiao YA, Cannon PL, Kaplan A, Cates CA, and Flynn ER.** The mouse heart attack research tool 1.0 database. *American Journal of Physiology-Heart and Circulatory Physiology* 315: H522-H530, 2018.
293. **Lindsey ML, Bolli R, Canty JM, Jr., Du XJ, Frangogiannis NG, Frantz S, Gourdie RG, Holmes JW, Jones SP, Kloner RA, Lefer DJ, Liao R, Murphy E, Ping P, Przyklenk K, Recchia FA, Schwartz Longacre L, Ripplinger CM, Van Eyk JE, and Heusch G.** Guidelines for experimental models of myocardial ischemia and infarction. *Am J Physiol Heart Circ Physiol* 314: H812-h838, 2018.

294. **Lindsey ML, Kassiri Z, Virag JAI, de Castro Brás LE, and Scherrer-Crosbie M.** Guidelines for measuring cardiac physiology in mice. *Am J Physiol Heart Circ Physiol* 314: H733-h752, 2018.
295. **Lindsey ML, de Castro Brás LE, DeLeon-Pennell KY, Frangogiannis NG, Halade GV, O'Meara CC, Spinale FG, Kassiri Z, Kirk JA, Kleinbongard P, Ripplinger CM, and Brunt KR.** Reperfused vs. nonreperfused myocardial infarction: when to use which model. *Am J Physiol Heart Circ Physiol* 321: H208-h213, 2021.
296. **Brooks HL, and Lindsey ML.** Guidelines for authors and reviewers on antibody use in physiology studies. *Am J Physiol Heart Circ Physiol* 314: H724-h732, 2018.
297. **Kaminski AR, Moore ET, Daseke MJ, 2nd, Valerio FM, Flynn ER, and Lindsey ML.** The compendium of matrix metalloproteinase expression in the left ventricle of mice following myocardial infarction. *Am J Physiol Heart Circ Physiol* 318: H706-h714, 2020.
298. **Lindsey ML, Jung M, Yabluchanskiy A, Cannon PL, Iyer RP, Flynn ER, DeLeon-Pennell KY, Valerio FM, Harrison CL, Ripplinger CM, Hall ME, and Ma Y.** Exogenous CXCL4 infusion inhibits macrophage phagocytosis by limiting CD36 signalling to enhance post-myocardial infarction cardiac dilation and mortality. *Cardiovasc Res* 115: 395-408, 2019.
299. **Lindsey ML, Gray GA, Wood SK, and Curran-Everett D.** Statistical considerations in reporting cardiovascular research. *Am J Physiol Heart Circ Physiol* 315: H303-h313, 2018.
300. **Chong J, and Xia J.** MetaboAnalystR: an R package for flexible and reproducible analysis of metabolomics data. *Bioinformatics* 34: 4313-4314, 2018.
301. **Kuleshov MV, Jones MR, Rouillard AD, Fernandez NF, Duan Q, Wang Z, Koplev S, Jenkins SL, Jagodnik KM, and Lachmann A.** Enrichr: a comprehensive gene set enrichment analysis web server 2016 update. *Nucleic acids research* 44: W90-W97, 2016.
302. **Florvall G, Basu S, and Larsson A.** Apolipoprotein A1 is a stronger prognostic marker than are HDL and LDL cholesterol for cardiovascular disease and mortality in elderly men. *The Journals of Gerontology Series A: Biological Sciences and Medical Sciences* 61: 1262-1266, 2006.
303. **Walldius G, Jungner I, Holme I, Aastveit AH, Kolar W, and Steiner E.** High apolipoprotein B, low apolipoprotein AI, and improvement in the prediction of fatal myocardial infarction (AMORIS study): a prospective study. *The Lancet* 358: 2026-2033, 2001.
304. **Xu Y, Ye J, Wang M, Liu J, Wang Z, Jiang H, Ye D, Zhang J, and Wan J.** The expression of interleukin-25 increases in human coronary artery disease and is associated with the severity of coronary stenosis. *Anatolian journal of cardiology* 23: 151, 2020.
305. **Jiang Z, Chen J, Du X, Cheng H, Wang X, and Dong C.** IL-25 blockade inhibits metastasis in breast cancer. *Protein & cell* 8: 191-201, 2017.
306. **Mantani PT, Dunér P, Bengtsson E, Alm R, Ljungcrantz I, Söderberg I, Sundius L, To F, Nilsson J, and Björkbacka H.** IL-25 inhibits atherosclerosis development in apolipoprotein E deficient mice. *PLoS one* 10: e0117255, 2015.
307. **Corrigan CJ, Wang W, Meng Q, Fang C, Wu H, Reay V, Lv Z, Fan Y, An Y, and Wang Y-H.** T-helper cell type 2 (Th2) memory T cell-potentiating cytokine IL-25 has the potential to promote angiogenesis in asthma. *Proceedings of the National Academy of Sciences* 108: 1579-1584, 2011.
308. **Hara K, Morita Y, Kamihata H, Iwasaka T, and Takahashi H.** Evidence for infection with *Helicobacter pylori* in patients with acute myocardial infarction. *Clinica chimica acta* 313: 87-94, 2001.
309. **Muscari A, Bozzoli C, Puddu GM, Rovinetti C, Vallar G, Renzi C, Scarani P, Molinaro N, and Puddu P.** Increased serum IgA levels in subjects with previous myocardial infarction or other major ischemic events. *Cardiology* 83: 383-389, 1993.
310. **Tsiantoulas D, Sage AP, Mallat Z, and Binder CJ.** Targeting B cells in atherosclerosis: closing the gap from bench to bedside. *Arteriosclerosis, thrombosis, and vascular biology* 35: 296-302, 2015.
311. **Porsch F, and Binder CJ.** Impact of B-cell-targeted therapies on cardiovascular disease. *Arteriosclerosis, thrombosis, and vascular biology* 39: 1705-1714, 2019.
312. **Zouggar Y, Ait-Oufella H, Bonnin P, Simon T, Sage AP, Guérin C, Vilar J, Caligiuri G, Tsiantoulas D, and Laurans L.** B lymphocytes trigger monocyte mobilization and impair heart function after acute myocardial infarction. *Nature medicine* 19: 1273-1280, 2013.

313. **Holme I, Aastveit AH, Hammar N, Jungner I, and Walldius G.** Haptoglobin and risk of myocardial infarction, stroke, and congestive heart failure in 342,125 men and women in the Apolipoprotein MORTality RISK study (AMORIS). *Annals of medicine* 41: 522-532, 2009.
314. **Blum S, Asaf R, Guetta J, Miller-Lotan R, Asleh R, Kremer R, Levy NS, Berger FG, Aronson D, and Fu X.** Haptoglobin genotype determines myocardial infarct size in diabetic mice. *Journal of the American College of Cardiology* 49: 82-87, 2007.
315. **Bilgrami G, Tyagi S, and Qasim A.** Serum haptoglobin in cases of ischemic heart diseases. *Japanese heart journal* 21: 505-510, 1980.
316. **Ebersole J, Machen R, Steffen M, and Willmann D.** Systemic acute-phase reactants, C-reactive protein and haptoglobin, in adult periodontitis. *Clinical & Experimental Immunology* 107: 347-352, 1997.
317. **Opstad TB, Seljeflot I, Bøhmer E, Arnesen H, and Halvorsen S.** MMP-9 and its regulators TIMP-1 and EMMPRIN in patients with acute ST-elevation myocardial infarction: a NORDISTEMI substudy. *Cardiology* 139: 17-24, 2018.
318. **Cavusoglu E, Ruwende C, Chopra V, Yanamadala S, Eng C, Clark LT, Pinsky DJ, and Marmur JD.** Tissue inhibitor of metalloproteinase-1 (TIMP-1) is an independent predictor of all-cause mortality, cardiac mortality, and myocardial infarction. *American heart journal* 151: 1101. e1101-1101. e1108, 2006.
319. **Kelly D, Khan SQ, Thompson M, Cockerill G, Ng LL, Samani N, and Squire IB.** Plasma tissue inhibitor of metalloproteinase-1 and matrix metalloproteinase-9: novel indicators of left ventricular remodelling and prognosis after acute myocardial infarction. *European heart journal* 29: 2116-2124, 2008.
320. **Glass C, and Singla DK.** Overexpression of TIMP-1 in embryonic stem cells attenuates adverse cardiac remodeling following myocardial infarction. *Cell transplantation* 21: 1931-1944, 2012.
321. **Tian S, Lei I, Gao W, Liu L, Guo Y, Creech J, Herron TJ, Xian S, Ma PX, and Chen YE.** HDAC inhibitor valproic acid protects heart function through Foxm1 pathway after acute myocardial infarction. *EBioMedicine* 39: 83-94, 2019.
322. **Bolte C, Zhang Y, Wang I-C, Kalin TV, Molkentin JD, and Kalinichenko VV.** Expression of Foxm1 transcription factor in cardiomyocytes is required for myocardial development. *PLoS one* 6: e22217, 2011.
323. **Krishnamurthy P, Rajasingh J, Lambers E, Qin G, Losordo DW, and Kishore R.** IL-10 inhibits inflammation and attenuates left ventricular remodeling after myocardial infarction via activation of STAT3 and suppression of HuR. *Circulation research* 104: e9-e18, 2009.
324. **Andreadou I, Efentakis P, Balafas E, Togliatto G, Davos CH, Varela A, Dimitriou CA, Nikolaou P-E, Maratou E, and Lambadiari V.** Empagliflozin limits myocardial infarction in vivo and cell death in vitro: role of STAT3, mitochondria, and redox aspects. *Frontiers in physiology* 8: 1077, 2017.
325. **Samidurai A, Roh SK, Prakash M, Durrant D, Salloum FN, Kukreja RC, and Das A.** STAT3-miR-17/20 signalling axis plays a critical role in attenuating myocardial infarction following rapamycin treatment in diabetic mice. *Cardiovascular research* 116: 2103-2115, 2020.
326. **McCormick J, Suleman N, Scarabelli T, Knight R, Latchman D, and Stephanou A.** STAT1 deficiency in the heart protects against myocardial infarction by enhancing autophagy. *Journal of cellular and molecular medicine* 16: 386-393, 2012.
327. **Zeng G, Lian C, Yang P, Zheng M, Ren H, and Wang H.** E3-ubiquitin ligase TRIM6 aggravates myocardial ischemia/reperfusion injury via promoting STAT1-dependent cardiomyocyte apoptosis. *Aging (Albany NY)* 11: 3536, 2019.
328. **Yang Y, Yang J, Sui F, Huo P, and Yang H.** Identification of potential molecular mechanisms and candidate genes involved in the acute phase of myocardial infarction. *Cell Journal (Yakhteh)* 20: 435, 2018.
329. **Simonis G, Mueller K, Schwarz P, Wiedemann S, Adler G, Strasser RH, and Kulaksiz H.** The iron-regulatory peptide hepcidin is upregulated in the ischemic and in the remote myocardium after myocardial infarction. *Peptides* 31: 1786-1790, 2010.
330. **Michels KB, and Yusuf S.** Does PTCA in acute myocardial infarction affect mortality and reinfarction rates? A quantitative overview (meta-analysis) of the randomized clinical trials. *Circulation* 91: 476-485, 1995.

331. **Sanada S, Komuro I, and Kitakaze M.** Pathophysiology of myocardial reperfusion injury: preconditioning, postconditioning, and translational aspects of protective measures. *Am J Physiol Heart Circ Physiol* 301: H1723-1741, 2011.
332. **Clark CL, Berman AD, McHugh A, Roe EJ, Boura J, and Swor RA.** Hospital process intervals, not EMS time intervals, are the most important predictors of rapid reperfusion in EMS Patients with ST-segment elevation myocardial infarction. *Prehosp Emerg Care* 16: 115-120, 2012.
333. **Eagle KA, Goodman SG, Avezum A, Budaj A, Sullivan CM, Lopez-Sendon J, and Investigators G.** Practice variation and missed opportunities for reperfusion in ST-segment-elevation myocardial infarction: findings from the Global Registry of Acute Coronary Events (GRACE). *Lancet* 359: 373-377, 2002.
334. **Goldberg RJ, Lamusta J, Darling C, DeWolf M, Saczynski JS, Lessard D, Ward J, and Gore JM.** Community trends in the use and characteristics of persons with acute myocardial infarction who are transported by emergency medical services. *Heart Lung* 41: 323-331, 2012.
335. **Ribichini F, Ferrero V, and Wijns W.** Reperfusion treatment of ST-elevation acute myocardial infarction. *Prog Cardiovasc Dis* 47: 131-157, 2004.
336. **Bui AL, Horwich TB, and Fonarow GC.** Epidemiology and risk profile of heart failure. *Nature Reviews Cardiology* 8: 30, 2011.
337. **Virani SS, Alonso A, Benjamin EJ, Bittencourt MS, Callaway CW, Carson AP, Chamberlain AM, Chang AR, Cheng S, and Delling FN.** Heart disease and stroke statistics—2020 update: a report from the American Heart Association. *Circulation* 141: e139-e596, 2020.
338. **Ziaeian B, and Fonarow GC.** Epidemiology and aetiology of heart failure. *Nat Rev Cardiol* 13: 368-378, 2016.
339. **Ezekowitz JA, Kaul P, Bakal JA, Armstrong PW, Welsh RC, and McAlister FA.** Declining in-hospital mortality and increasing heart failure incidence in elderly patients with first myocardial infarction. *J Am Coll Cardiol* 53: 13-20, 2009.
340. **Frangogiannis NG.** Regulation of the inflammatory response in cardiac repair. *Circulation research* 110: 159-173, 2012.
341. **Jung K, Kim P, Leuschner F, Gorbatov R, Kim JK, Ueno T, Nahrendorf M, and Yun SH.** Endoscopic time-lapse imaging of immune cells in infarcted mouse hearts. *Circulation research* 112: 891-899, 2013.
342. **Carbone F, Nencioni A, Mach F, Vuilleumier N, and Montecucco F.** Pathophysiological role of neutrophils in acute myocardial infarction. *Thrombosis and haemostasis* 110: 501-514, 2013.
343. **Weil BR, and Neelamegham S.** Selectins and Immune Cells in Acute Myocardial Infarction and Post-infarction Ventricular Remodeling: Pathophysiology and Novel Treatments. *Front Immunol* 10: 300, 2019.
344. **Mouton AJ, Ma Y, Gonzalez OJR, Daseke MJ, Flynn ER, Freeman TC, Garrett MR, DeLeon-Pennell KY, and Lindsey ML.** Fibroblast polarization over the myocardial infarction time continuum shifts roles from inflammation to angiogenesis. *Basic research in cardiology* 114: 6, 2019.
345. **Sokol CL, and Luster AD.** The chemokine system in innate immunity. *Cold Spring Harbor perspectives in biology* 7: a016303, 2015.
346. **Mann DL.** The emerging role of innate immunity in the heart and vascular system: for whom the cell tolls. *Circulation research* 108: 1133-1145, 2011.
347. **Shinde AV, and Frangogiannis NG.** Fibroblasts in myocardial infarction: a role in inflammation and repair. *Journal of molecular and cellular cardiology* 70: 74-82, 2014.
348. **Kawaguchi M, Takahashi M, Hata T, Kashima Y, Usui F, Morimoto H, Izawa A, Takahashi Y, Masumoto J, and Koyama J.** Inflammasome activation of cardiac fibroblasts is essential for myocardial ischemia/reperfusion injury. *Circulation* 123: 594-604, 2011.
349. **Saxena A, Chen W, Su Y, Rai V, Uche OU, Li N, and Frangogiannis NG.** IL-1 induces proinflammatory leukocyte infiltration and regulates fibroblast phenotype in the infarcted myocardium. *The Journal of Immunology* 191: 4838-4848, 2013.
350. **Galli A, and Lombardi F.** Postinfarct left ventricular remodelling: a prevailing cause of heart failure. *Cardiology research and practice* 2016: 2016.

351. **Huang S, and Frangogiannis NG.** Anti-inflammatory therapies in myocardial infarction: failures, hopes and challenges. *British journal of pharmacology* 175: 1377-1400, 2018.
352. **Serhan CN, Chiang N, and Dalli J.** The resolution code of acute inflammation: Novel pro-resolving lipid mediators in resolution. In: *Seminars in immunology* Elsevier, 2015, p. 200-215.
353. **Penna C, Granata R, Gabriele Tocchetti C, Pia Gallo M, Alloatti G, and Pagliaro P.** Endogenous cardioprotective agents: role in pre and postconditioning. *Current drug targets* 16: 843-867, 2015.
354. **Dalli J, Norling LV, Renshaw D, Cooper D, Leung K-Y, and Perretti M.** Annexin 1 mediates the rapid anti-inflammatory effects of neutrophil-derived microparticles. *Blood, The Journal of the American Society of Hematology* 112: 2512-2519, 2008.
355. **La M, D'Amico M, Bandiera S, Filippo CD, Oliani SM, Gavins FN, Flower RJ, and Perretti M.** Annexin 1 peptides protect against experimental myocardial ischemia-reperfusion: analysis of their mechanism of action. *The FASEB Journal* 15: 2247-2256, 2001.
356. **Ma Y.** Role of Neutrophils in Cardiac Injury and Repair Following Myocardial Infarction. *Cells* 10: 1676, 2021.
357. **Hanash S.** Disease proteomics. *Nature* 422: 226-232, 2003.
358. **Lam MP, Ping P, and Murphy E.** Proteomics research in cardiovascular medicine and biomarker discovery. *Journal of the American College of Cardiology* 68: 2819-2830, 2016.
359. **Lindsey ML, Hall ME, Harmancey R, and Ma Y.** Adapting extracellular matrix proteomics for clinical studies on cardiac remodeling post-myocardial infarction. *Clinical proteomics* 13: 1-8, 2016.
360. **Lindsey ML, Weintraub ST, and Lange RA.** Using extracellular matrix proteomics to understand left ventricular remodeling. *Circulation: Cardiovascular Genetics* 5: o1-o7, 2012.
361. **Liddy KA, White MY, and Cordwell SJ.** Functional decorations: post-translational modifications and heart disease delineated by targeted proteomics. *Genome medicine* 5: 1-12, 2013.
362. **Brunetti ND, Pellegrino PL, Correale M, De Gennaro L, Cuculo A, and Di Biase M.** Acute phase proteins and systolic dysfunction in subjects with acute myocardial infarction. *Journal of thrombosis and thrombolysis* 26: 196-202, 2008.
363. **Porsch F, Mallat Z, and Binder CJ.** Humoral immunity in atherosclerosis and myocardial infarction: from B cells to antibodies. *Cardiovascular research* 117: 2544-2562, 2021.
364. **Cordero-Reyes AM, Youker KA, Trevino AR, Celis R, Hamilton DJ, Flores-Arredondo JH, Orrego CM, Bhimaraj A, Estep JD, and Torre-Amione G.** Full expression of cardiomyopathy is partly dependent on B-cells: a pathway that involves cytokine activation, immunoglobulin deposition, and activation of apoptosis. *Journal of the American Heart Association* 5: e002484, 2016.
365. **Cisek K, Krochmal M, Klein J, and Mischak H.** The application of multi-omics and systems biology to identify therapeutic targets in chronic kidney disease. *Nephrology Dialysis Transplantation* 31: 2003-2011, 2016.
366. **Lau E, Cao Q, Lam MP, Wang J, Ng DC, Bleakley BJ, Lee JM, Liem DA, Wang D, and Hermjakob H.** Integrated omics dissection of proteome dynamics during cardiac remodeling. *Nature communications* 9: 1-14, 2018.
367. **Munafò MR, and Smith GD.** Robust research needs many lines of evidence. Nature Publishing Group, 2018.
368. **Pigozzo AB, Macedo GC, Dos Santos RW, and Lobosco M.** On the computational modeling of the innate immune system. In: *BMC bioinformatics* Springer, 2013, p. 1-20.
369. **Zeigler AC, Richardson WJ, Holmes JW, and Saucerman JJ.** Computational modeling of cardiac fibroblasts and fibrosis. *Journal of molecular and cellular cardiology* 93: 73-83, 2016.
370. **Yang JH, and Saucerman JJ.** Computational models reduce complexity and accelerate insight into cardiac signaling networks. *Circulation research* 108: 85-97, 2011.